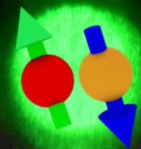


The 11th School of Mesoscopic Physics: Quantum Control and Sensing

Quantum Sensing and Imaging

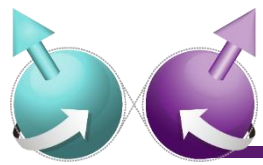
Using Diamond NV Center



Donghun Lee

Department of Physics, Korea University

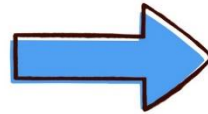




Beginning the era of quantum technology

Quantum Mechanics

- Duality
- Uncertainty
- Superposition
- Entanglement



Quantum Technology

- Quantum computation
- Quantum communication
- Quantum simulation
- Quantum sensing

반도체 이론, 기초 실험

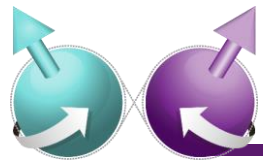
양자정보 이론, 기초 실험

Se photocell (1931, Weston)

양자 센서 (?)

진공튜브 컴퓨터 (1946, ENIAC)

양자컴퓨터 (?)

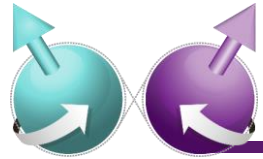


Quantum sensing ?

개념 및 정의	참고문헌
양자시스템(예, 큐비트) 또는 양자결맞음(예, 중첩)을 이용하여 물리량(예, 온도, 자기장)을 측정하는 기술	[1]
양자얽힘(entanglement), 압착(squeezing) 등 양자특성을 이용하여 물리량을 양자한계(standard quantum limit) 이하로 측정하는 기술	[1]
고전시스템만을 사용했을 때 얻을 수 있는 것보다 더 나은 민감도와 분해능을 얻기 위해 양자얽힘과 같은 양자특성을 활용하는 기술	[2]
기존 센서/이미징의 정밀도를 획기적으로 개선하고 새로운 초정밀 양자센서/이미징 산업을 창출할 수 있는 기술을 포함	[2]

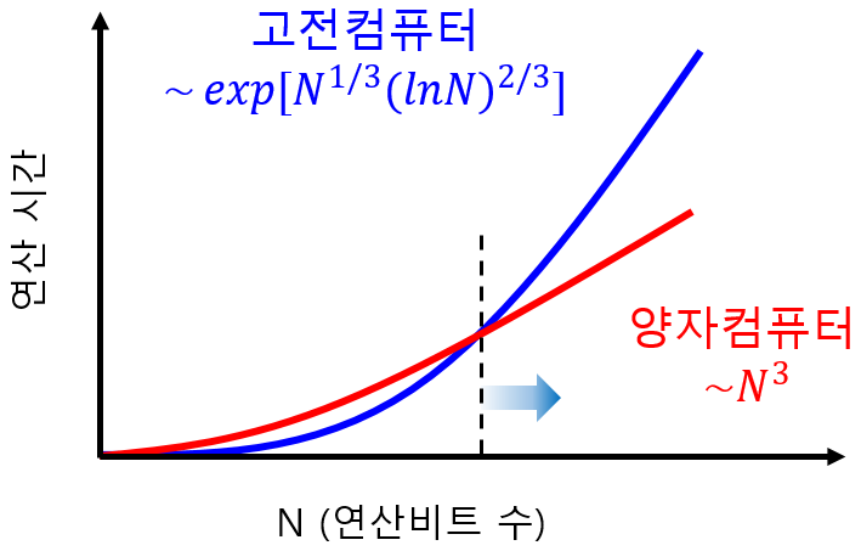
[1] C. L. Degen, F. Reinhard, P. Cappellaro, "Quantum Sensing", Reviews of Modern Physics 89, 0034-6861, 2017.

[2] 정보통신기술진흥센터 ICT R&D 기술로드맵 2023.

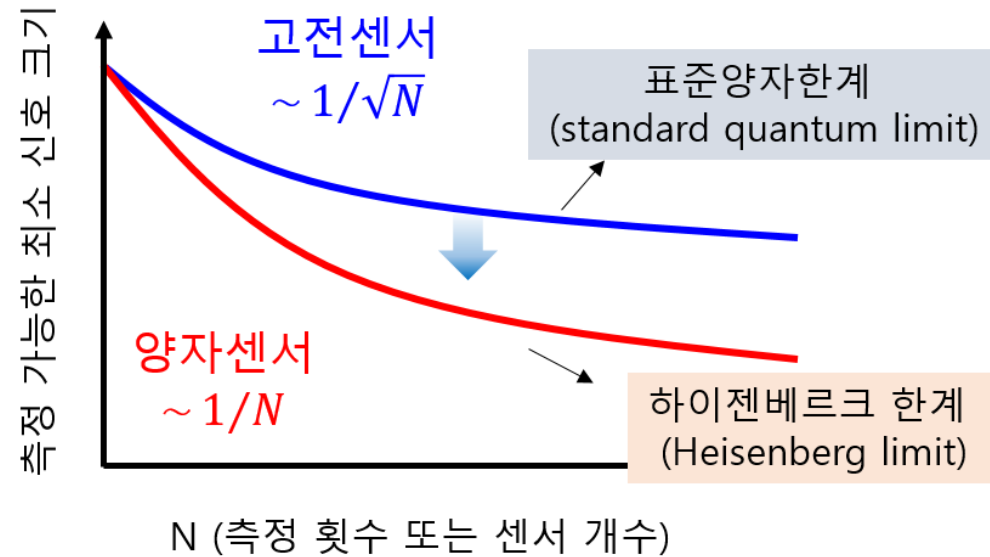


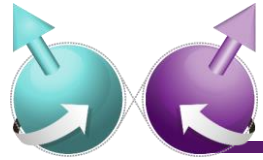
Quantum sensing and quantum limit

양자컴퓨팅 / 양자우월성



양자센싱 / 양자한계





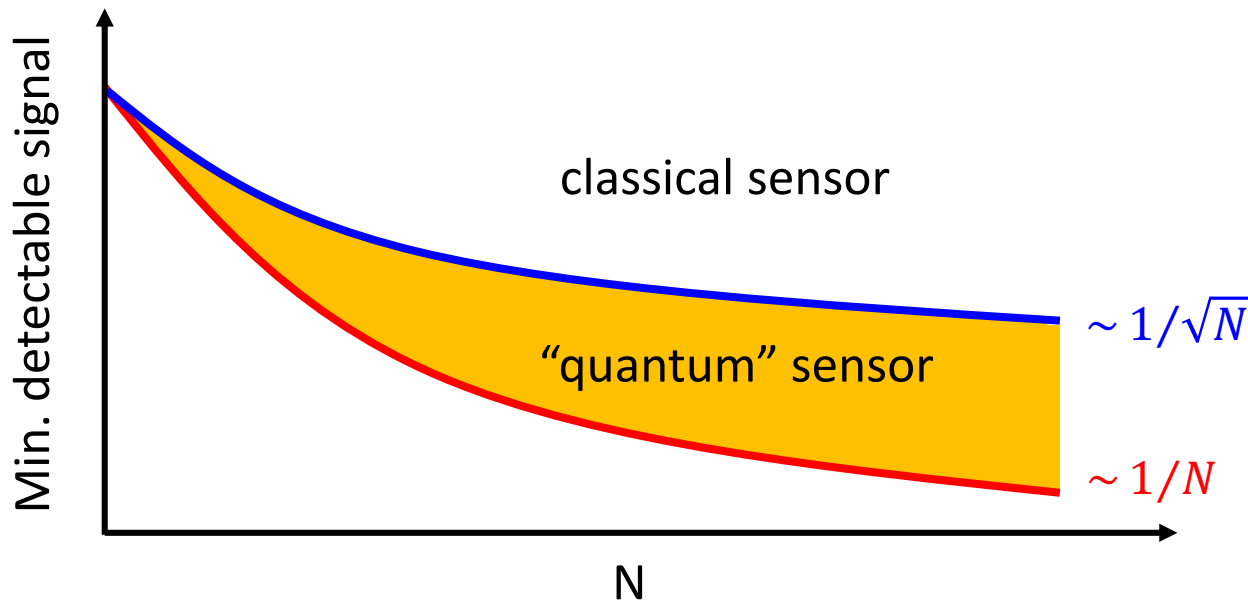
Sensitivity of quantum sensor

$$\text{민감도 (sensitivity)} \approx \frac{1}{\sqrt{N}} \frac{1}{\sqrt{T}}$$

$$\left[\frac{\text{물리량}}{\sqrt{\text{Hz}}} \right]$$

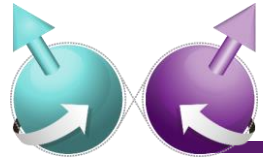
N : # of measurements or # of sensors

T : Coherence time , T_1, T_2, T_2^*



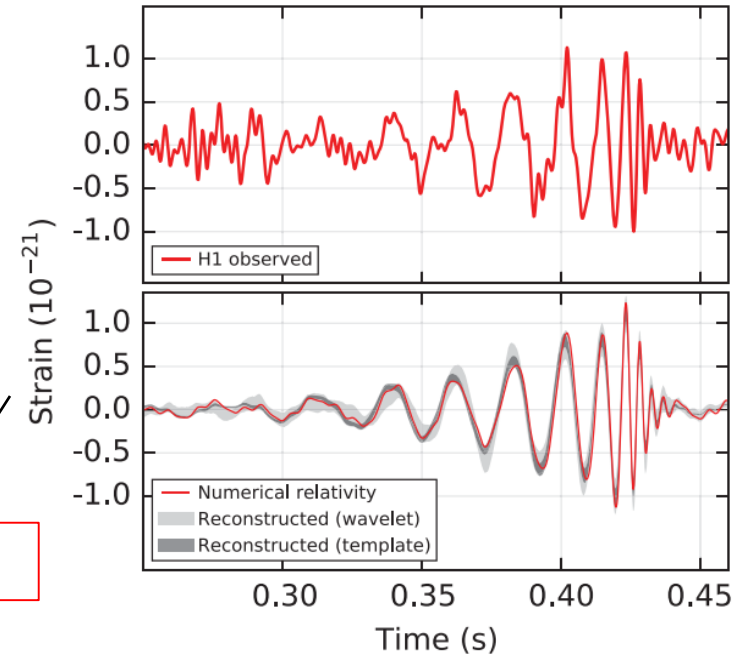
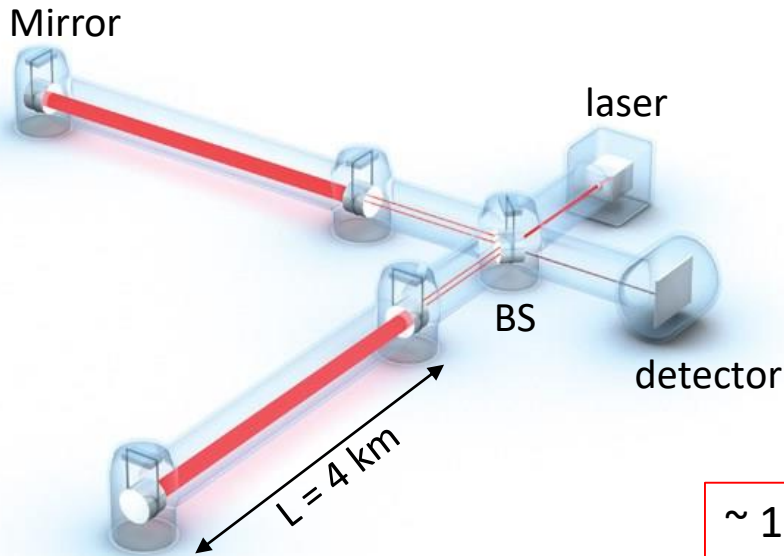
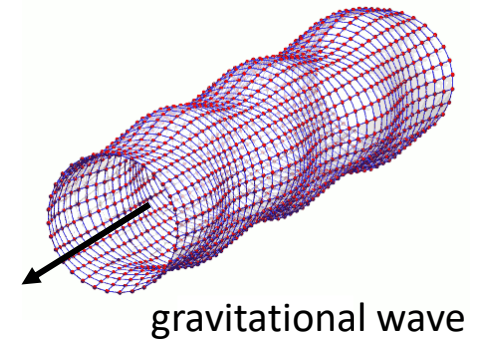
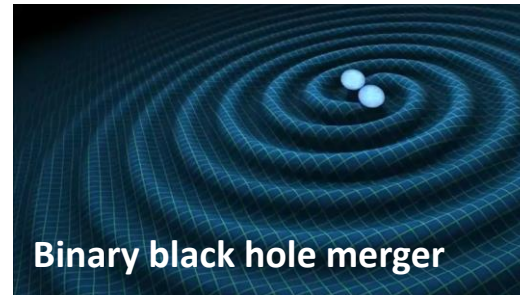
표준양자한계
(standard quantum limit)

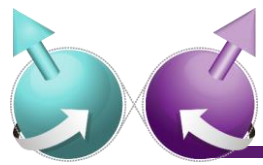
하이젠베르크 한계
(Heisenberg limit)



Example : Gravitational Wave Detection

LIGO (Laser Interferometer Gravitational-Wave Observatory), Nobel prize at 2017

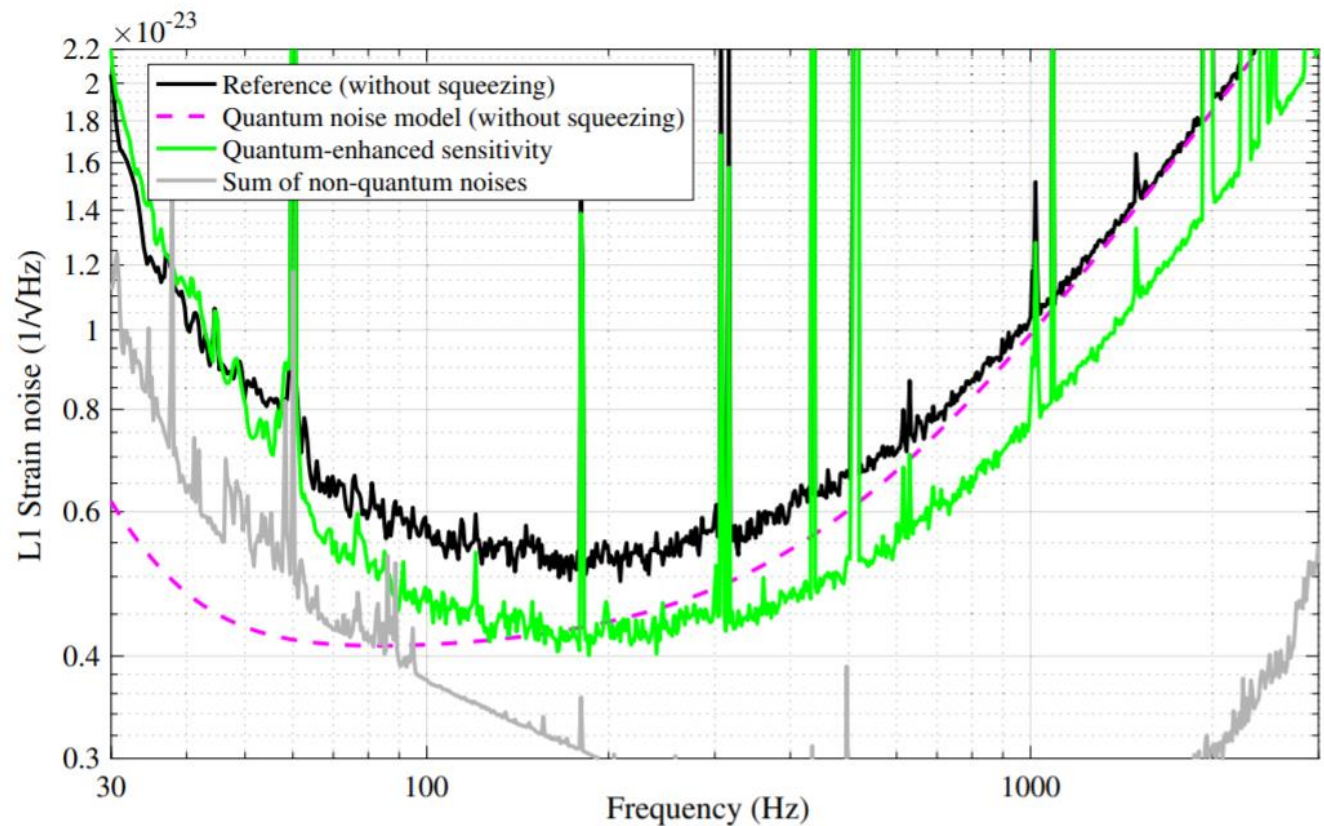
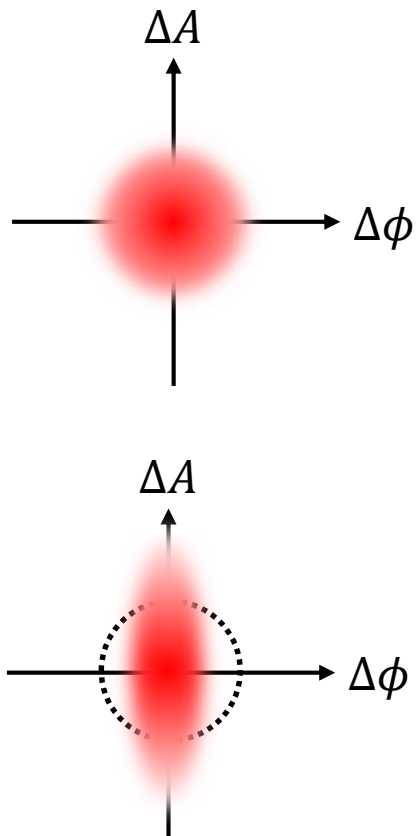


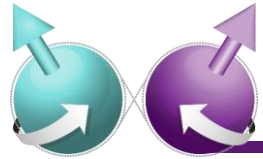


Example : Gravitational Wave Detection

LIGO (Laser Interferometer Gravitational-Wave Observatory), Nobel prize at 2017

50 % improvement with quantum squeezed light

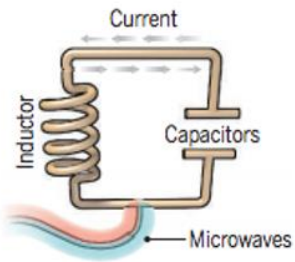




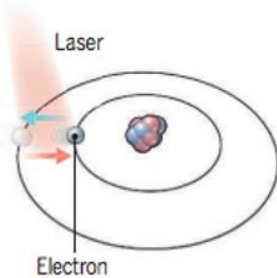
Classification of quantum sensing

▶ 양자센서에 따른 분류

초전도 소자



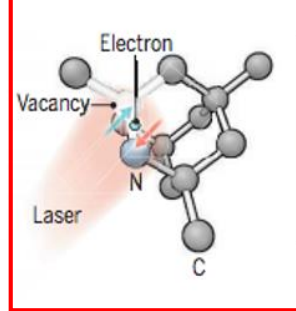
이온, 원자



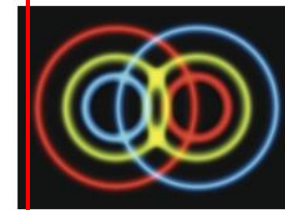
반도체 양자점



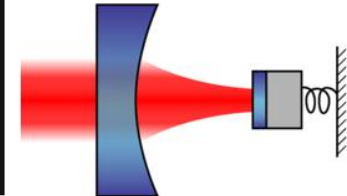
NV 센터



광자

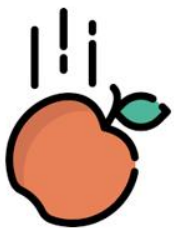


역학계



▶ 센싱 물리량에 따른 분류

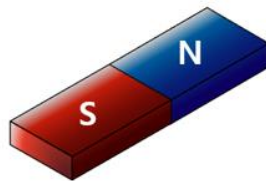
중력/힘



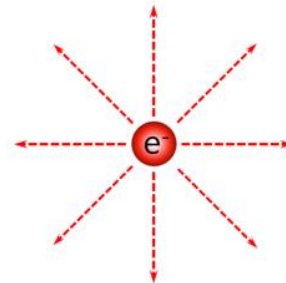
회전/각속도



자기장/스핀



전기장/전하



온도



시간





Classification of quantum sensing

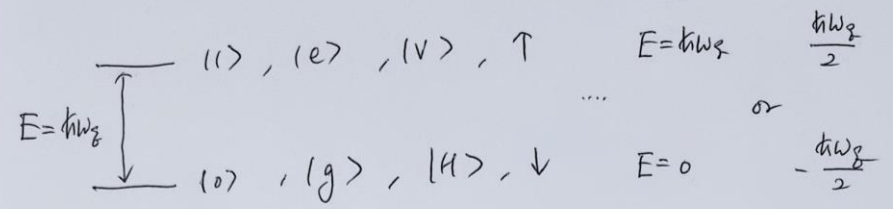
대분류	소분류	큐비트	측정하는양	진동수	초기화	상태읽기
중성 원자	원자 증기	원자 스핀	자기장, 회전, 시간/진동수	dc-GHz	광학	광학
	차가운 구름	원자 스핀	자기장, 가속도, 시간/진동수	dc-GHz	광학	광학
갇힌 이온	-	수명이 긴 전자 상태	시간/진동수	THz	광학	광학
			회전	-	광학	광학
	진동 모드	전기장, 힘	MHz	광학	광학	
리드버그 원자	-	리드버그 상태	전기장	dc, GHz	광학	광학
고체 스핀 (양상블)	NMR 센서	핵 스핀	자기장	dc	열	픽업 코일
	NV 센터 양상블	전자 스핀	자기장, 전기장, 온도, 압력, 회전	dc-GHz	광학	광학
고체 스핀 (단일 스핀)	Si 반도체의 P 도너	전자 스핀	자기장	dc-GHz	열	전기
	반도체 양자 점	전자 스핀	자기장, 전기장	dc-GHz	전기, 광학	전기, 광학
	단일 NV 센터	전자 스핀	자기장, 전기장, 온도, 압력, 회전	dc-GHz	광학	광학
초전도 회로	SQUID	초전류	자기장	dc-GHz	열	전기
	Flux 큐비트	순환 전류	자기장	dc-GHz	열	전기
	전하 큐비트	전하 고유상태	전기장	dc-GHz	열	전기
기본 입자	뮤온	뮤온 스핀	자기장	dc	방사성 붕괴	방사성 붕괴
	중성자	핵스핀	자기장, 포논 밀도, 중력	dc	브래그 산란	브래그 산란
기타 센서	SET	전하 고유상태	전기장	dc-MHz	열	전기
	광역학계	포논	힘, 가속도, 질량, 자기장, 전압	-	-	-
	간섭계	광자, (원자, 분자)	변위, 굴절률	-	-	-

강의 계획

- Part 1 : 스핀 큐비트 기반 양자센싱 기초 원리
- Part 2 : 다이아몬드 NV 센터 소개
- Part 3 : NV 센터 기반 양자센싱 및 이미징 연구 소개

Part 1 : 스핀 큐비트 기반 양자센싱 기초 원리

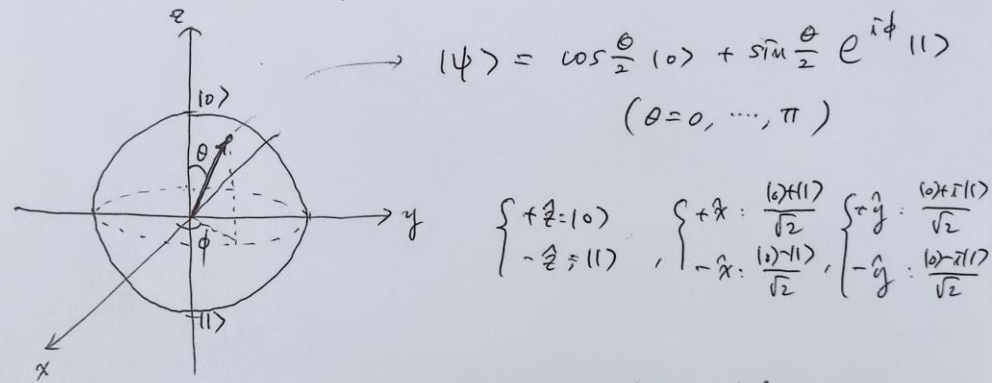
1.1 Qubit (Two level system)



Qubit state : $|\psi\rangle = \alpha|0\rangle + \beta|1\rangle$
 ($|\alpha|^2 + |\beta|^2 = 1$)

$\rightarrow |\psi\rangle = \alpha|0\rangle + \beta e^{i\phi}|1\rangle$ ϕ : relative phase

1.2 Bloch representation



$$\begin{cases} +z = |0\rangle \\ -z = |1\rangle \end{cases}, \begin{cases} +x = \frac{|0\rangle + |1\rangle}{\sqrt{2}} \\ -x = \frac{|0\rangle - |1\rangle}{\sqrt{2}} \end{cases}, \begin{cases} +y = \frac{|0\rangle + i|1\rangle}{\sqrt{2}} \\ -y = \frac{|0\rangle - i|1\rangle}{\sqrt{2}} \end{cases}$$

• π (180°) turn around z : $|\psi\rangle \rightarrow |\psi'\rangle$

$$|\psi'\rangle = \cos\frac{\theta}{2}|0\rangle + \sin\frac{\theta}{2}e^{i(\phi+\pi)}|1\rangle$$

$$= \cos\frac{\theta}{2}|0\rangle - \sin\frac{\theta}{2}|1\rangle$$

$$\mathbb{Z} \equiv \begin{pmatrix} 1 & 0 \\ 0 & -1 \end{pmatrix} = \sigma_z$$

• Π around \hat{x} : $|0\rangle \rightarrow |1\rangle$, $|1\rangle \rightarrow |0\rangle$

$$X \equiv \begin{pmatrix} 0 & 1 \\ 1 & 0 \end{pmatrix} = \sigma_x$$

• Π around \hat{y} :

$$Y \equiv \begin{pmatrix} 0 & -i \\ i & 0 \end{pmatrix} = \sigma_y$$

1.3. Qubit Hamiltonian

$$H = \hbar\omega_z |1\rangle\langle 1| + 0 \cdot |0\rangle\langle 0|$$

$$= \frac{\hbar\omega_z}{2} |1\rangle\langle 1| - \frac{\hbar\omega_z}{2} |0\rangle\langle 0|$$

$$= -\frac{\hbar\omega_z}{2} \begin{pmatrix} 1 & 0 \\ 0 & -1 \end{pmatrix} = -\frac{\hbar\omega_z}{2} \sigma_z$$

① time evolution

$$\frac{\partial}{\partial t} |\psi\rangle = -\frac{i}{\hbar} H |\psi\rangle, \quad H = -\frac{\hbar\omega_z}{2} \sigma_z$$

$$\rightarrow \frac{\partial}{\partial t} \begin{pmatrix} \alpha \\ \beta \end{pmatrix} = -\frac{i}{\hbar} \left(-\frac{\hbar\omega_z}{2}\right) \begin{pmatrix} 1 & 0 \\ 0 & -1 \end{pmatrix} \begin{pmatrix} \alpha \\ \beta \end{pmatrix}$$

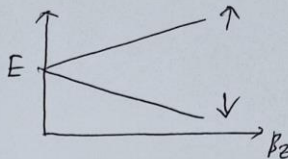
$$\rightarrow \begin{pmatrix} \dot{\alpha} \\ \dot{\beta} \end{pmatrix} = \begin{pmatrix} i \frac{\omega_z}{2} \alpha \\ -i \frac{\omega_z}{2} \beta \end{pmatrix}$$

$$\therefore \alpha(t) = e^{+i \frac{\omega_z}{2} t} \alpha(0), \quad \beta(t) = e^{-i \frac{\omega_z}{2} t} \beta(0)$$

\therefore process at ω_z

② Zeeman splitting

$\uparrow m_s = +\frac{1}{2}$
 $\downarrow m_s = -\frac{1}{2}$

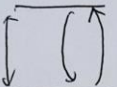


$$H = -\frac{\hbar\omega_L}{2} \sigma_z - \frac{\hbar\gamma}{2} B_z \sigma_z$$

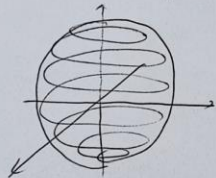
\therefore precess at $\omega_L + \gamma B_z$

"1/22" at $B_z = 100$ Gauss

③ Driving with $H_{\perp}(x, y)$

$E = \hbar\omega_L$  ω, Ω , $H = -\frac{\hbar\omega_L}{2} \sigma_z + \hbar\Omega \cos\omega t \sigma_x$

time evolution: $i\hbar \frac{d}{dt} \begin{pmatrix} \alpha \\ \beta \end{pmatrix} = \begin{pmatrix} -\frac{\hbar\omega_L}{2} \alpha \\ +\frac{\hbar\omega_L}{2} \beta \end{pmatrix} + \hbar\Omega \cos\omega t \begin{pmatrix} \beta \\ \alpha \end{pmatrix}$



at lab frame,

$\left\{ \begin{array}{l} \text{precess freq} \sim \omega_L(\omega) \text{ (fast)} \\ \uparrow \downarrow \text{ freq} \sim \Omega \text{ (slow)} \end{array} \right.$

Go into "rotating frame"

$$\begin{pmatrix} \alpha \\ \beta \end{pmatrix} = \begin{pmatrix} \tilde{\alpha} e^{+i\frac{\omega}{2}t} \\ \tilde{\beta} e^{-i\frac{\omega}{2}t} \end{pmatrix}$$

$$\rightarrow \underbrace{i\hbar \left(+i\frac{\omega}{2} \right)}_{= -\frac{\hbar\omega}{2}} \begin{pmatrix} \tilde{\alpha} e^{i\frac{\omega}{2}t} \\ -\tilde{\beta} e^{-i\frac{\omega}{2}t} \end{pmatrix} + i\hbar \begin{pmatrix} \tilde{\alpha} e^{i\frac{\omega}{2}t} \\ \tilde{\beta} e^{-i\frac{\omega}{2}t} \end{pmatrix}$$

$$\begin{aligned}
 (\cos \omega t) \rho &= \frac{1}{2} (e^{i\omega t} + e^{-i\omega t}) \tilde{\rho} \approx e^{-i\frac{\omega}{2}t} \\
 &= \frac{1}{2} (e^{i\frac{\omega}{2}t} + e^{-i\frac{3\omega}{2}t}) \tilde{\rho} \approx \frac{1}{2} e^{i\frac{\omega}{2}t} \tilde{\rho} \\
 &\approx_0 \quad \text{RWA (rotating wave approx.)}
 \end{aligned}$$

$$\rightarrow \approx -\frac{\hbar\omega_f}{2} \begin{pmatrix} \tilde{\alpha} e^{+i\frac{\omega}{2}t} \\ -\tilde{\beta} e^{-i\frac{\omega}{2}t} \end{pmatrix} + \frac{\hbar\Omega}{2} \begin{pmatrix} \tilde{\rho} e^{+i\frac{\omega}{2}t} \\ \tilde{\alpha} e^{-i\frac{\omega}{2}t} \end{pmatrix}$$

Cancel $e^{\pm i\frac{\omega}{2}t}$

$$\begin{aligned}
 \rightarrow i\hbar \begin{pmatrix} \dot{\tilde{\alpha}} \\ \dot{\tilde{\beta}} \end{pmatrix} &= -\left(\frac{\hbar\omega_f}{2} - \frac{\hbar\omega}{2}\right) \begin{pmatrix} \tilde{\alpha} \\ -\tilde{\beta} \end{pmatrix} + \frac{\hbar\Omega}{2} \begin{pmatrix} \tilde{\rho} \\ \tilde{\alpha} \end{pmatrix} \\
 &= -\frac{\hbar\delta}{2} \sigma_z \begin{pmatrix} \tilde{\alpha} \\ \tilde{\beta} \end{pmatrix} + \frac{\hbar\Omega}{2} \sigma_x \begin{pmatrix} \tilde{\alpha} \\ \tilde{\beta} \end{pmatrix}
 \end{aligned}$$

$(\delta \equiv \omega_f - \omega, \text{ detuning } \begin{array}{|c|} \hline \delta \\ \hline \omega_f \\ \hline \omega \\ \hline \end{array})$

$$= \tilde{H} \begin{pmatrix} \tilde{\alpha} \\ \tilde{\beta} \end{pmatrix}, \quad \tilde{H} = -\frac{\hbar\delta}{2} \sigma_z + \frac{\hbar\Omega}{2} \sigma_x$$

on resonance, $\delta = 0$

$$i\hbar \begin{pmatrix} \dot{\tilde{\alpha}} \\ \dot{\tilde{\beta}} \end{pmatrix} = \frac{\hbar\Omega}{2} \sigma_x \begin{pmatrix} \tilde{\alpha} \\ \tilde{\beta} \end{pmatrix}$$

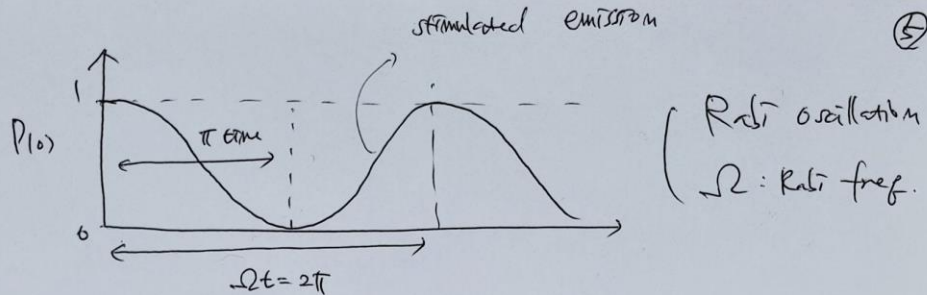
rotates around \hat{x} at freq $\frac{\hbar\Omega}{2}$

— $|1\rangle, P_{11}$

— $|0\rangle, P_{10}$

$$\langle \sigma_z \rangle = P_{10} - P_{11} = P_{10} - (1 - P_{10}) = 2P_{10} - 1$$

$$\therefore P_{10}(t) = \frac{1}{2} (1 + \langle \sigma_z \rangle) = \frac{1}{2} (1 + \cos \Omega t)$$



pulse

$\left\{ \begin{array}{l} \Omega \tau = \pi \quad : \quad \text{"}\pi\text{-pulse"} \\ \Omega \tau = \frac{\pi}{2} \quad : \quad \text{"}\frac{\pi}{2}\text{-pulse"} \end{array} \right.$

$\begin{array}{l} |0\rangle \xrightarrow{\frac{\pi}{2}} \frac{|0\rangle + |1\rangle}{\sqrt{2}} \\ |1\rangle \xrightarrow{\frac{\pi}{2}} \frac{|0\rangle - |1\rangle}{\sqrt{2}} \end{array} \rightarrow \frac{1}{\sqrt{2}} \begin{pmatrix} 1 & 1 \\ 1 & -1 \end{pmatrix} \begin{pmatrix} |0\rangle \\ |1\rangle \end{pmatrix}$

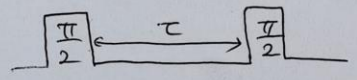
$\equiv H$ (Hadamard gate)

"A23"

④ Ramsey interferometry (DC field sensing)

$$H = -\frac{\hbar \omega_L}{2} \sigma_z - \frac{\hbar \delta}{2} B_z \sigma_x$$

rotating frame \rightarrow $\tilde{H} = -\left(\frac{\hbar \delta}{2} + \frac{\hbar \delta}{2} B_z\right) \sigma_x$ "A24 - Ramsey"



cf)

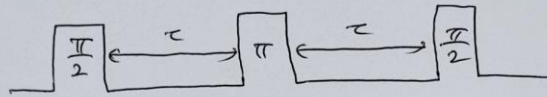
$\begin{array}{l} |0\rangle \\ |1\rangle \end{array} \xrightarrow{\frac{\pi}{2}} \frac{|0\rangle + |1\rangle}{\sqrt{2}}$ (pi-pulse)

insert material with m and $\delta \rightarrow$

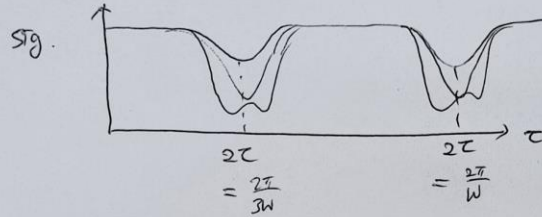
$\begin{array}{l} \text{cf) } \delta=0, B_z=0 \\ \text{cf) } \delta \neq 0, B_z=0 \\ \text{cf) } \delta \neq 0, B_z \neq 0 \end{array}$

⑤ (SPM) Hahn echo (AC field sensing)

$$\tilde{H} = -\frac{\hbar\omega}{2}\sigma_z - \frac{\hbar\gamma}{2}\beta_z \sin(\omega t + \phi)\sigma_z$$

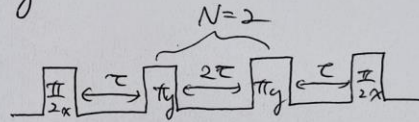


"Art-echo"

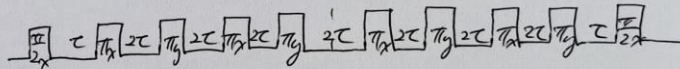


⑥ Dynamical decoupling

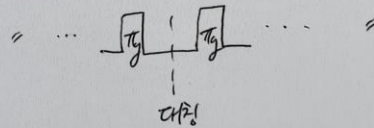
• CPMG (-N)
(Car-Purcell-Meiboom-Gill)



• XT-4



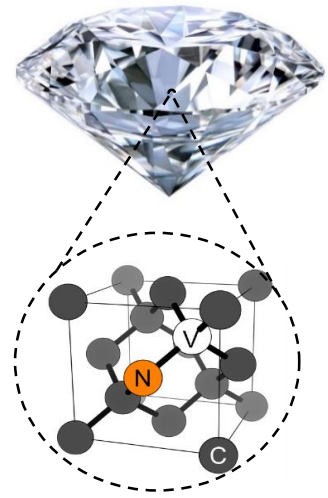
• XT-8



Part 2 : 다이아몬드 NV 센터 소개



Nitrogen-vacancy (NV) defect centers in diamond



Quantum Point Defects (QPDs)

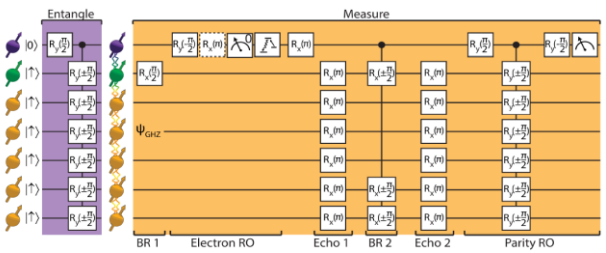
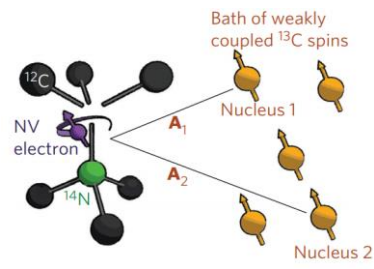
“trapped ions” in solids

- long coherence time
- atomic size
- optically addressable
- room temperature operation

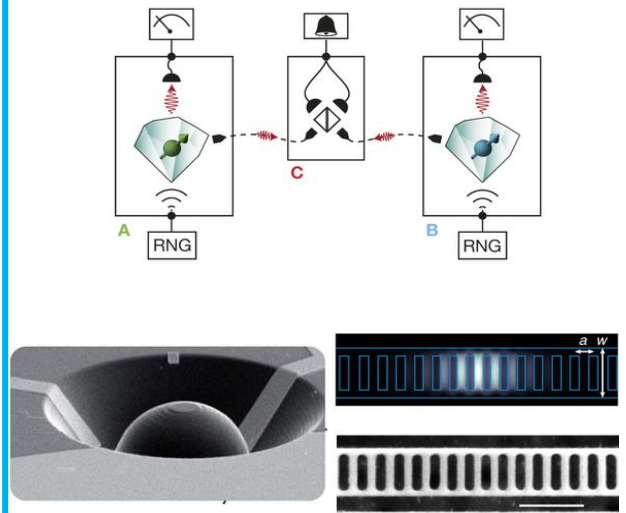
defects in semiconductors

- fast manipulation
- nano fabrication
- scalable
- integrated, devices on-chip

Quantum computation



Quantum communication



Quantum sensing

Microscope objective

Diamond tip

NV e spin

RF

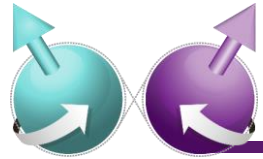
30 nm

5 μm

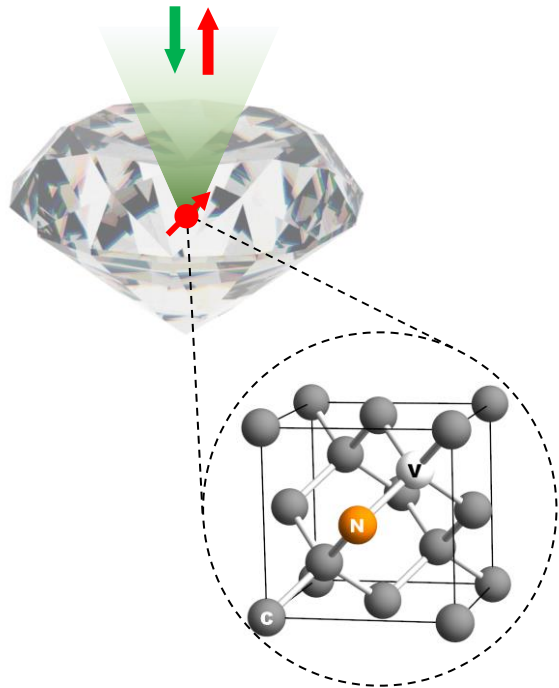
5 μm

Normalized $f(F_2^T)$

Chemical shift (ppm)

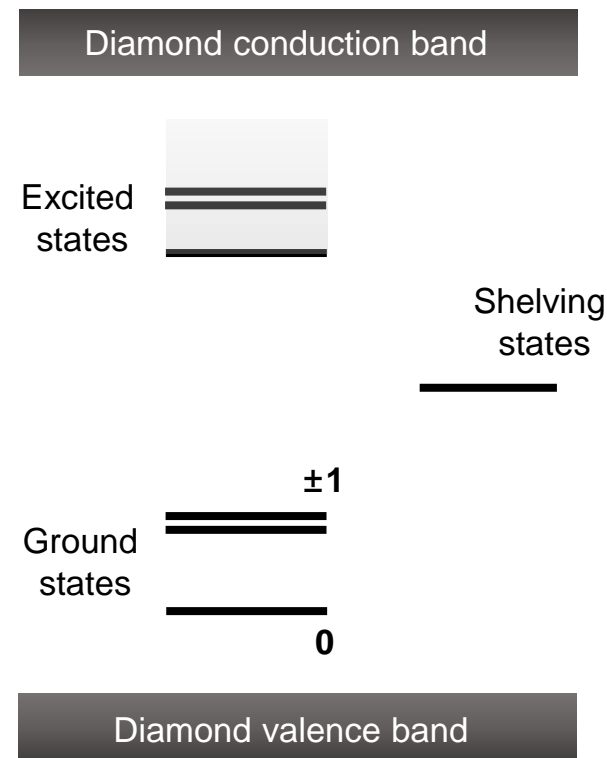
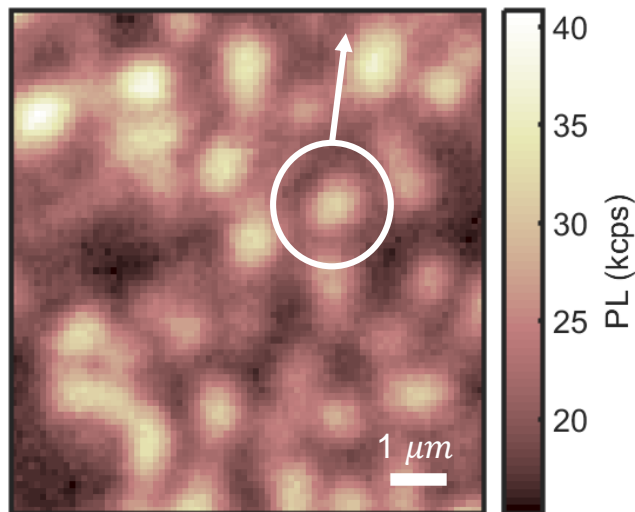


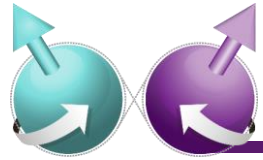
Nitrogen-vacancy (NV) defect centers in diamond



NV defect centers in diamond

- $S = 1$ ground states i.e. $m_s = 0, m_s = \pm 1$
- Spin levels are very sensitive to external magnetic field
- Magnetic signal is optically detected (ODMR)

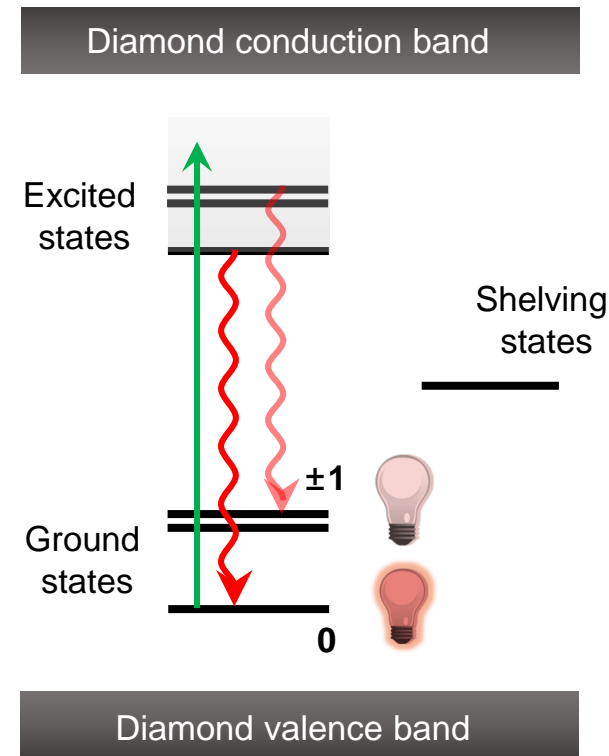
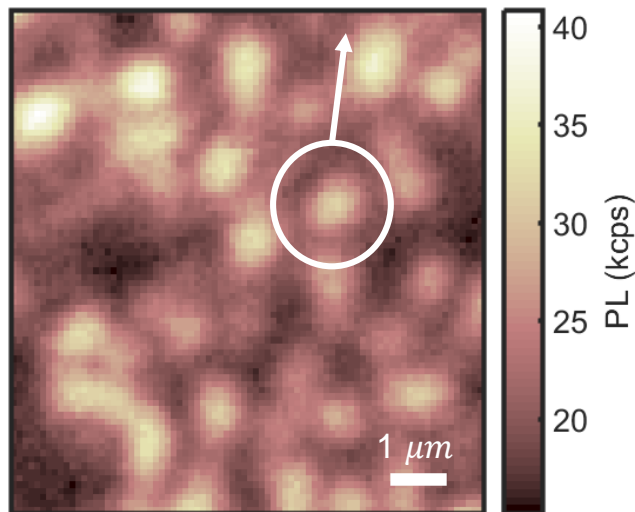
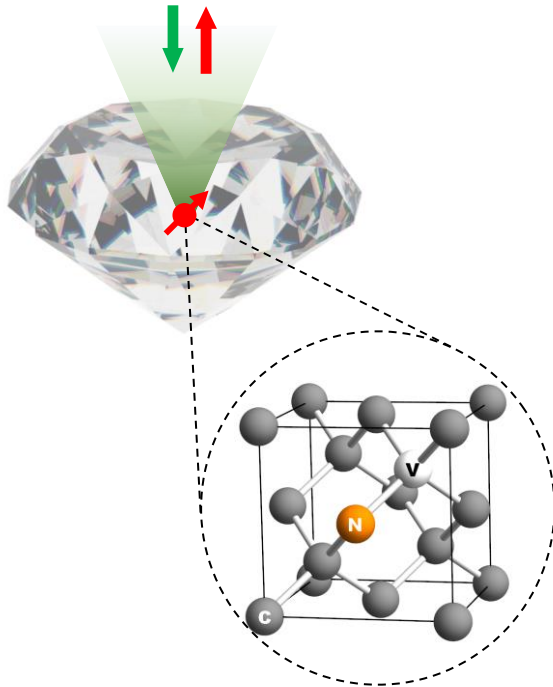


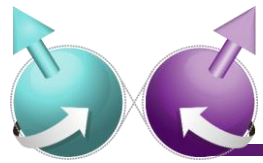


Nitrogen-vacancy (NV) defect centers in diamond

NV defect centers in diamond

- $S = 1$ ground states i.e. $m_s = 0$, $m_s = \pm 1$
- Spin levels are very sensitive to external magnetic field
- Magnetic signal is optically detected (ODMR)

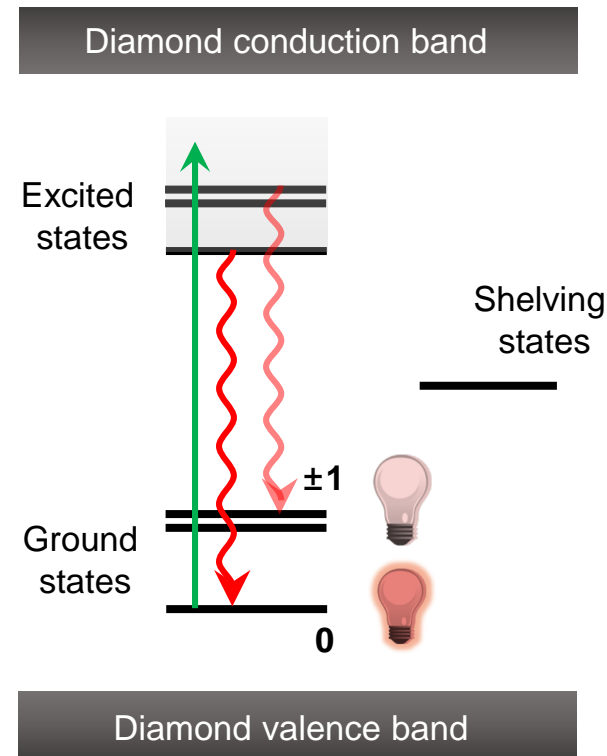
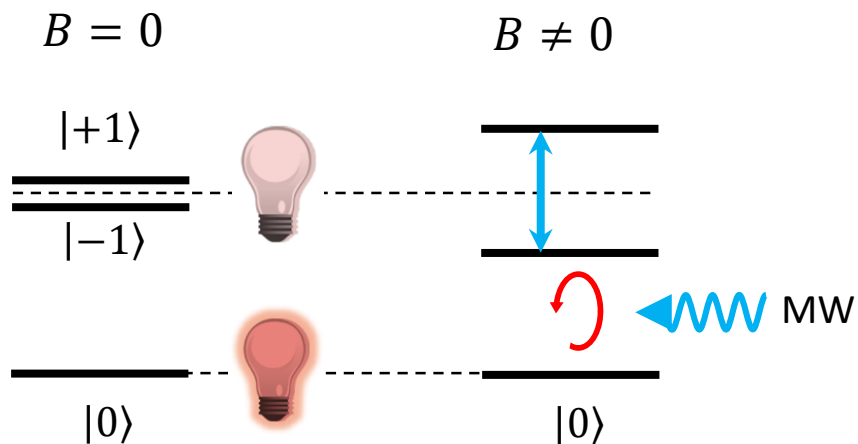


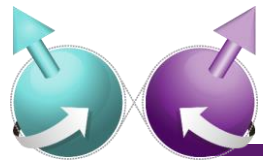


Nitrogen-vacancy (NV) defect centers in diamond

NV defect centers in diamond

- $S = 1$ ground states i.e. $m_s = 0$, $m_s = \pm 1$
- Spin levels are very sensitive to external magnetic field
- Magnetic signal is optically detected (ODMR)



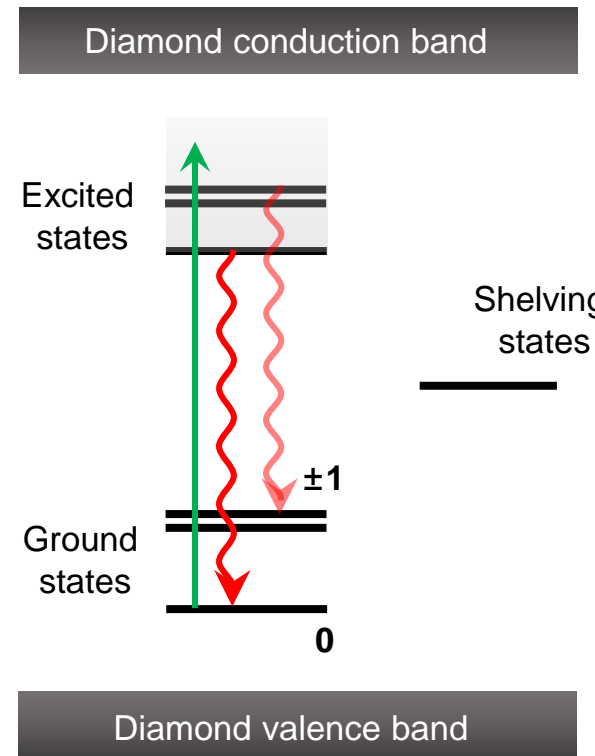
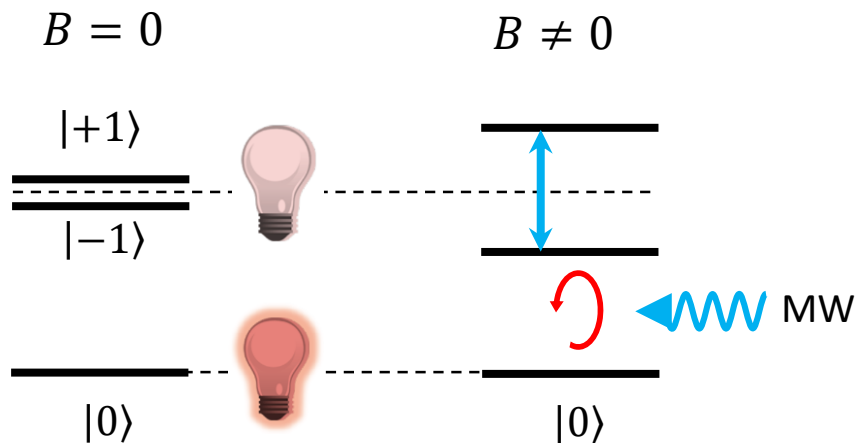
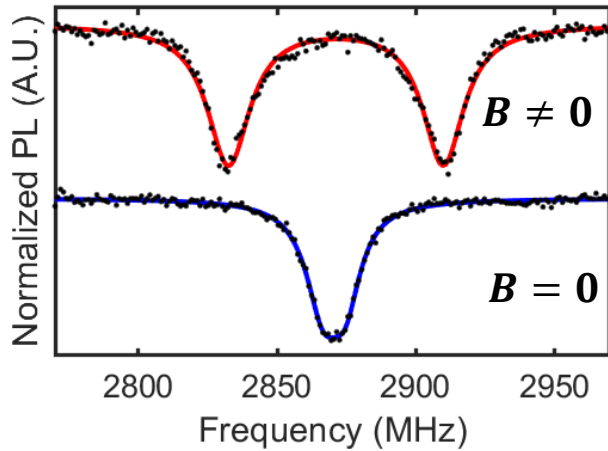


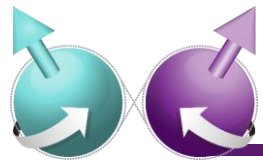
Nitrogen-vacancy (NV) defect centers in diamond

NV defect centers in diamond

- $S = 1$ ground states i.e. $m_s = 0$, $m_s = \pm 1$
- Spin levels are very sensitive to external magnetic field
- Magnetic signal is optically detected (ODMR)

Optically-detected ESR



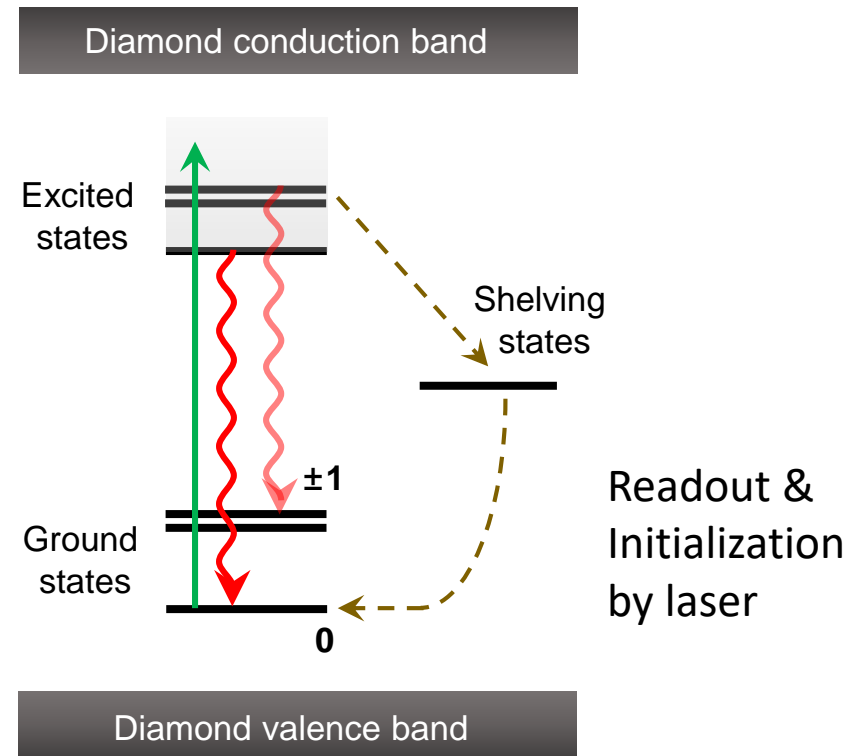
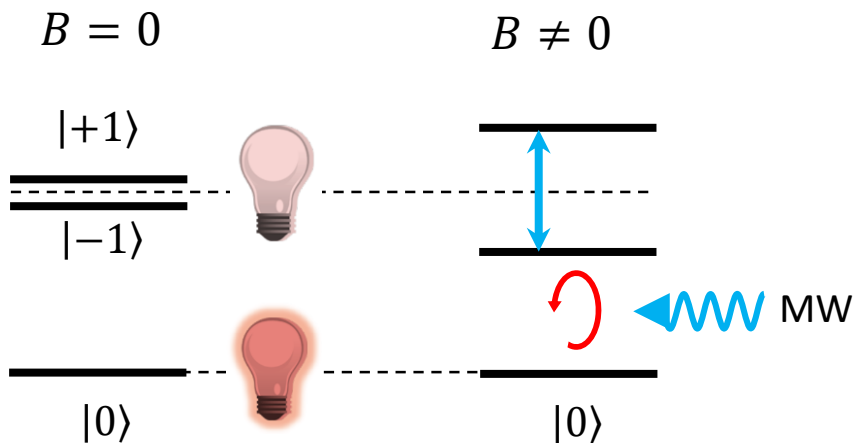
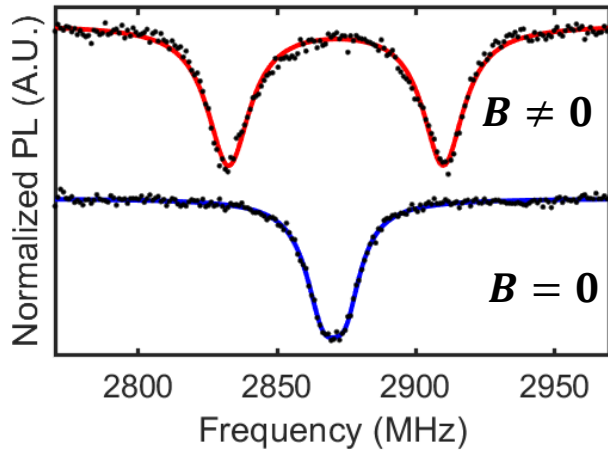


Nitrogen-vacancy (NV) defect centers in diamond

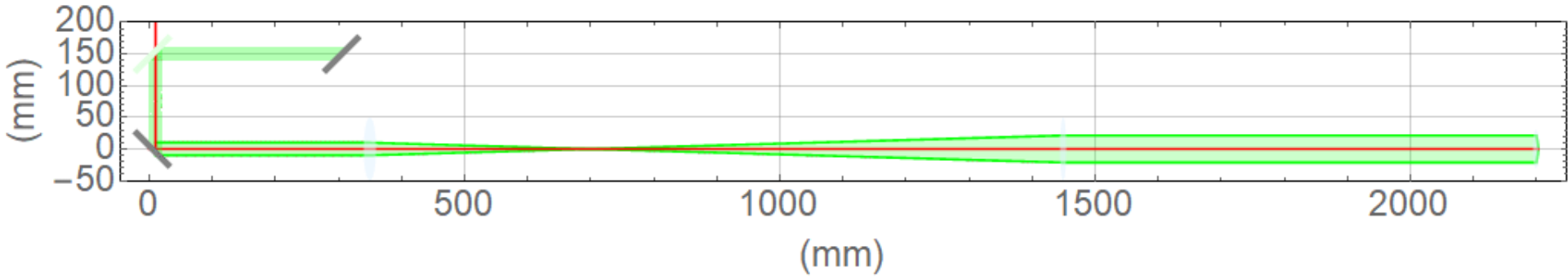
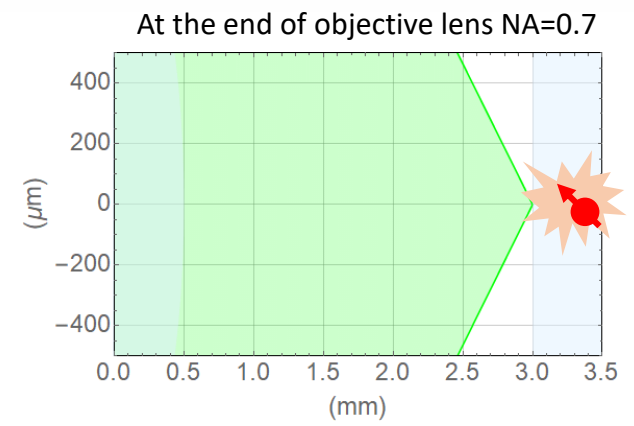
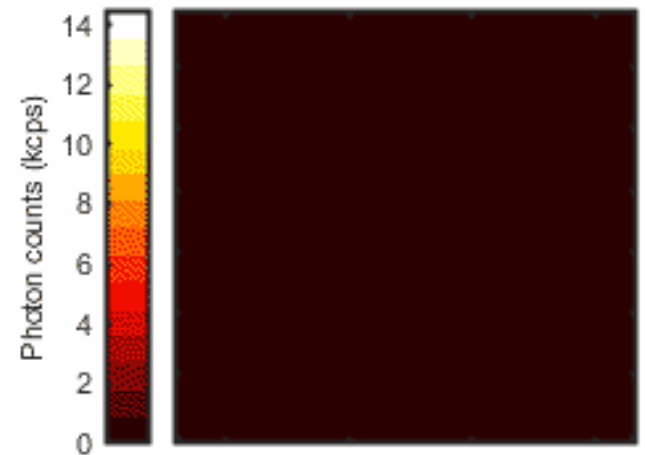
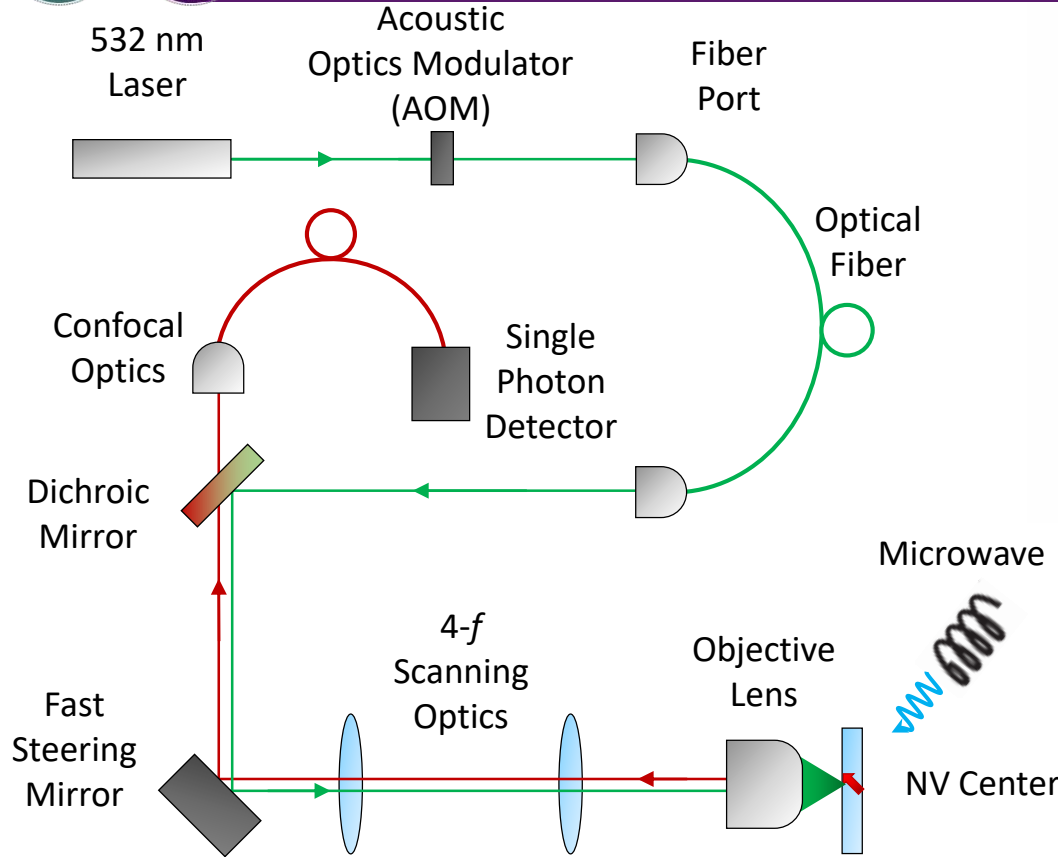
NV defect centers in diamond

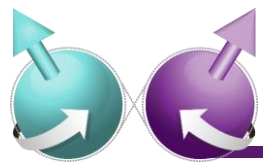
- $S = 1$ ground states i.e. $m_s = 0, m_s = \pm 1$
- Spin levels are very sensitive to external magnetic field
- Magnetic signal is optically detected (ODMR)

Optically-detected ESR



Experimental confocal optics setup

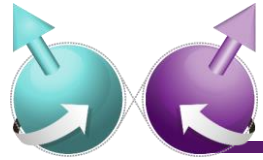




Sensitivity of diamond NV center

Physical property	Sensitivity	Physical property	Sensitivity	References	
Magnetic field	$< 1 \text{ nT/Hz}^{1/2}$ (single NV) $< 1 \text{ pT/Hz}^{1/2}$ (ensemble)	Temperature	$< 1 \text{ mK/Hz}^{1/2}$	J. Taylor et al., Nat. Phys. 2008 T. Wolf et al., PRX 2015 F. Dolde et al., PRL 2014 K. Lee et al., PR Applied 2016 G. Kuscko et al., Nature 2013 A. Ajoy et al., PRA 2012 M. Doherty et al., PRL 2014 R. Schirhagl et al., Ann. Rev. Phys. Chem. 2014	
Electric field	$< 100 \text{ Vcm}^{-1}/\text{Hz}^{1/2}$	Rotation	$< 1 \text{ mdeg /Hz}^{1/2}$		
Strain field	$< 10^{-7}/\text{Hz}^{1/2}$	Pressure	$< 0.1 \text{ MPa/Hz}^{1/2}$		
Spatial resolution	$\sim 10 \text{ nm}$	Detection bandwidth	DC – GHz	Operating temperature	Sub K to RT
Other advantages	<ul style="list-style-type: none"> chemically stable, non-toxic and bio-friendly optically stable (free from photobleaching) suitable for devices (nano fabrication) 				

Part 3 : NV 센터 기반 양자센싱 및 이미징 연구 소개



Quantum sensing examples

Static magnetism

Domain wall

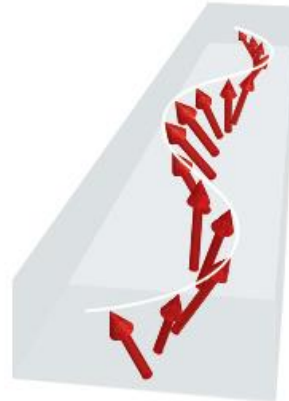


Skyrmion

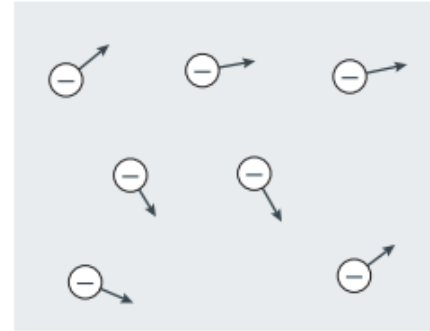


Magnetic excitations

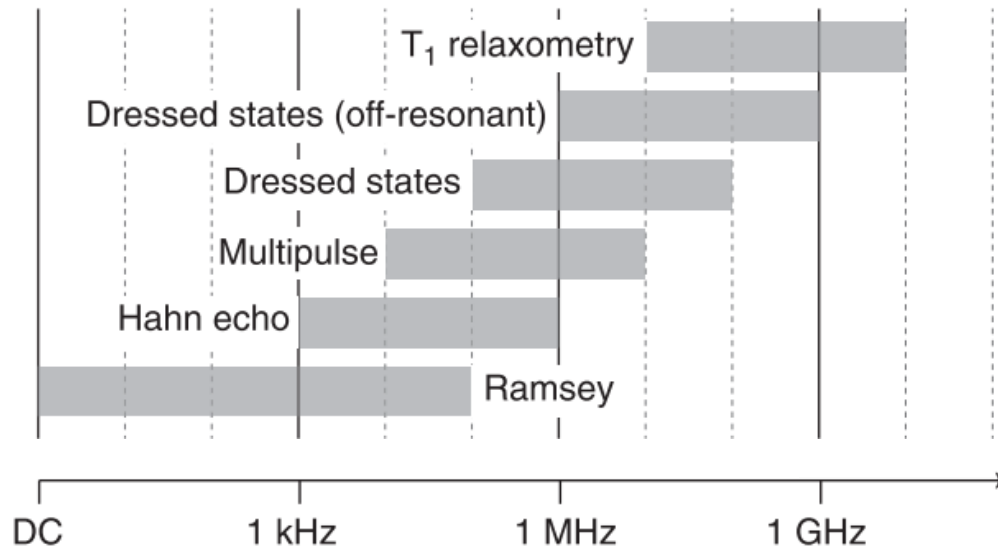
Spin wave



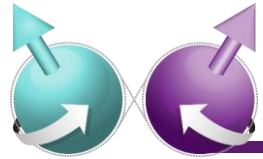
Noise currents



F. Casola *et al.*, Nat. Rev. Mater. (2018)



C. Degen *et al.*, Rev. of Mod. Phys. (2017)



Quantum sensing examples

Static magnetism

Domain wall



Skyrmion

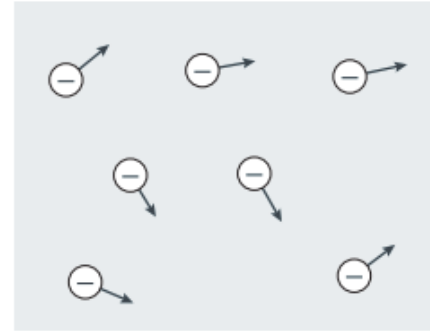


Magnetic excitations

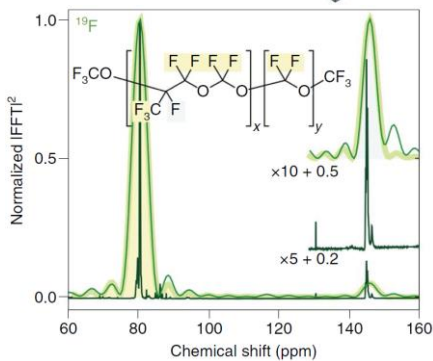
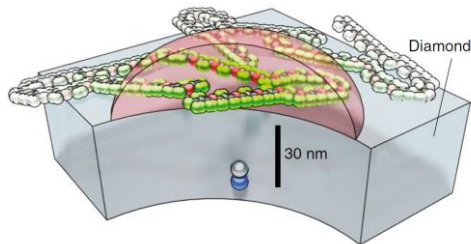
Spin wave



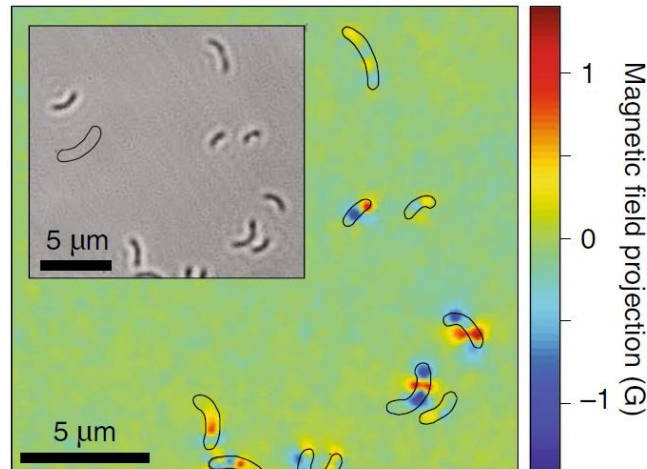
Noise currents



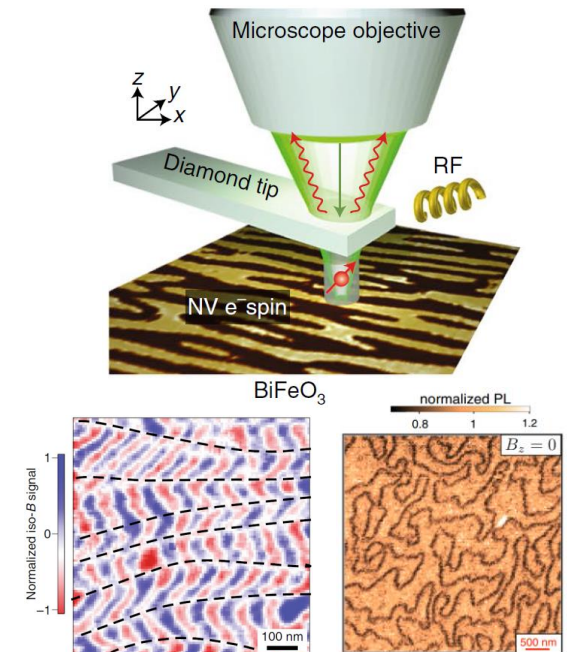
F. Casola *et al.*, Nat. Rev. Mater. (2018)



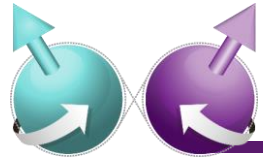
N. Aslam *et al.* Science 2017



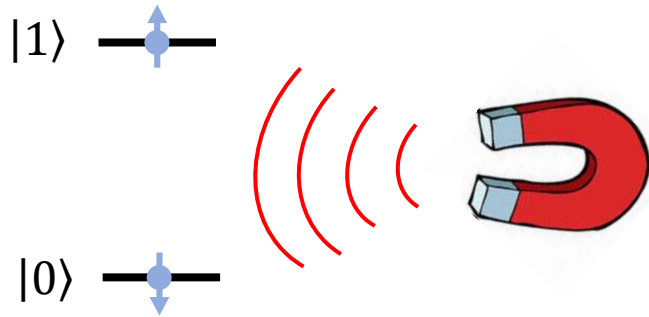
Le Sage *et al.* Nature 2013



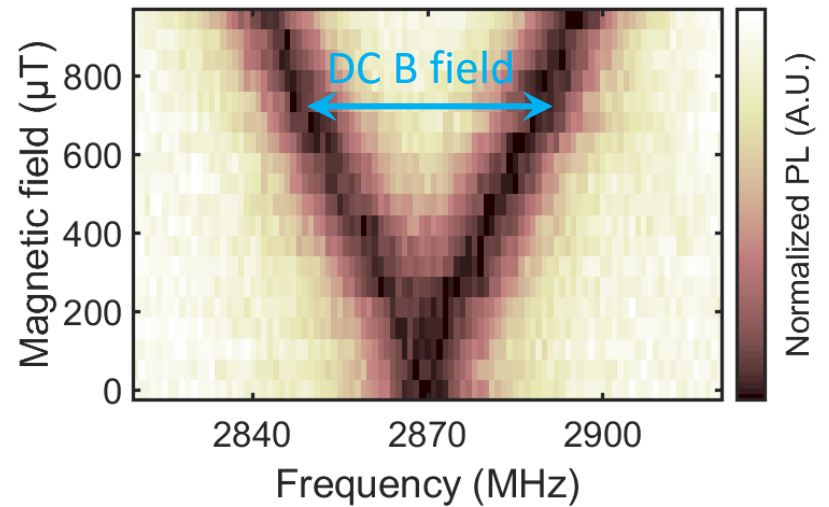
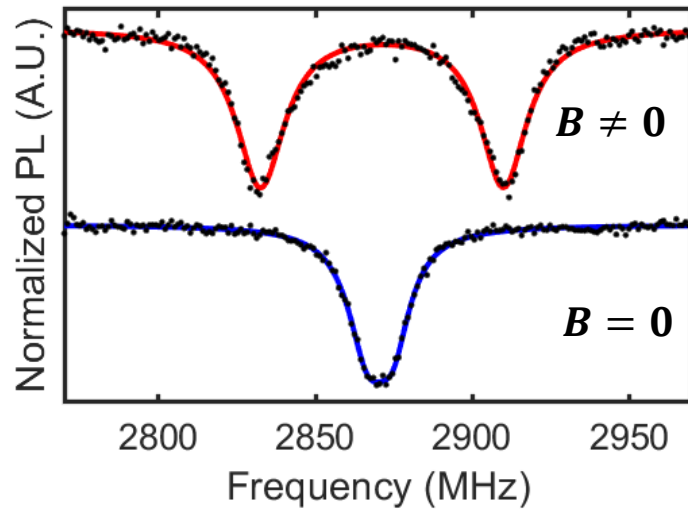
I. Gross *et al.* Nature 2017

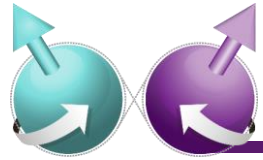


Sensing static (DC) B field

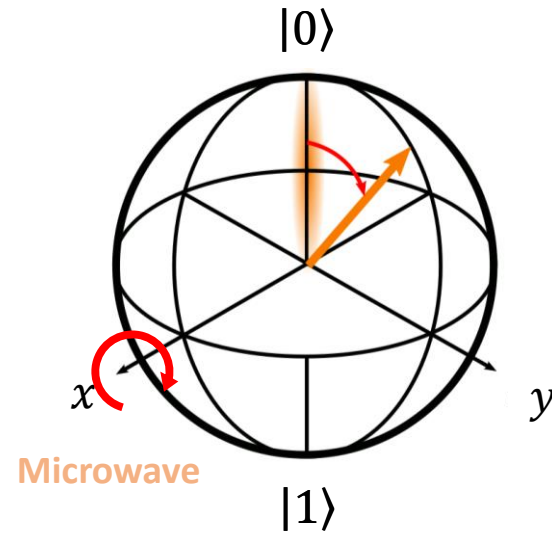
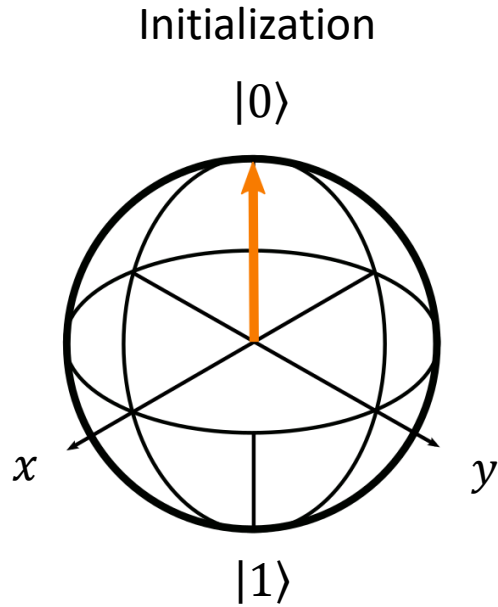
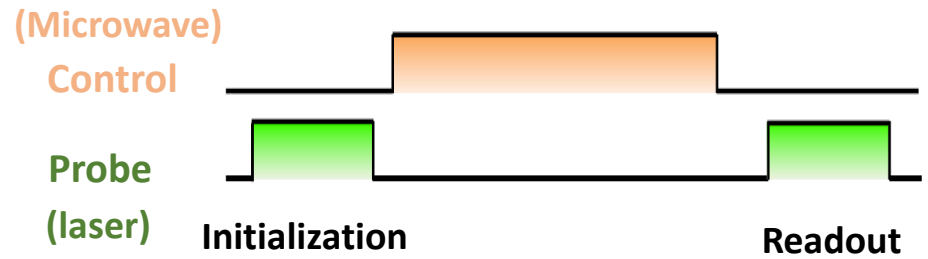
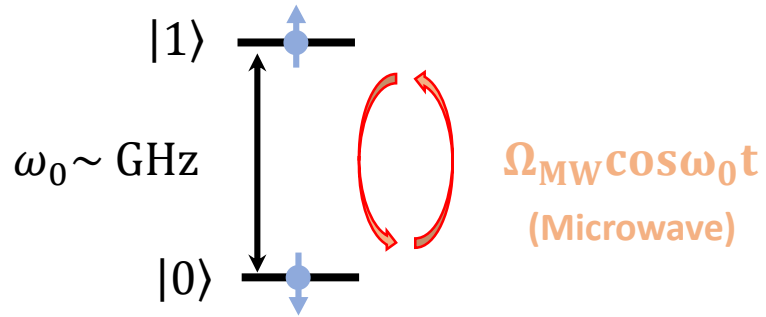


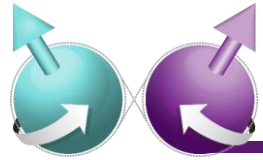
Optically-detected ESR



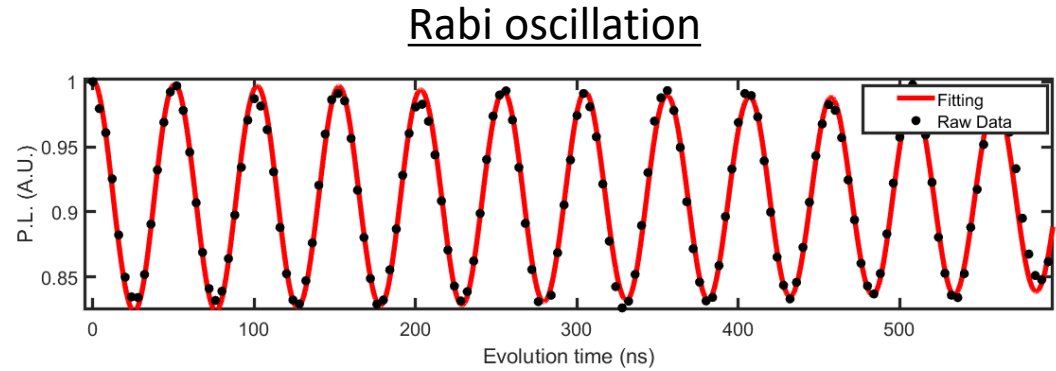
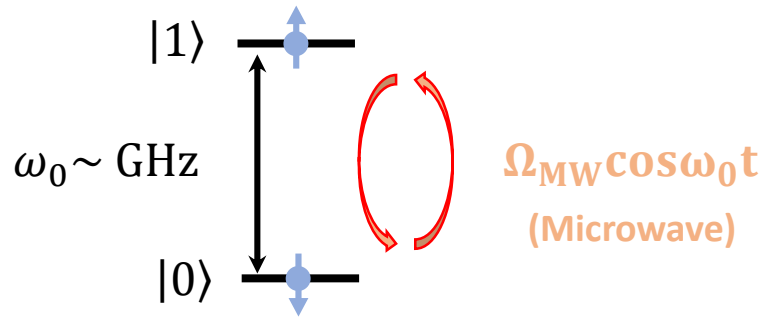


Sensing static (DC) B field

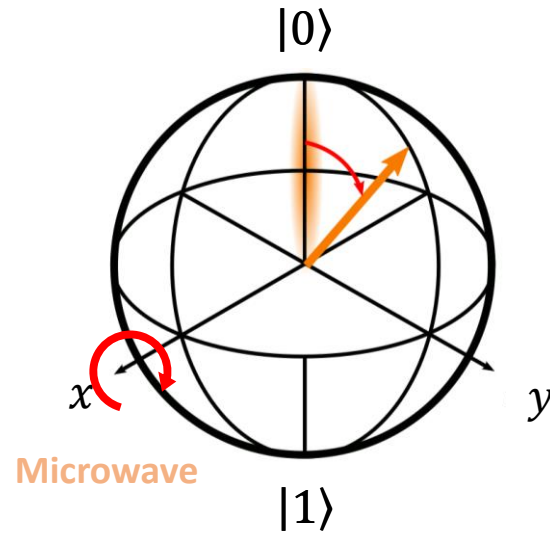
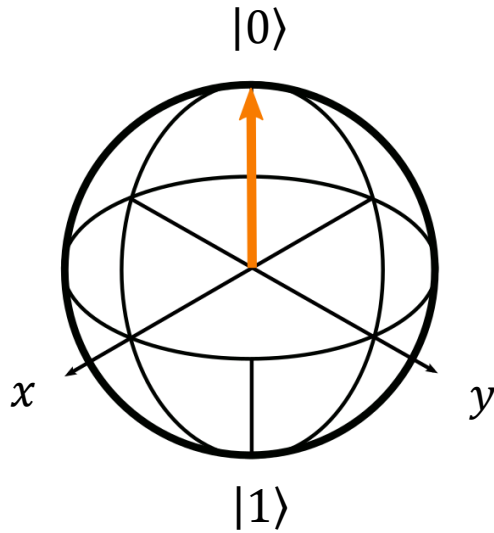


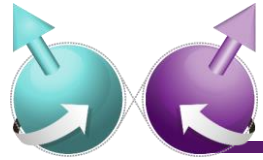


Sensing static (DC) B field

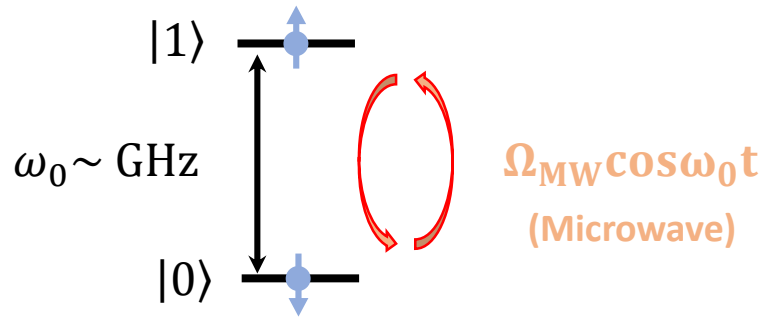


Initialization

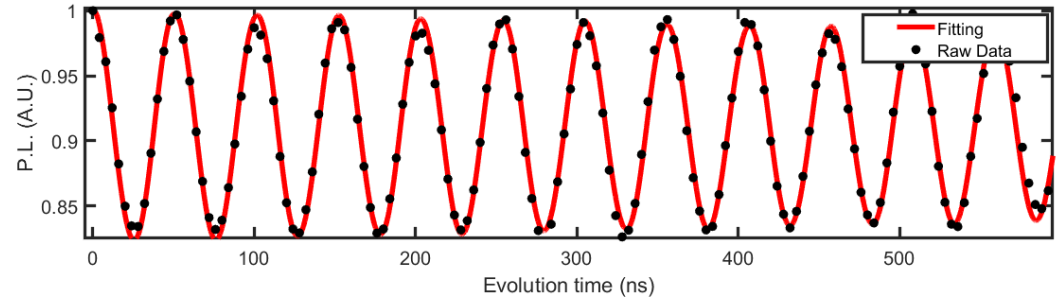




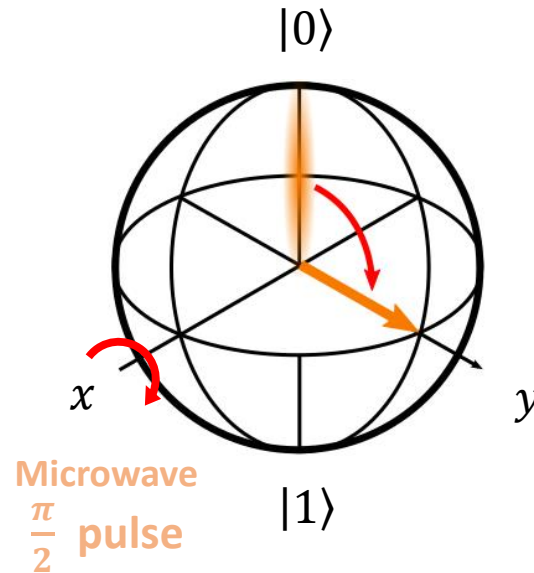
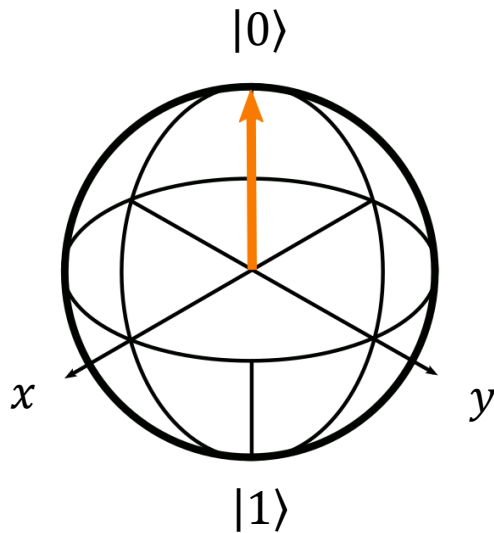
Sensing static (DC) B field



Rabi oscillation

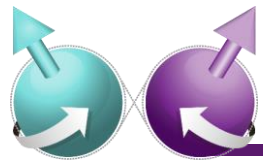


Initialization



$$|\psi\rangle = \frac{1}{\sqrt{2}} (|0\rangle + |1\rangle)$$



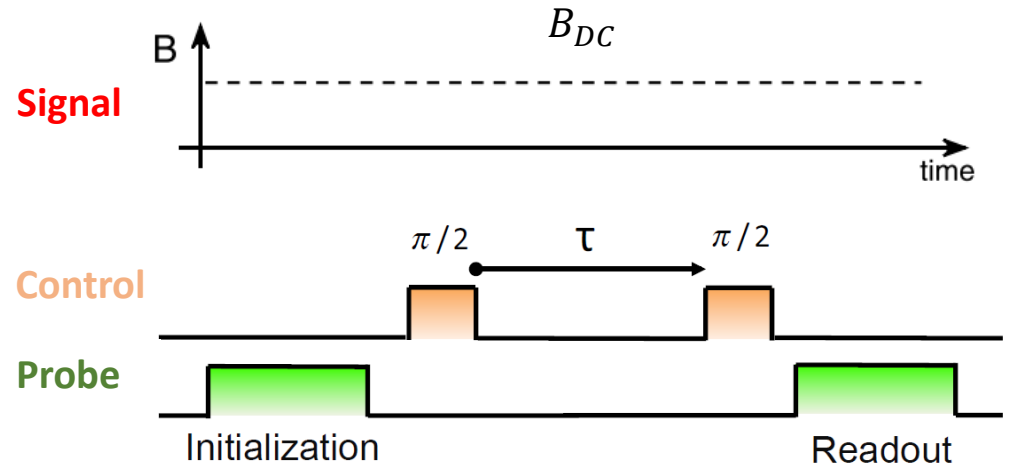


Sensing static (DC) B field

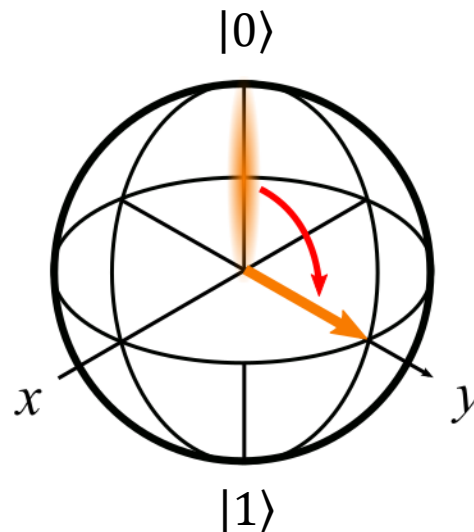
Ramsey Interferometry

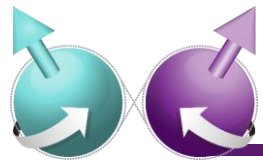
$|1\rangle$ ———

$|0\rangle$ ———



$$|\psi\rangle = \frac{1}{\sqrt{2}} (|0\rangle + |1\rangle)$$



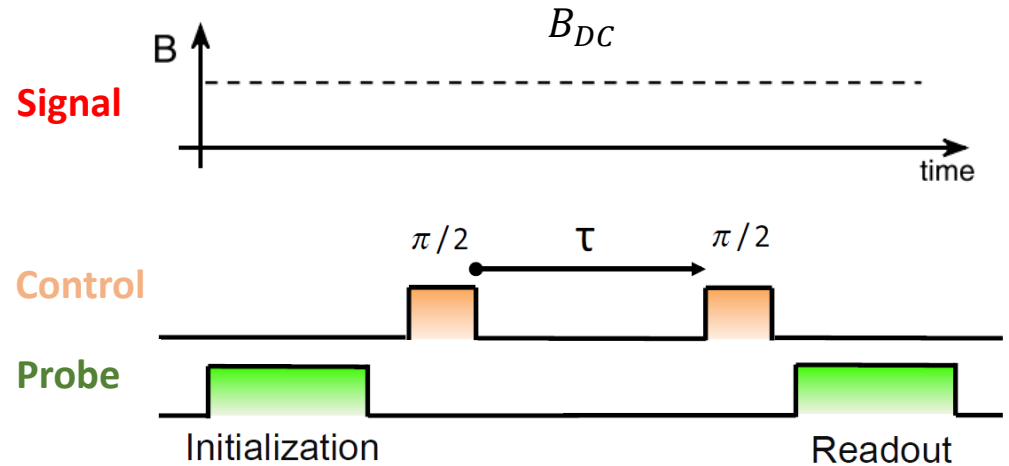


Sensing static (DC) B field

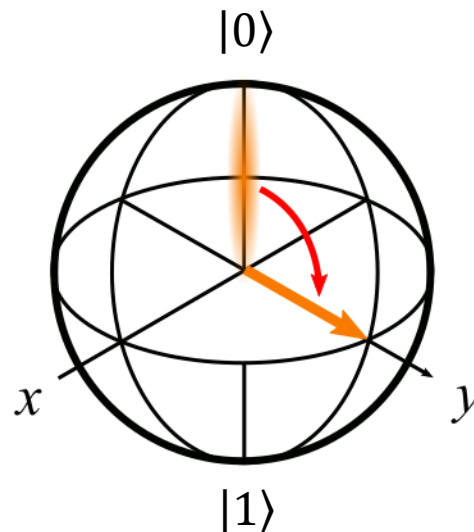
Ramsey Interferometry

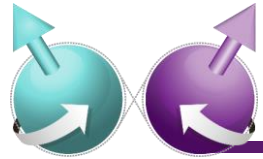
$|1\rangle$ ———

$|0\rangle$ ———



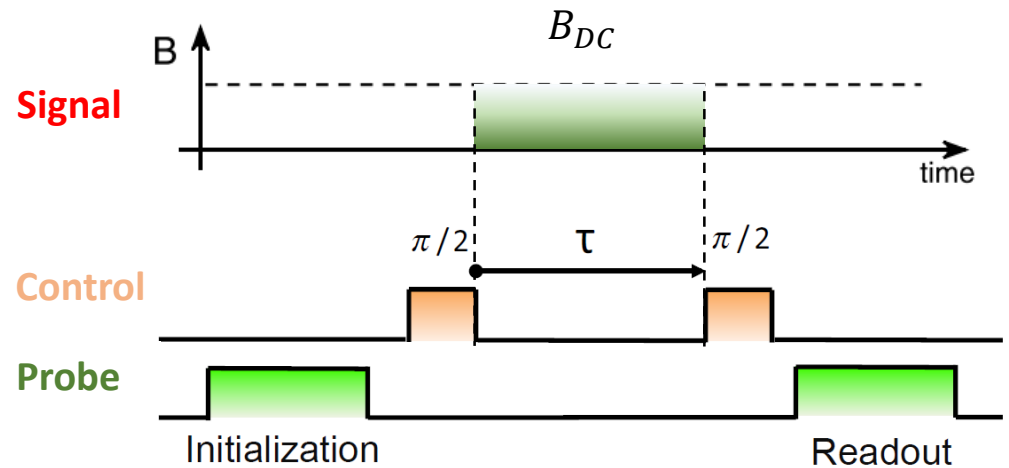
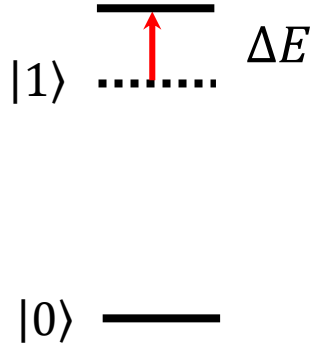
$$|\psi\rangle = \frac{1}{\sqrt{2}} (|0\rangle + |1\rangle)$$



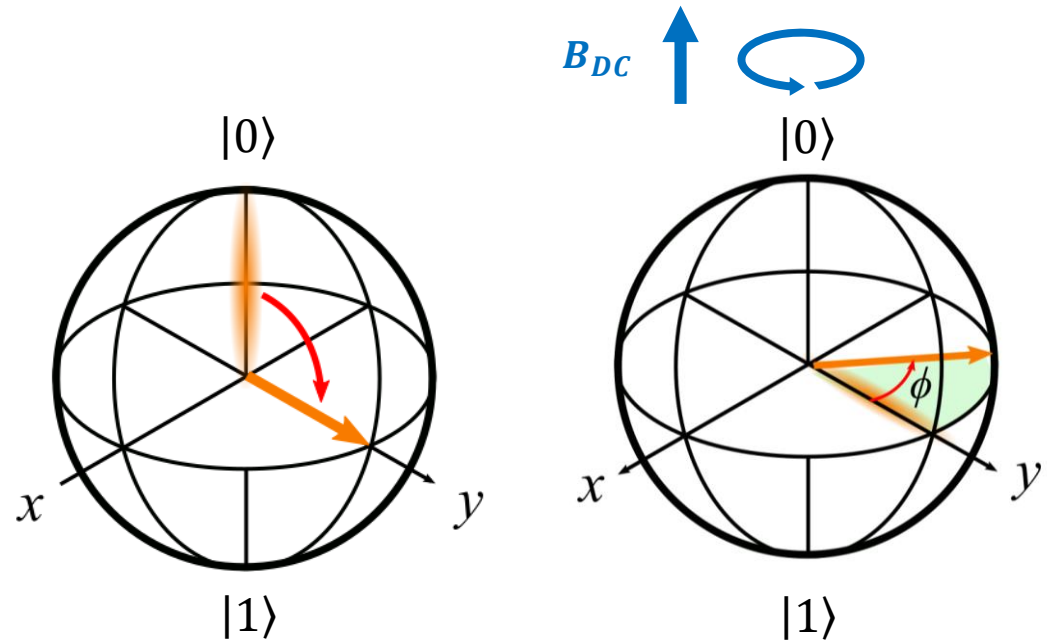


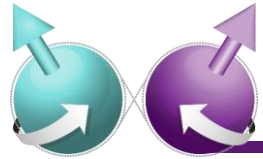
Sensing static (DC) B field

Ramsey Interferometry

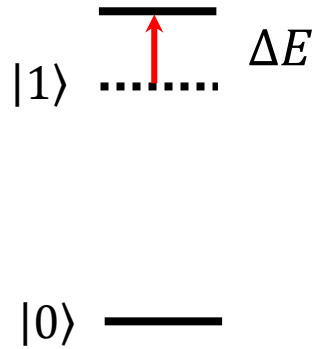


$$|\psi\rangle = \frac{1}{\sqrt{2}} (|0\rangle + e^{i\phi} |1\rangle)$$

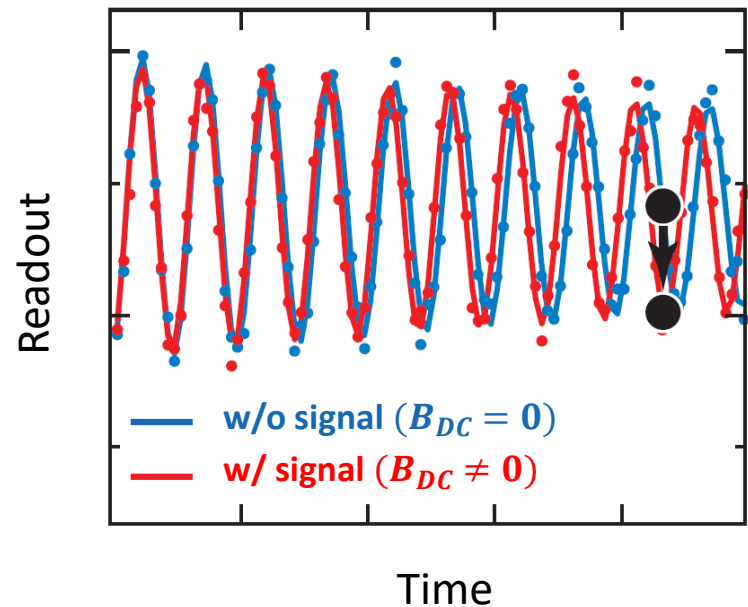
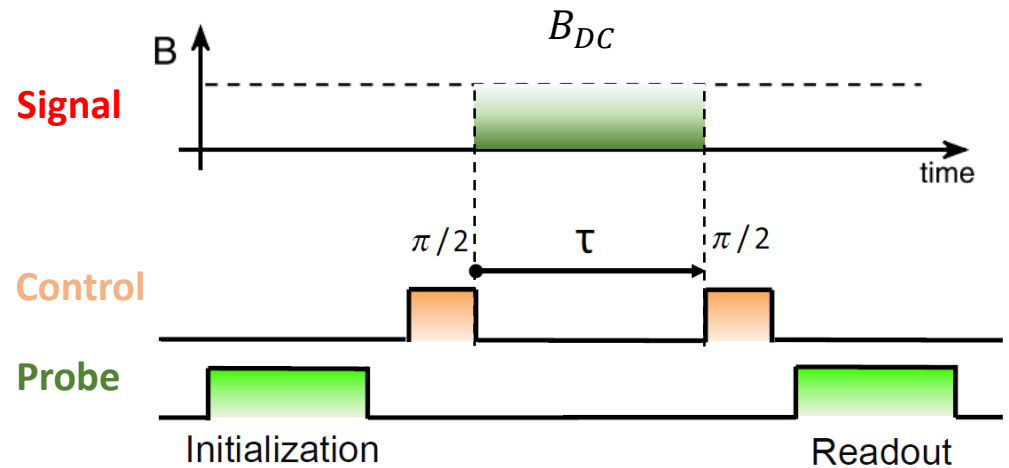


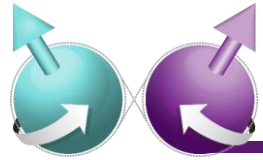


Sensing static (DC) B field

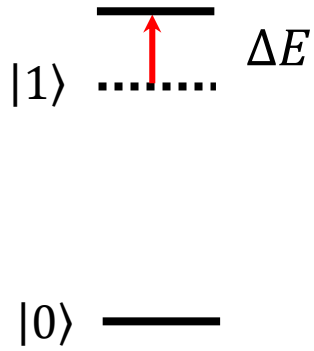


Ramsey Interferometry

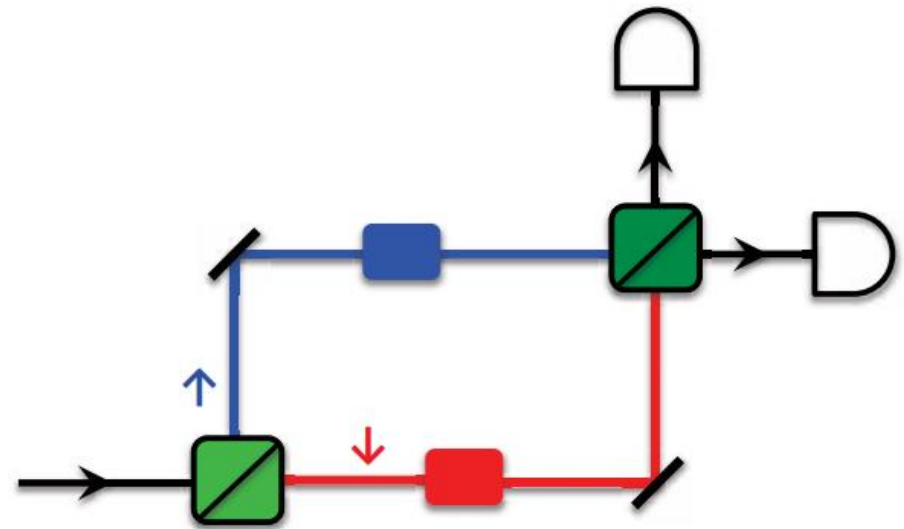
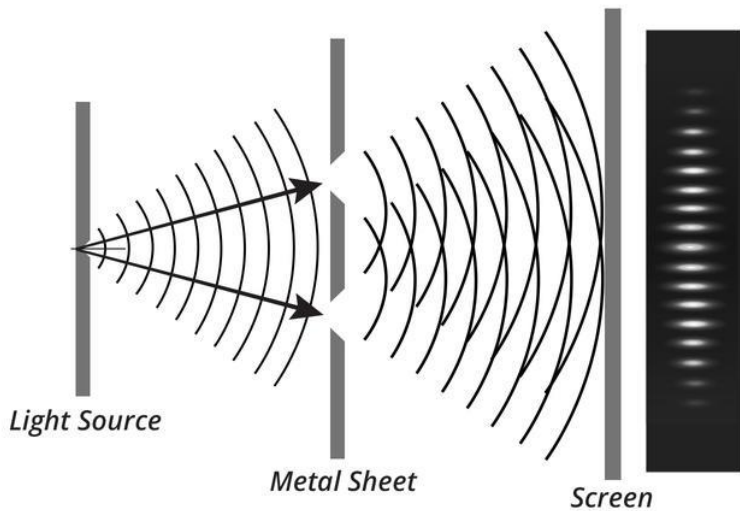
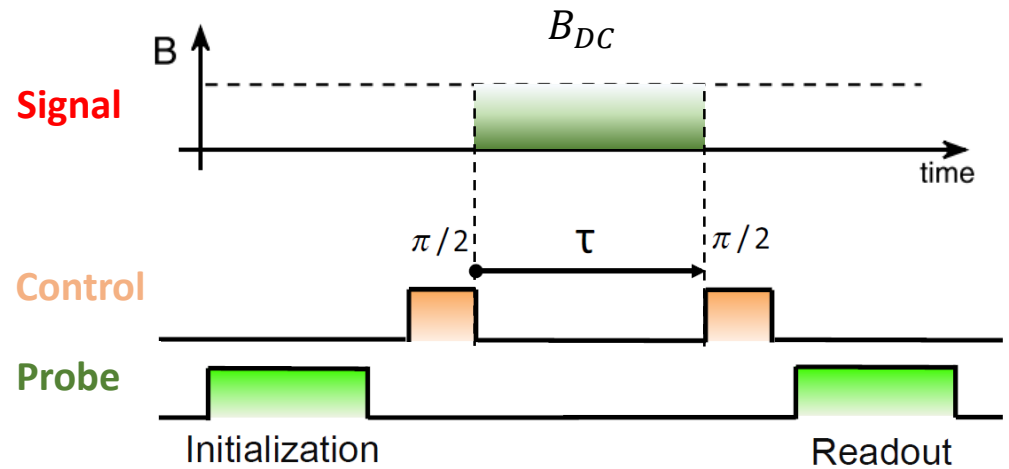


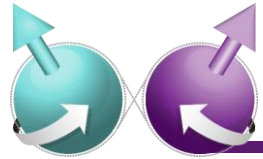


Sensing static (DC) B field

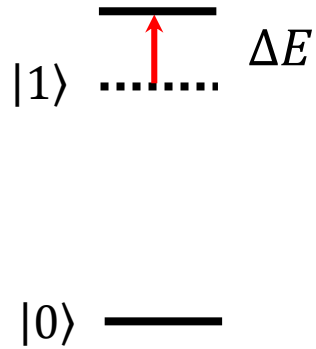


Ramsey Interferometry

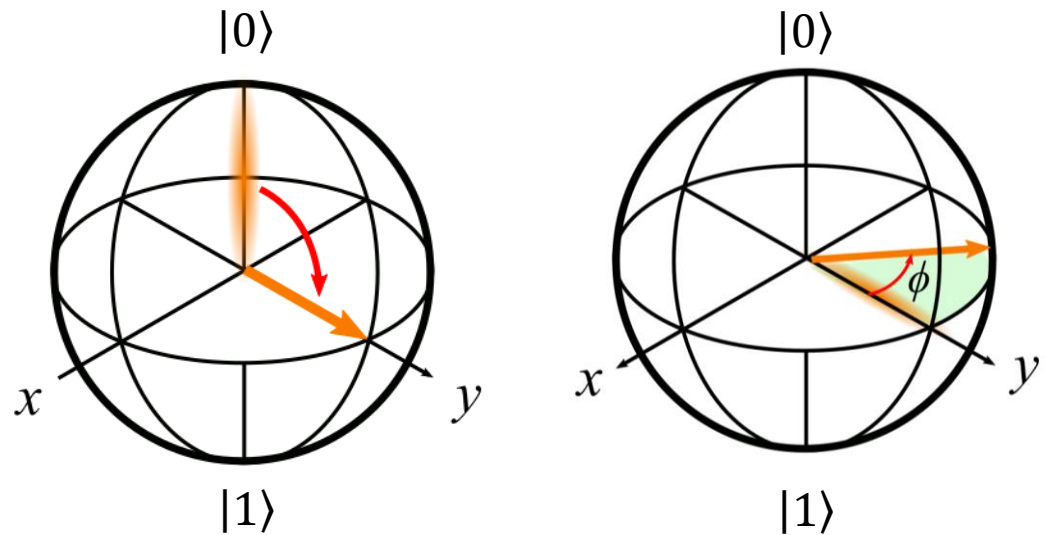
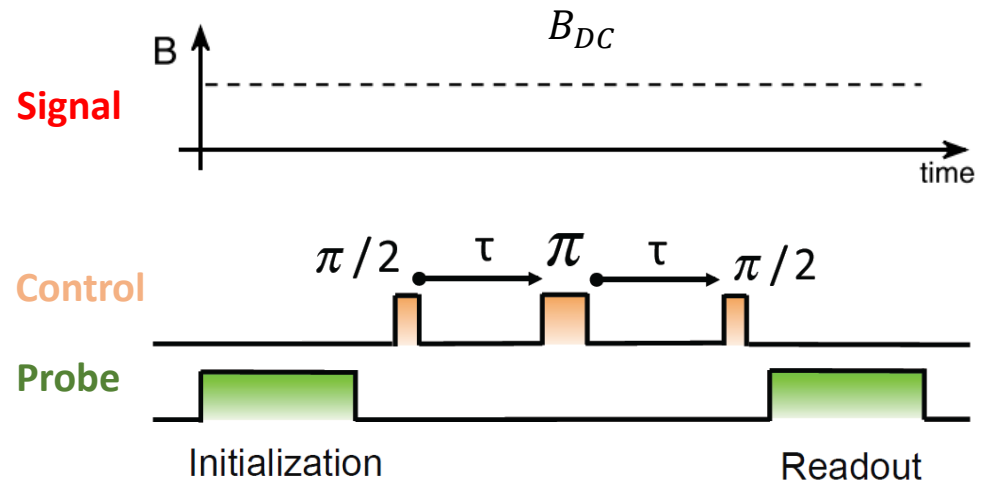


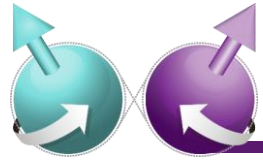


Sensing dynamics (AC) B field

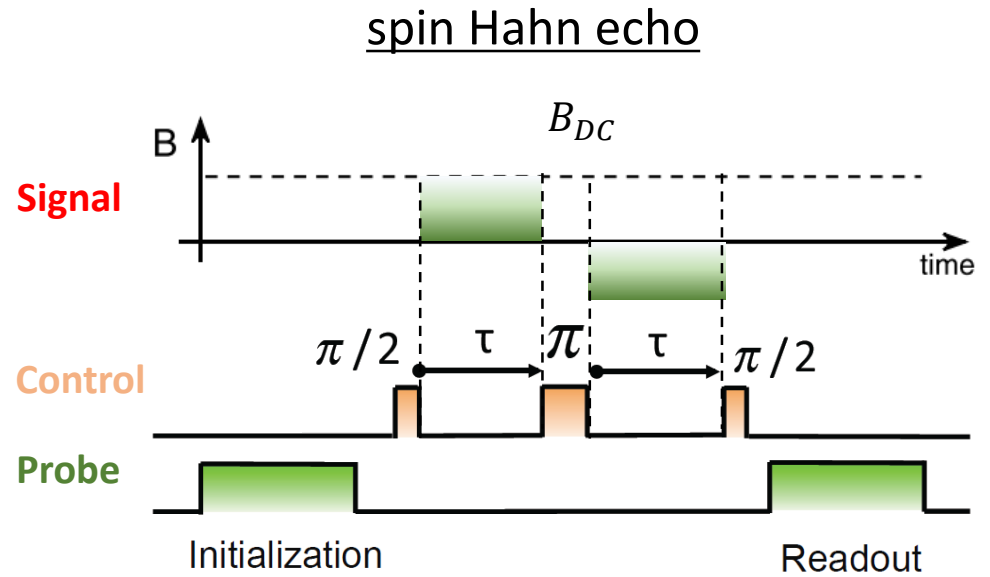
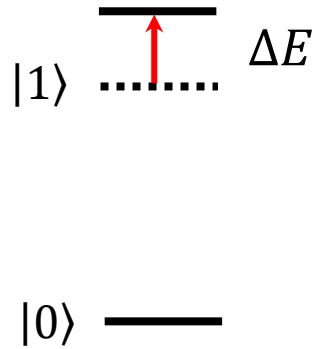


spin Hahn echo



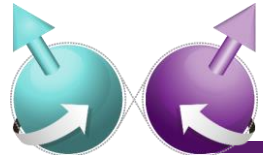


Sensing dynamics (AC) B field

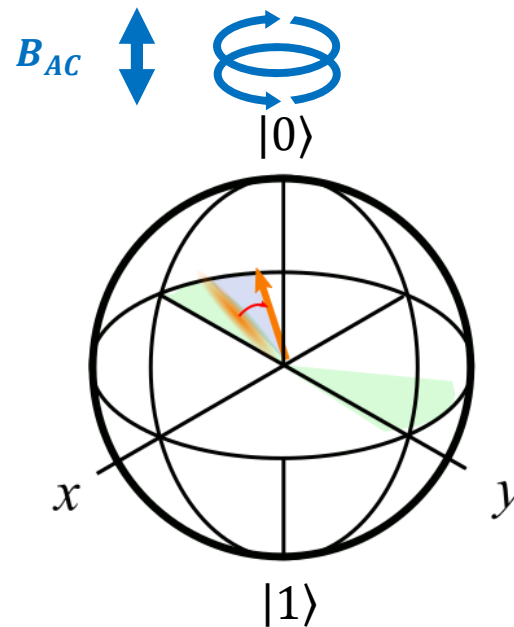
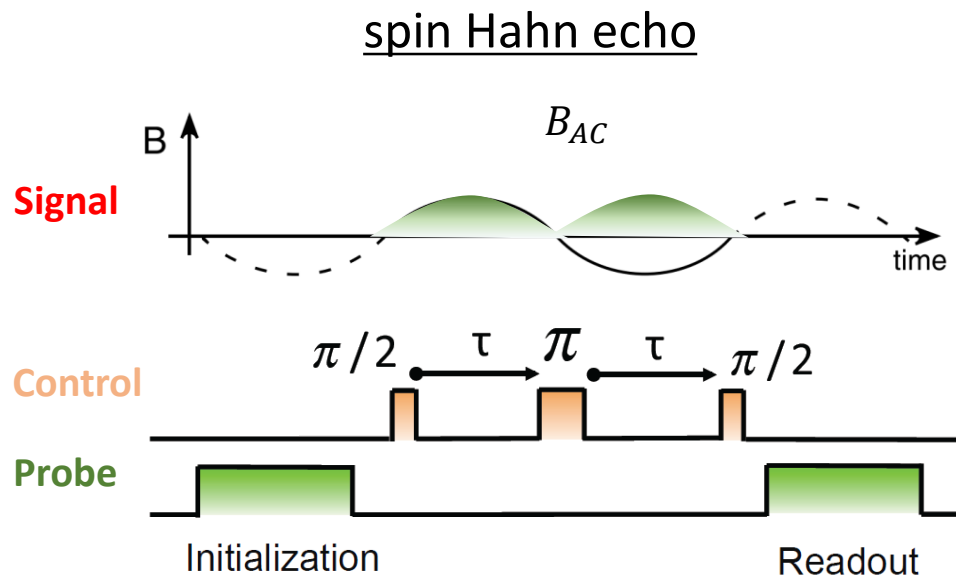
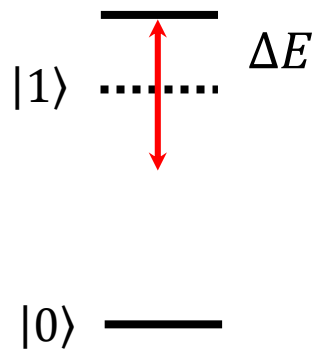


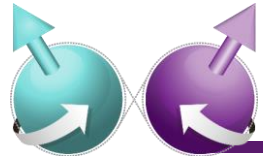
$$\phi = \phi_1 - \phi_2 = 0$$

for DC signal

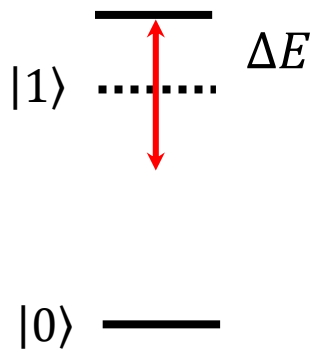


Sensing dynamics (AC) B field

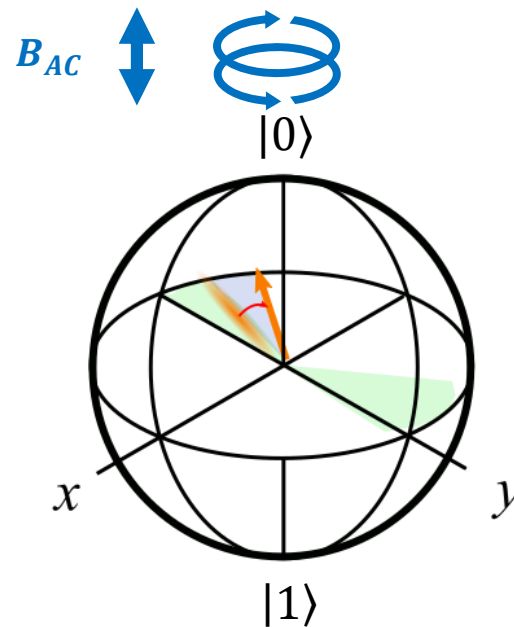
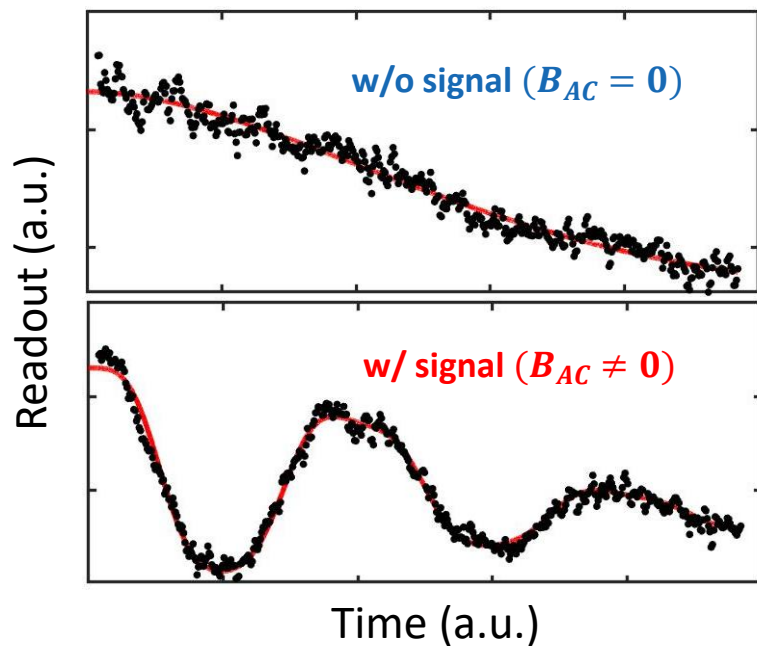
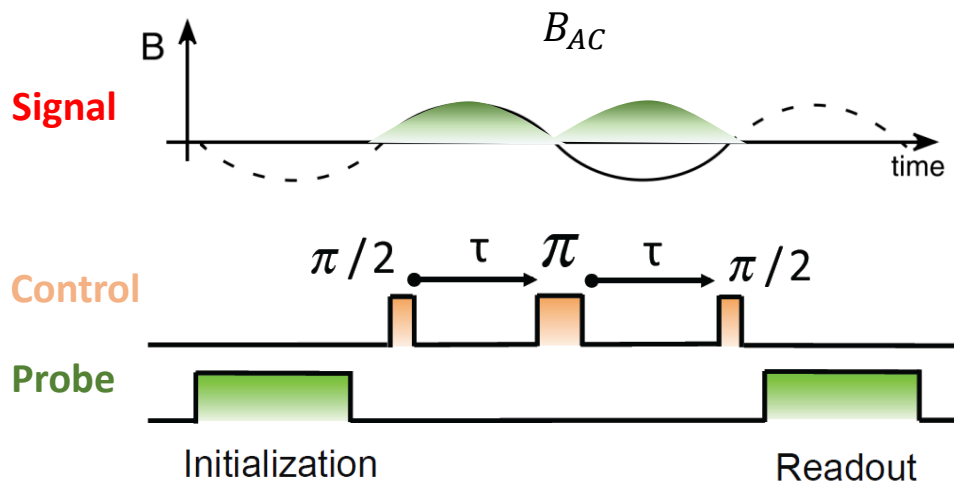


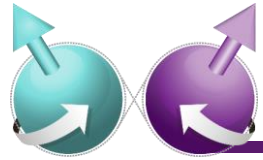


Sensing dynamics (AC) B field



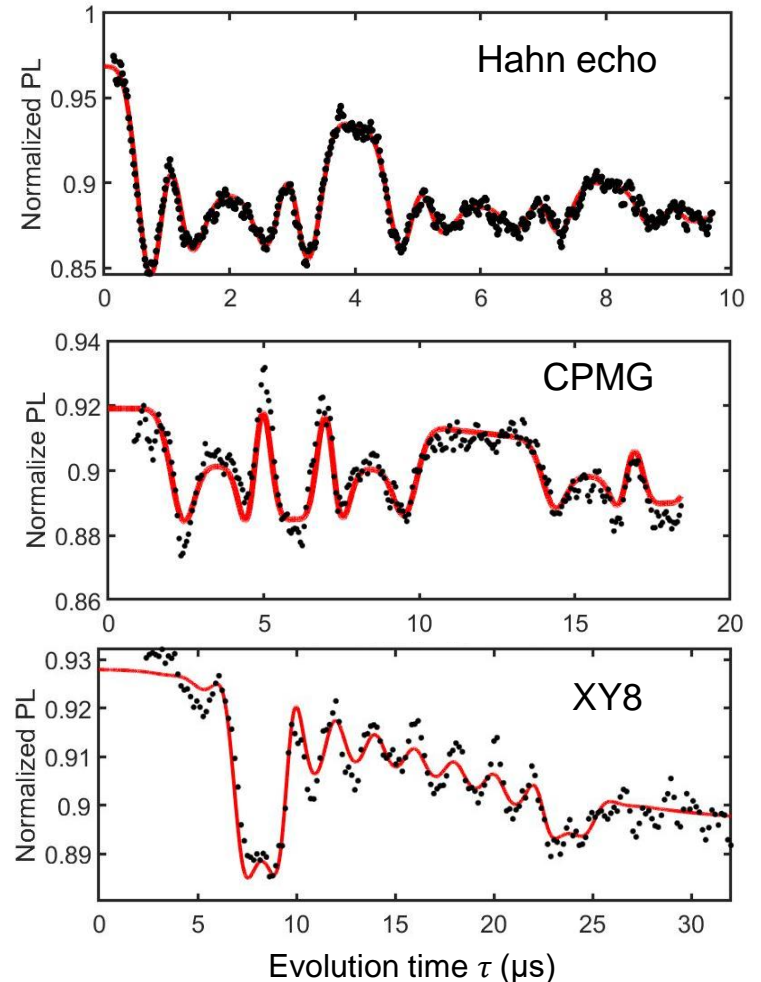
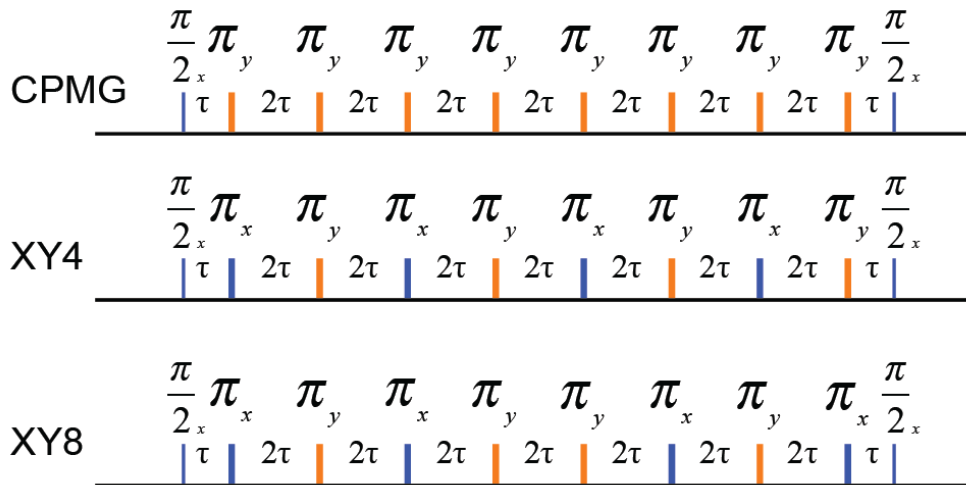
spin Hahn echo

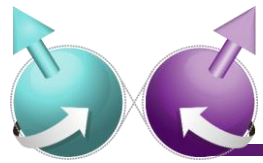




Sensing dynamics (AC) B field

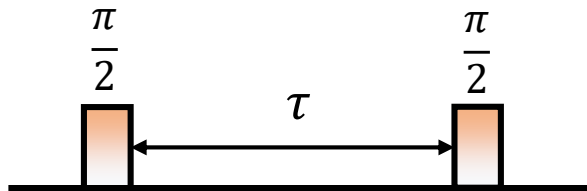
Dynamical decoupling



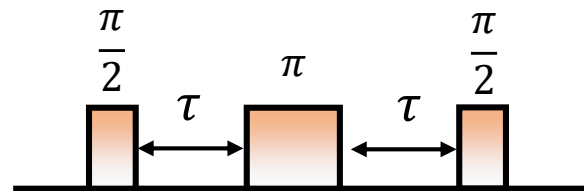


Sensing dynamics (AC) B field

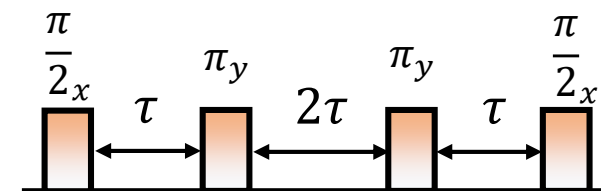
Ramsey



Hahn echo



CPMG-N

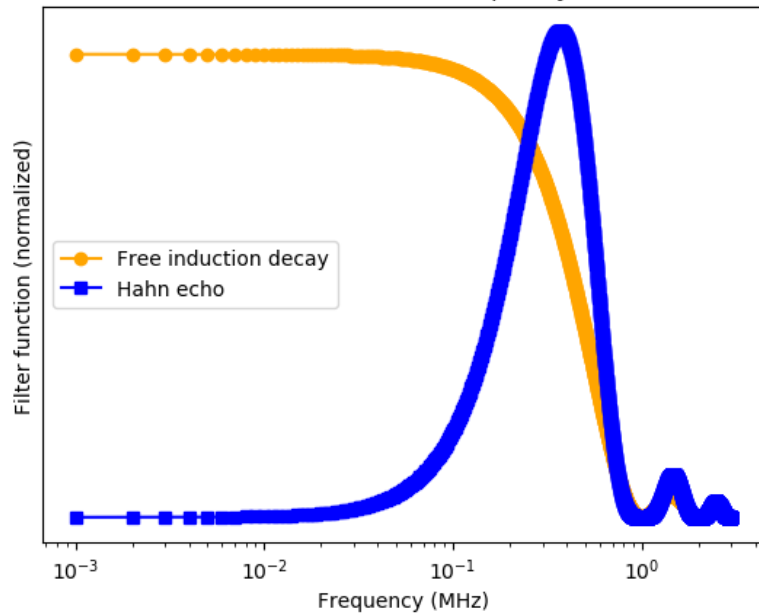


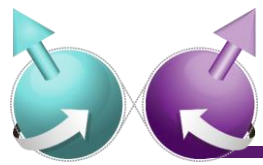
$$\langle 0|\rho|1\rangle \sim \exp\left\{-\frac{1}{\hbar^2} \int_{-\infty}^{\infty} d\omega \tilde{S}(\omega) F(\tau, \omega)\right\}$$

signal

filter function

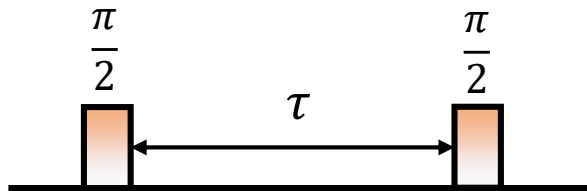
Filter function vs frequency



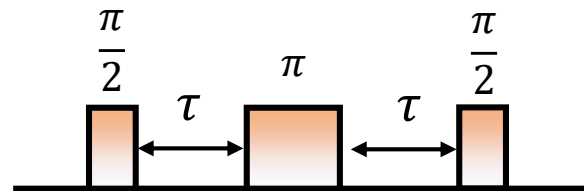


Sensing dynamics (AC) B field

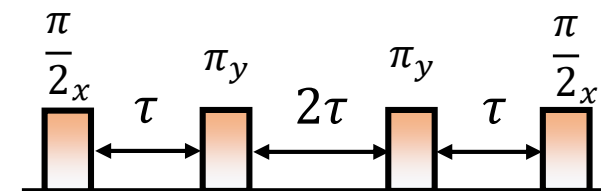
Ramsey



Hahn echo



CPMG-N

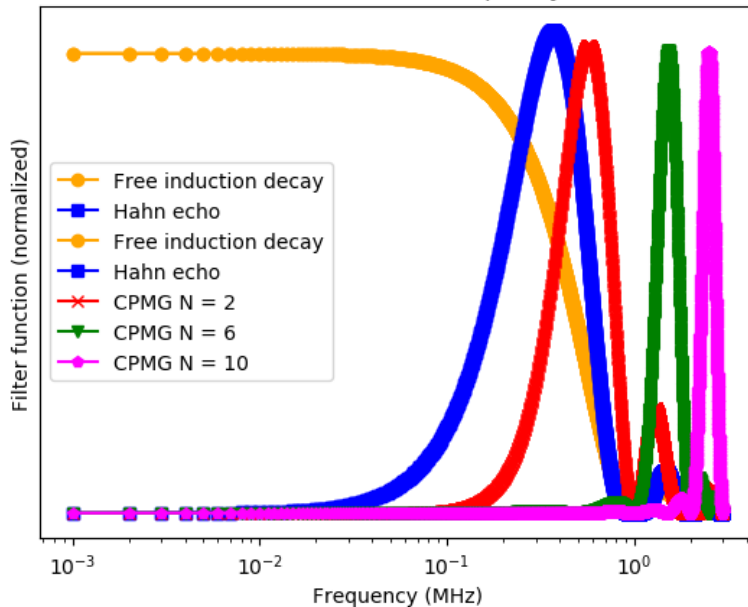


$$\langle 0|\rho|1\rangle \sim \exp\left\{-\frac{1}{\hbar^2} \int_{-\infty}^{\infty} d\omega \tilde{S}(\omega) F(\tau, \omega)\right\}$$

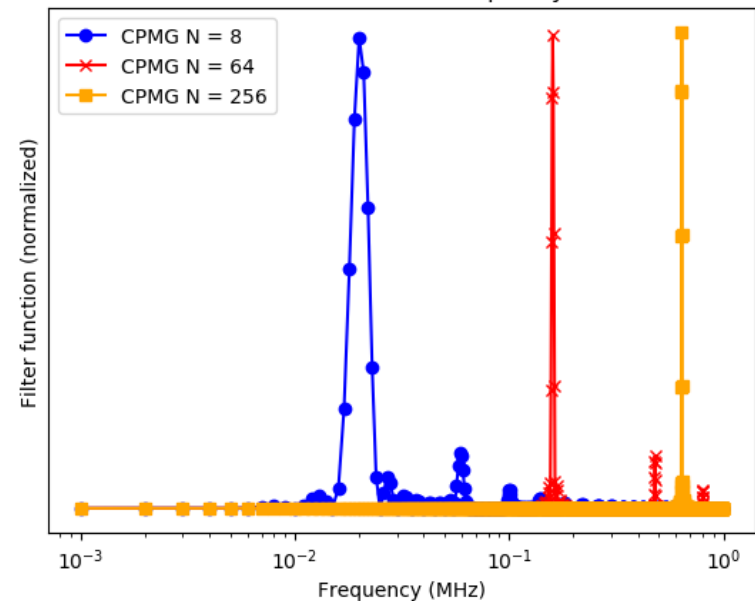
signal

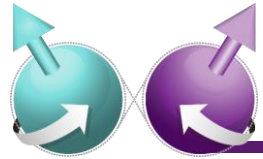
filter function

Filter function vs frequency



Filter function vs frequency





Sensing dynamics (AC) B field

General quantum sensing methods

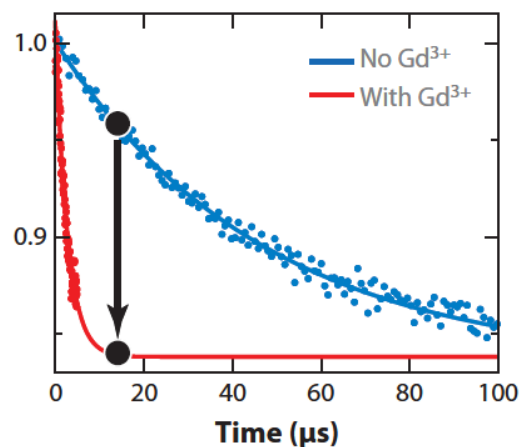
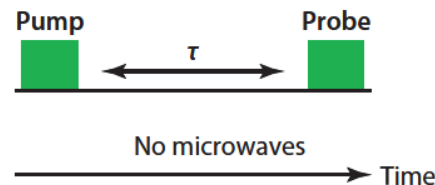
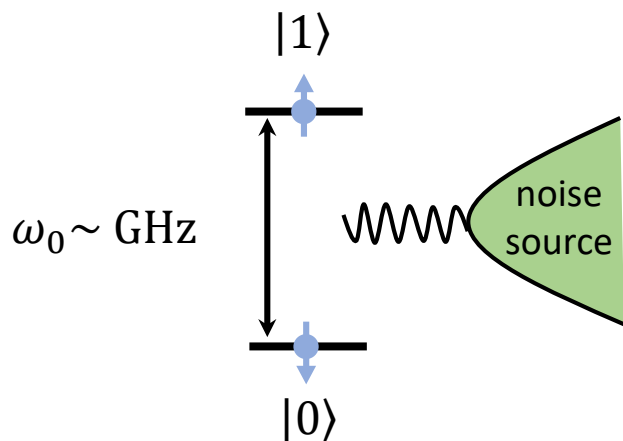
DC (dc ~ kHz) : Ramsey

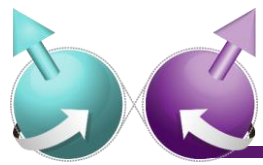
AC (kHz ~ 100 kHz) : Echo

AC (~ MHz) : CPMG, XY4, XY8

⋮

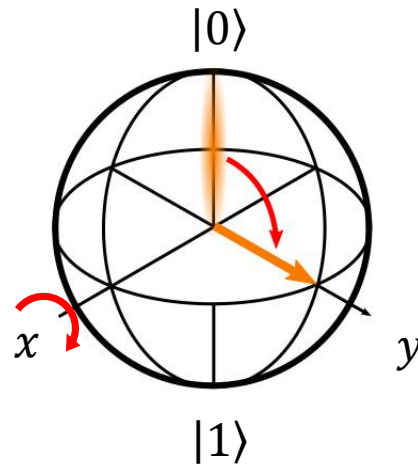
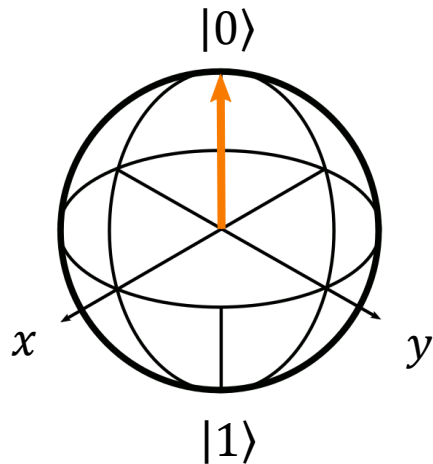
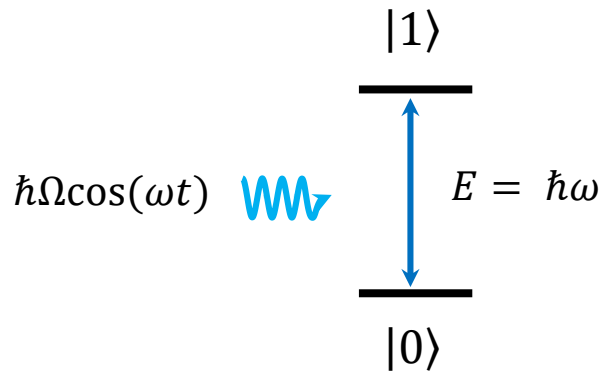
AC (~ GHz) : T_1 relaxometry



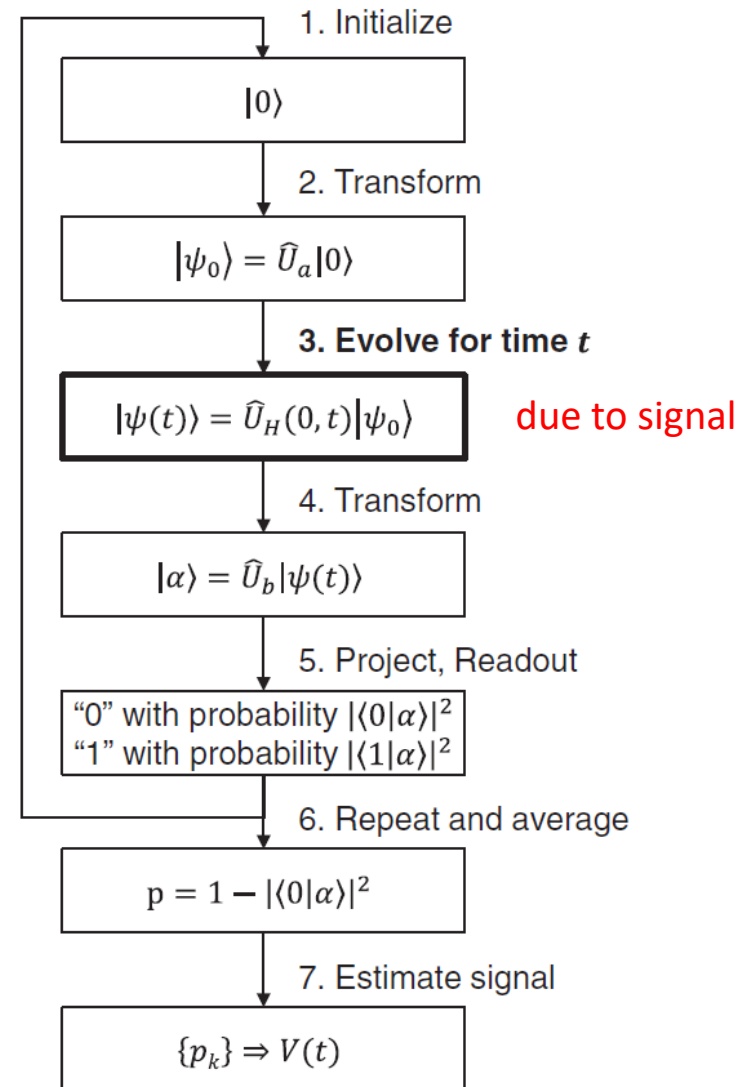


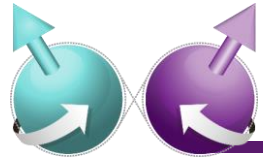
Quantum sensing protocol

Qubit

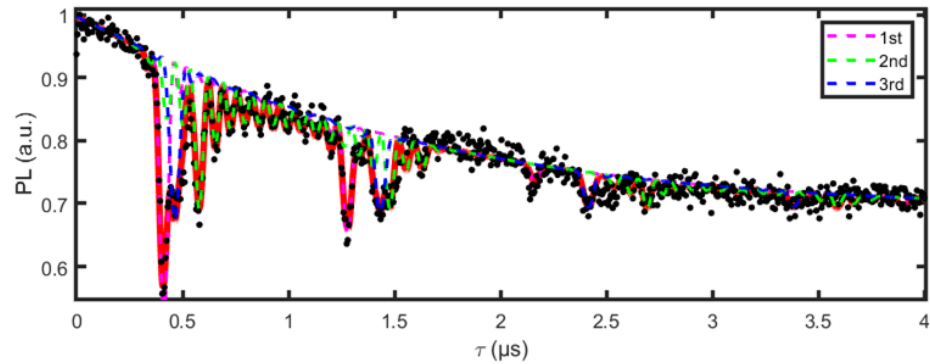
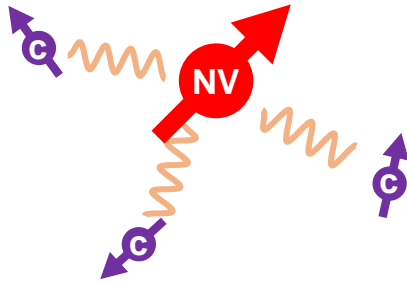


$$|\psi\rangle = \frac{1}{\sqrt{2}}(|0\rangle + |1\rangle)$$



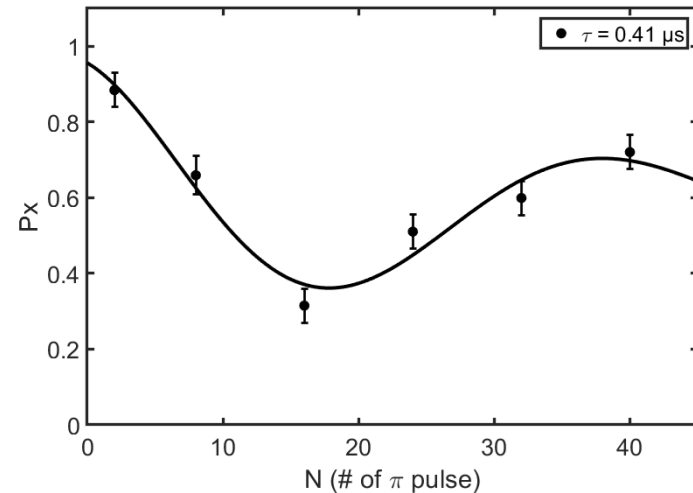
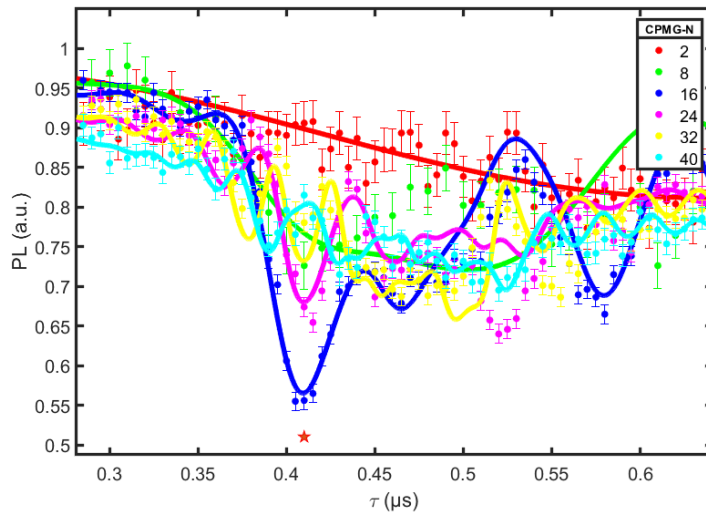


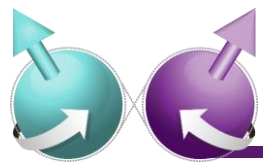
Advanced quantum sensing with multi-qubits



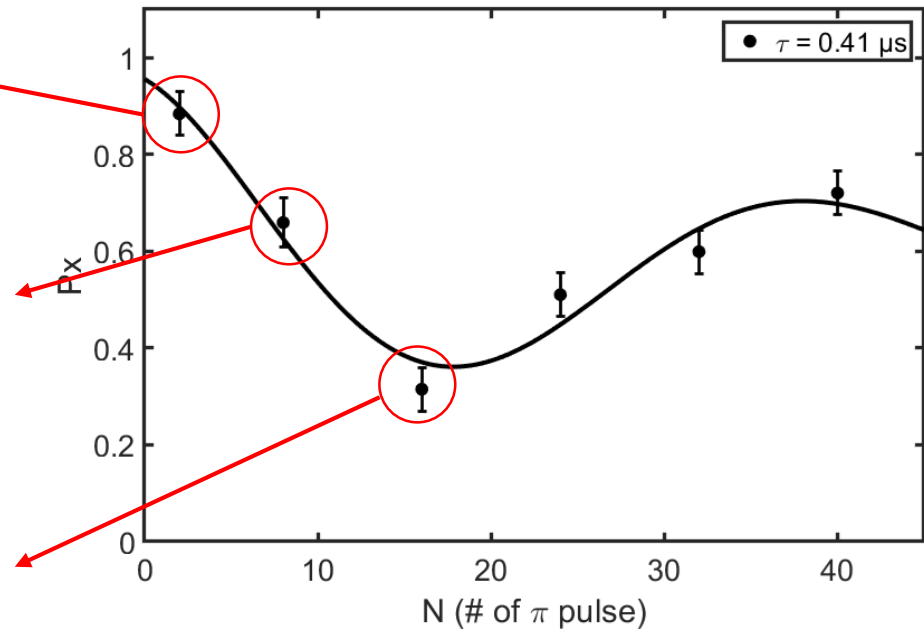
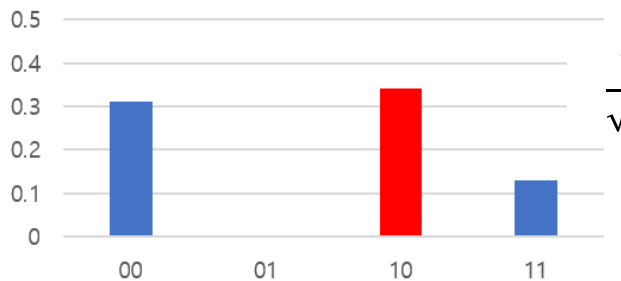
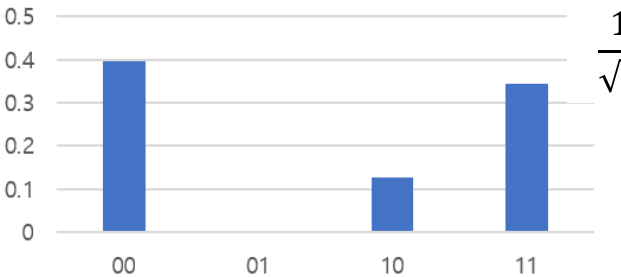
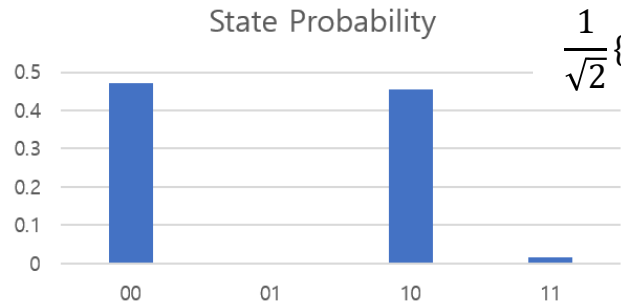
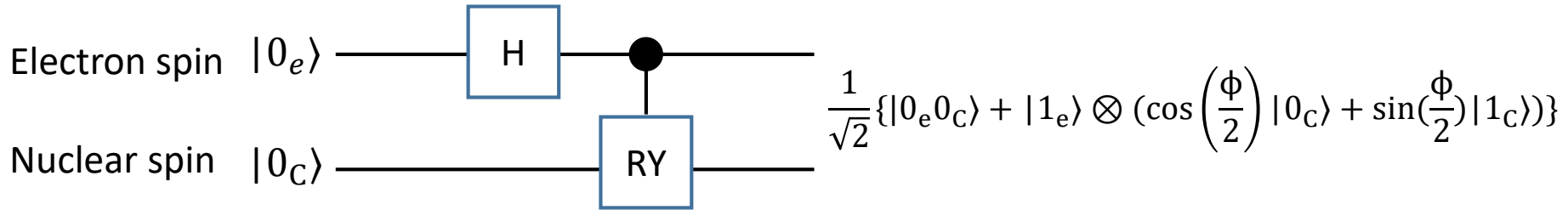
^{13}C index	1	2	3
A_{\parallel} (kHz)	167.7 ± 11.2	-46.2 ± 11.8	54.6 ± 12.0
A_{\perp} (kHz)	99.65 ± 6.9	148.8 ± 2.4	55.1 ± 2.9

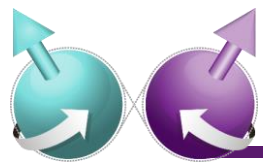
CPMG based $C_e\text{NOT}_n$ operation





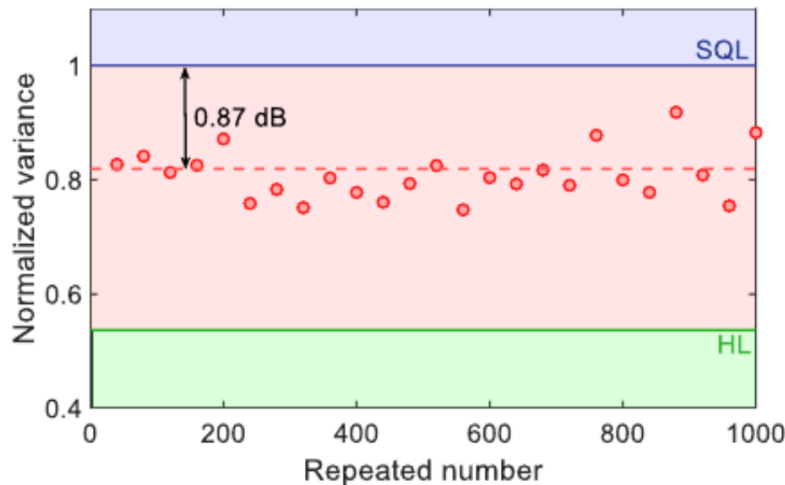
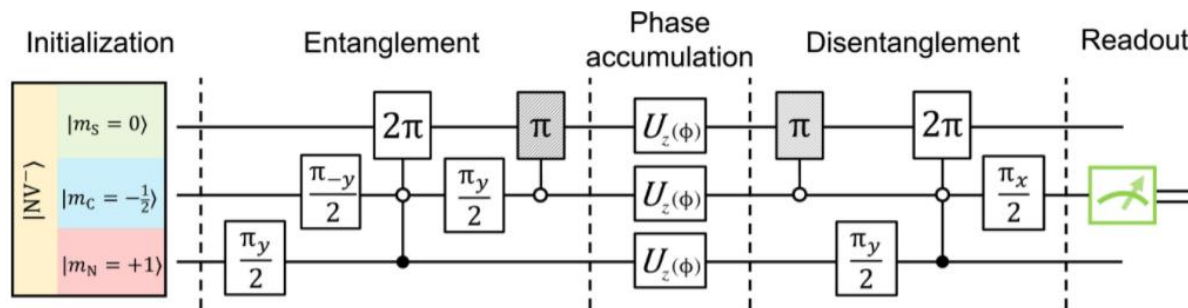
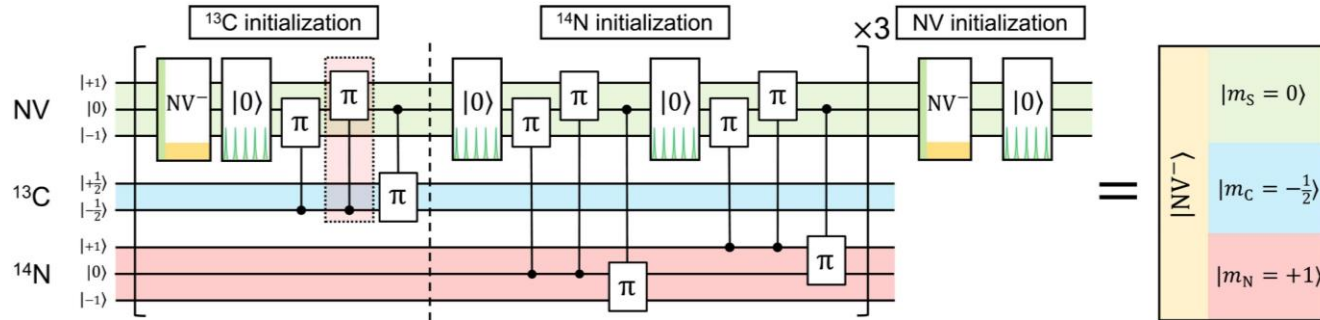
Advanced quantum sensing with multi-qubits

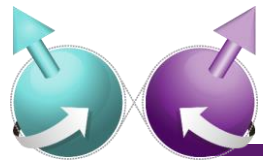




Advanced quantum sensing with multi-qubits

Quantum sensing below standard quantum limit

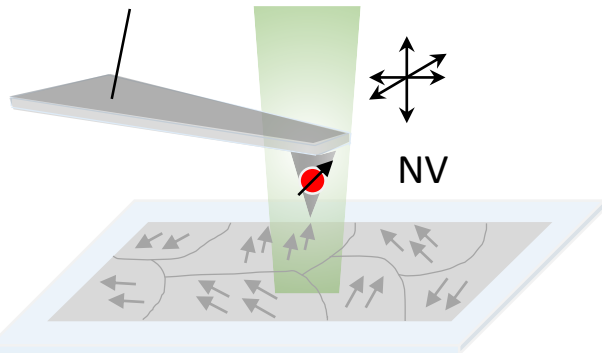




Quantum imaging based on diamond NV centers

nm scale imaging

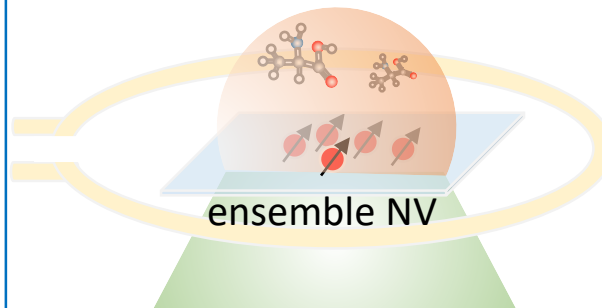
Scanning probe



magnetic sample

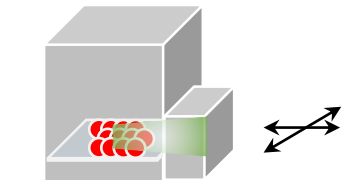
μm scale imaging

magnetic sample



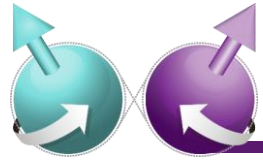
ensemble NV

mm scale imaging

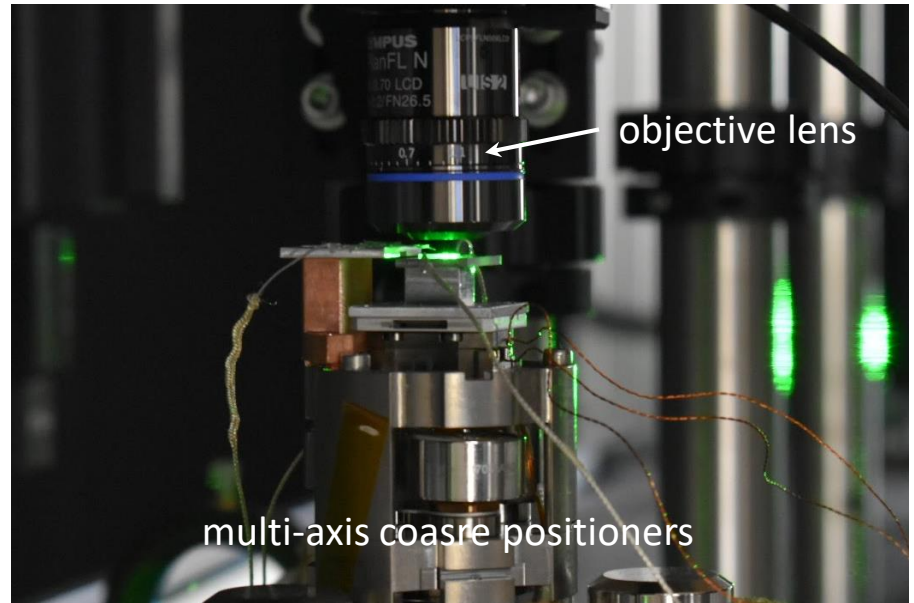
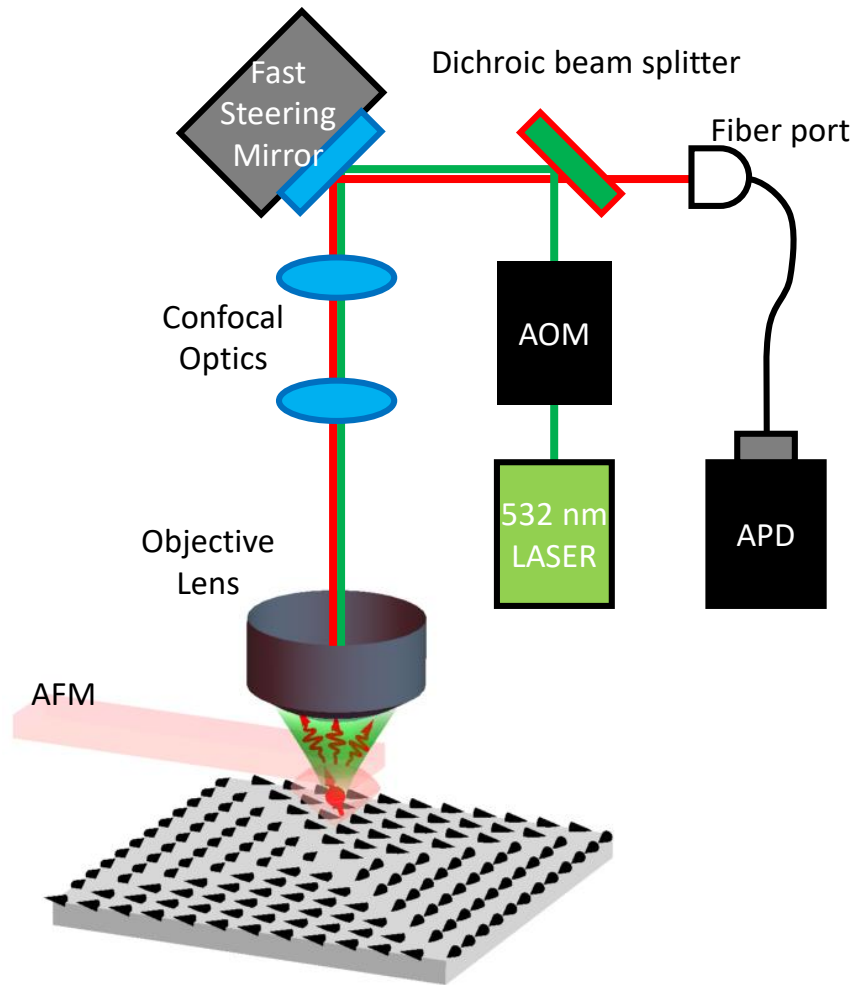


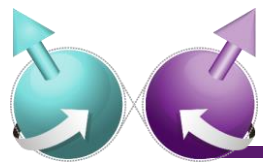
ensemble NV

magnetic sample

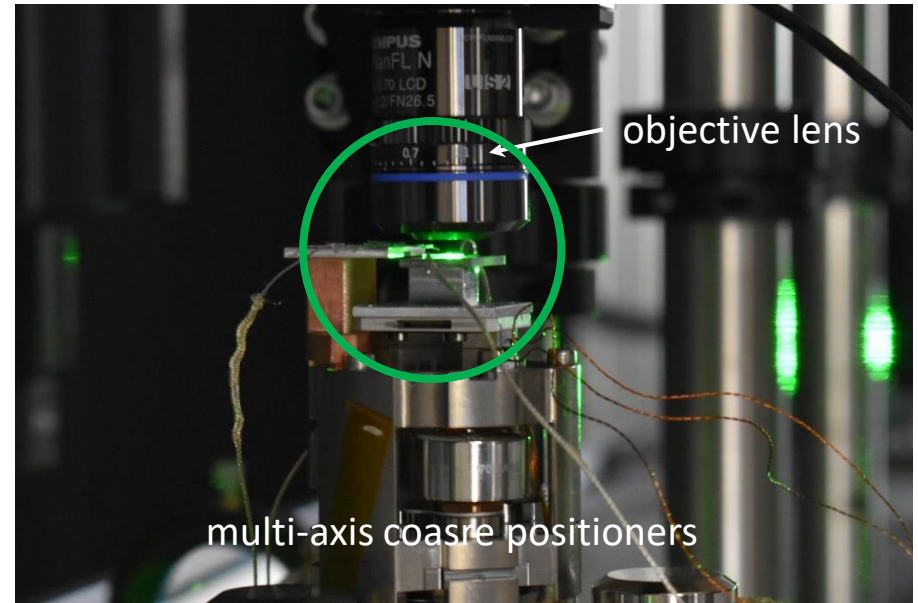
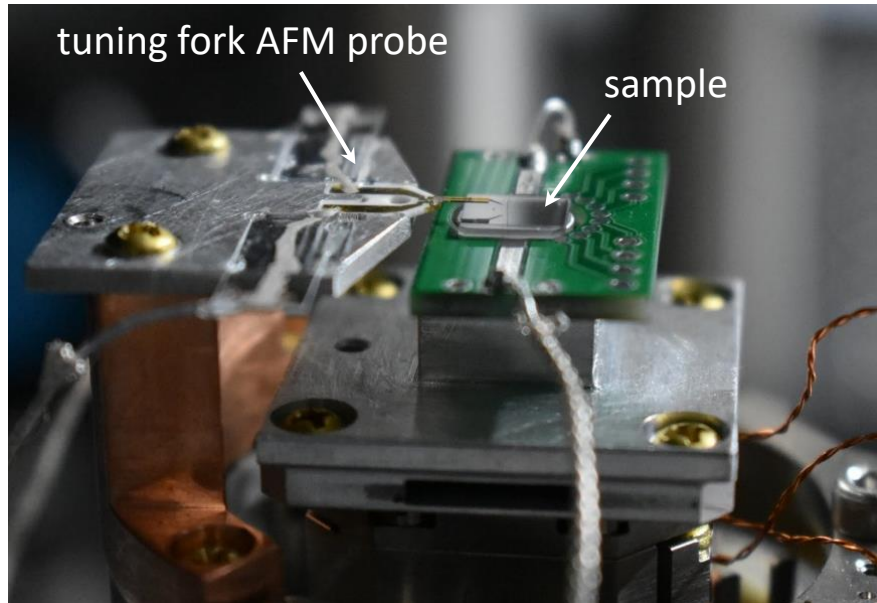


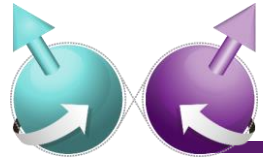
Imaging with single spin scanning magnetometer



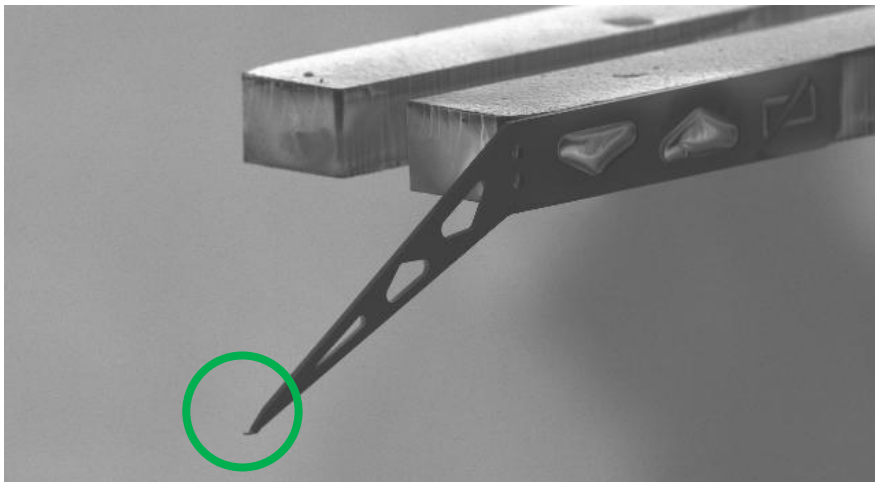
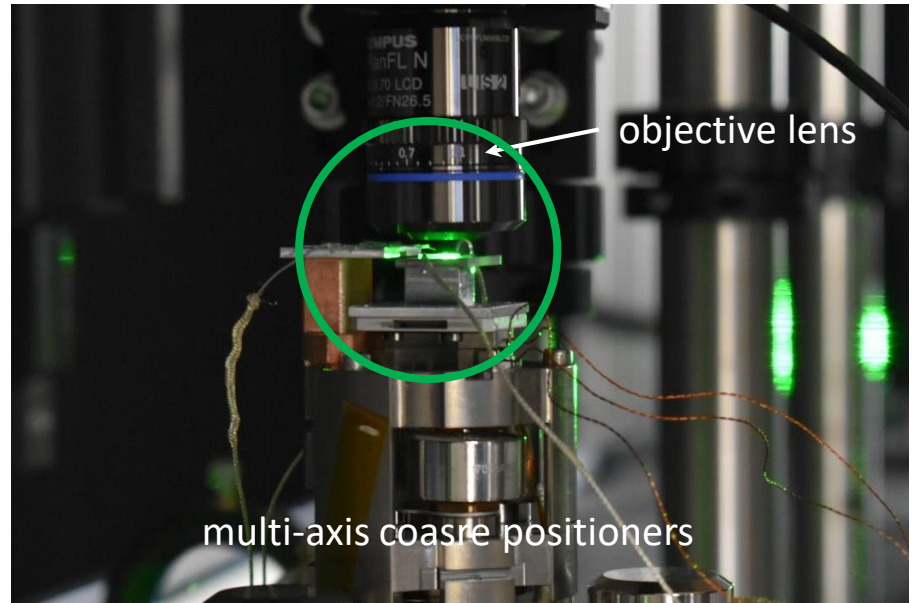
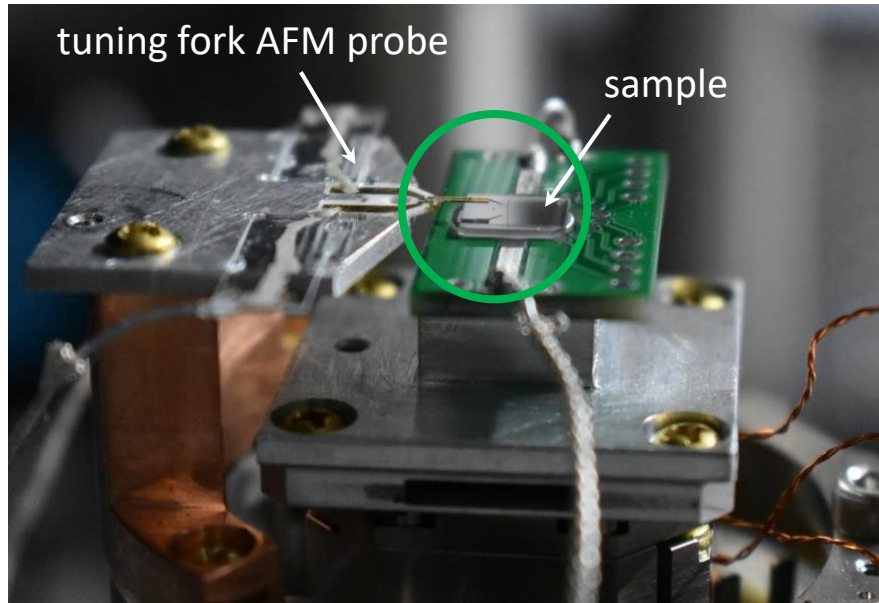


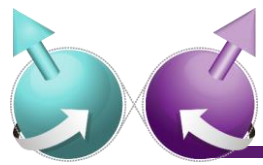
Imaging with single spin scanning magnetometer



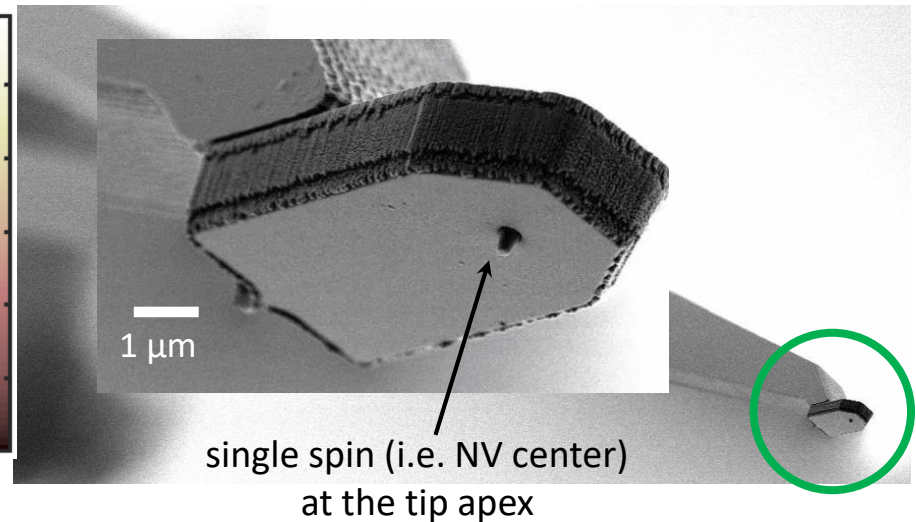
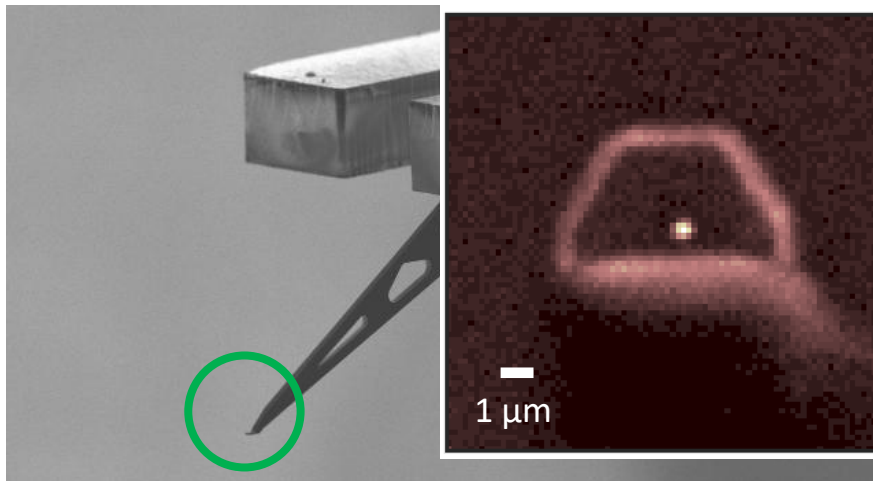
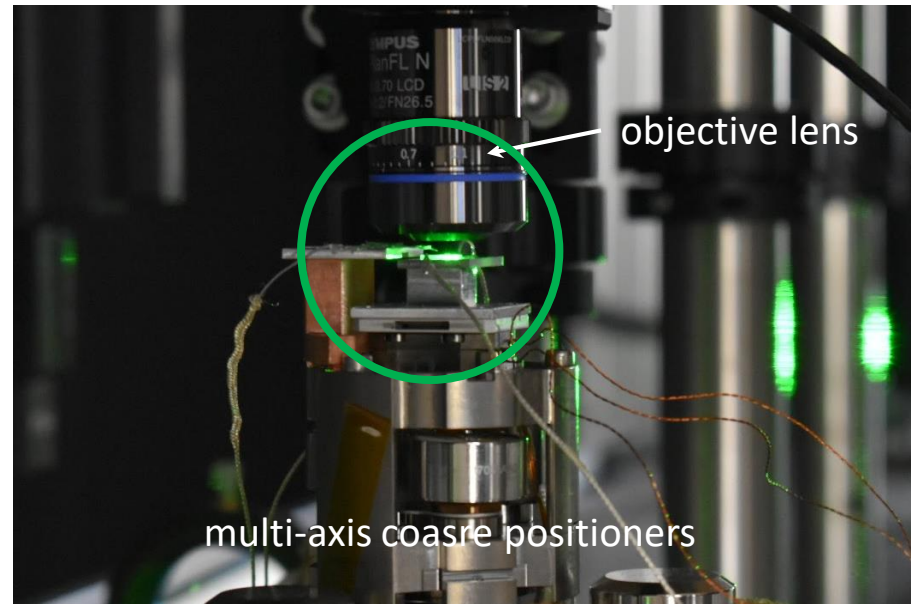
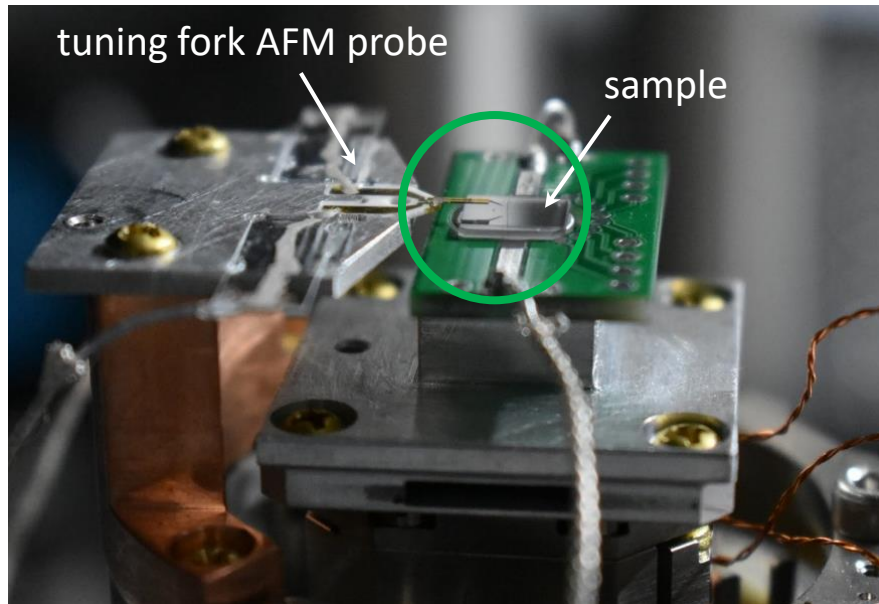


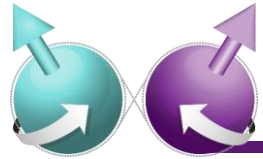
Imaging with single spin scanning magnetometer





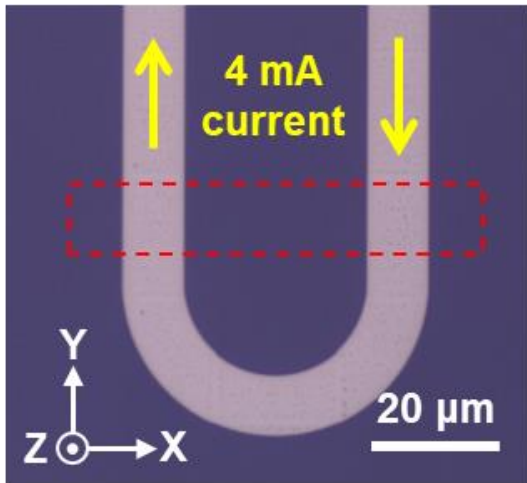
Imaging with single spin scanning magnetometer



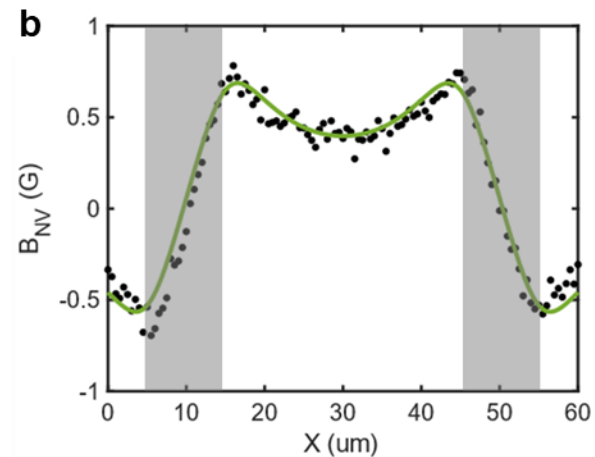
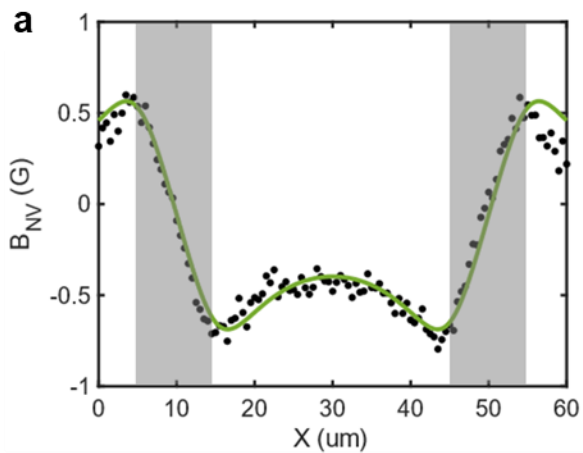
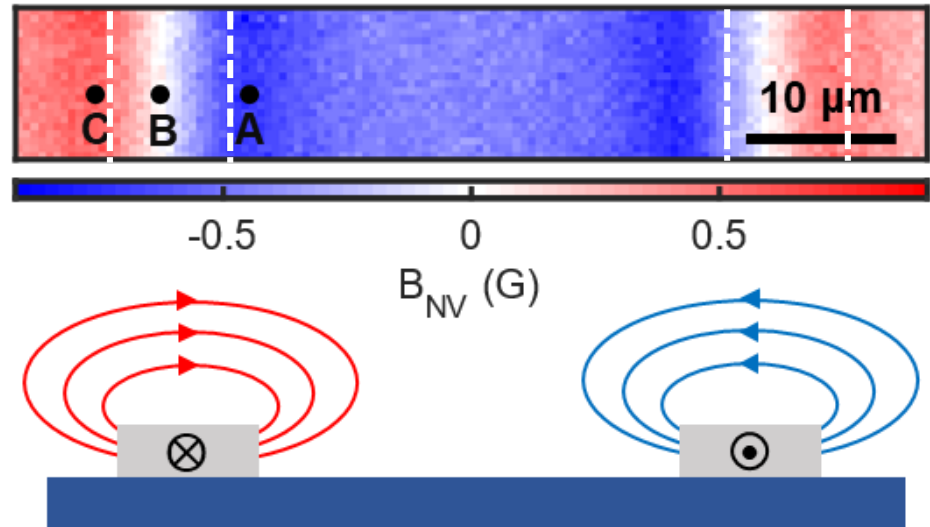


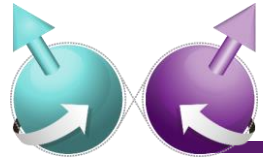
Imaging example with current device

- Optical image of Pt wire



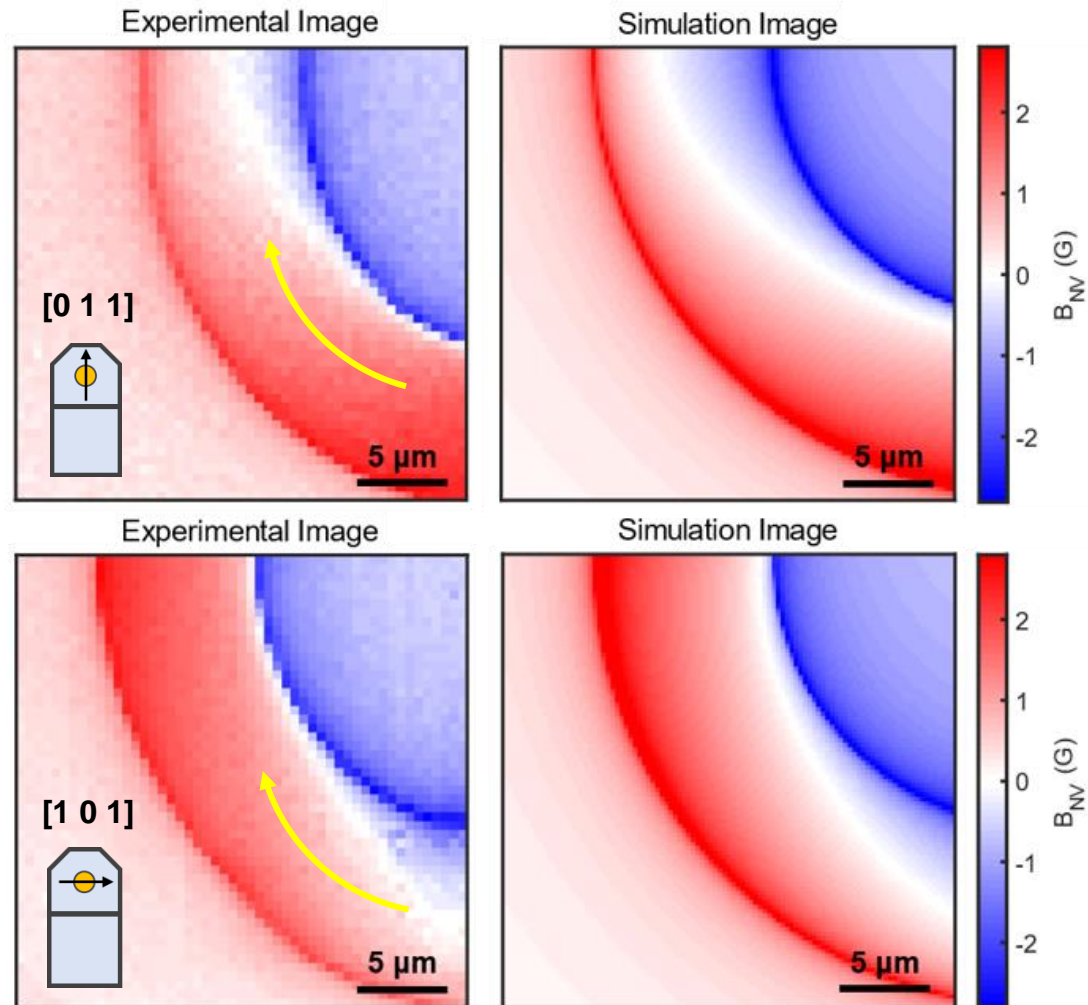
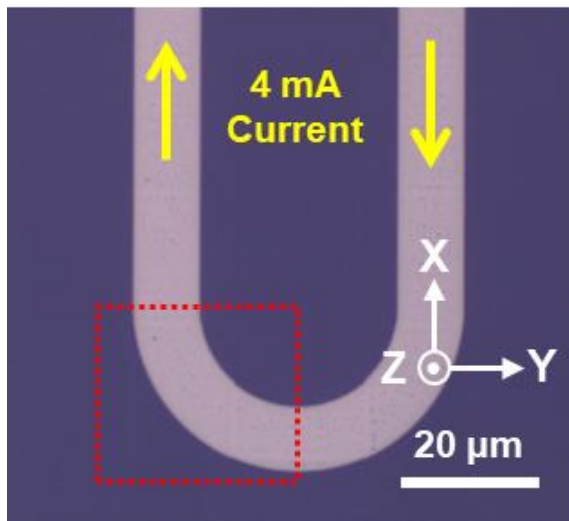
- Magnetic field image of the dashed area

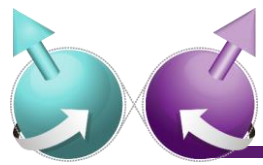




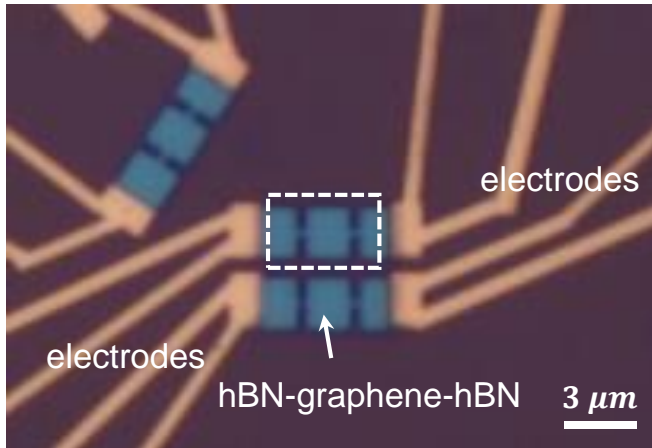
Imaging example with current device

- Optical image of Pt wire

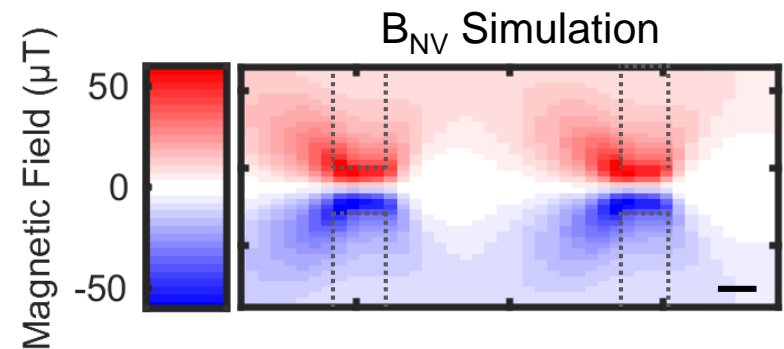
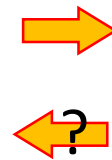
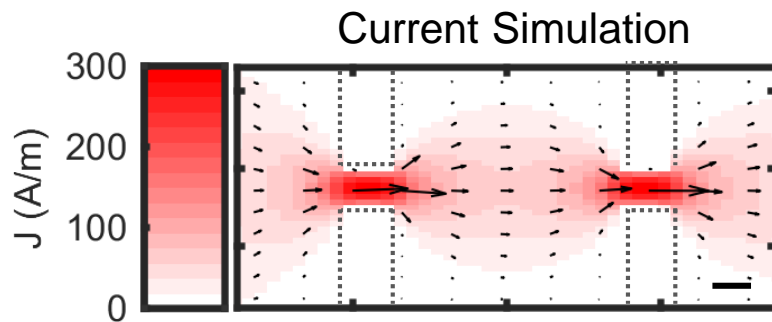
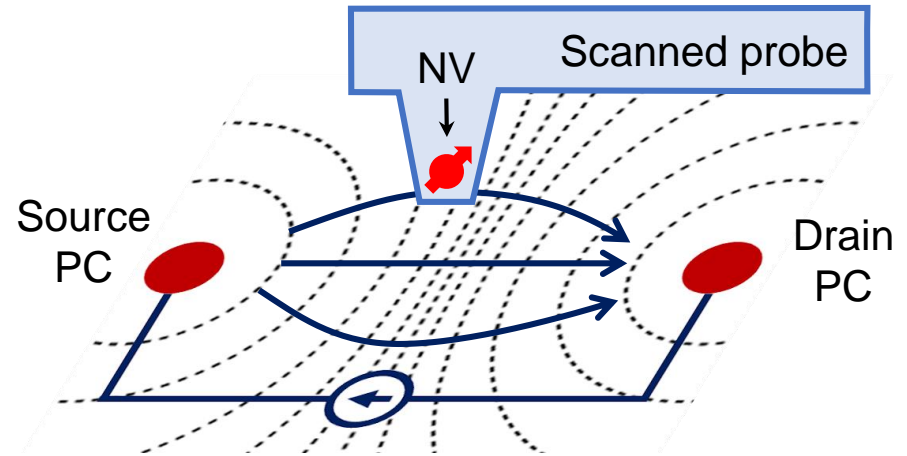




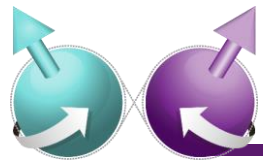
Imaging example with graphene device



Graphene sample (Prof. Gil-Ho Lee, POSTECH)

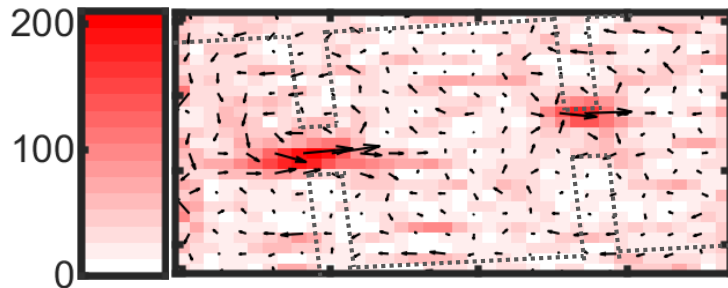


Is a single component of magnetic field enough to reconstruct current profile? Yes!

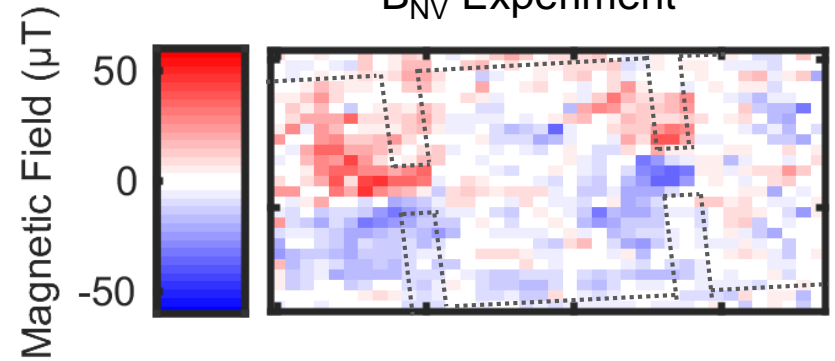


Imaging example with graphene device

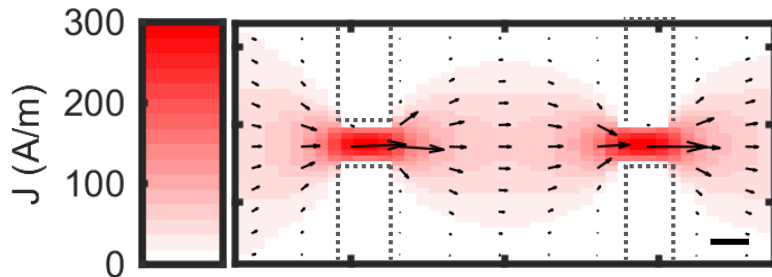
Reconstructed current density



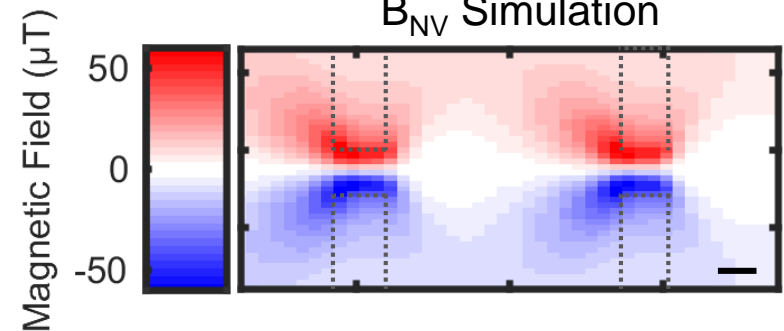
B_{NV} Experiment



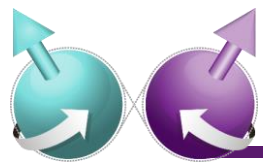
Current Simulation



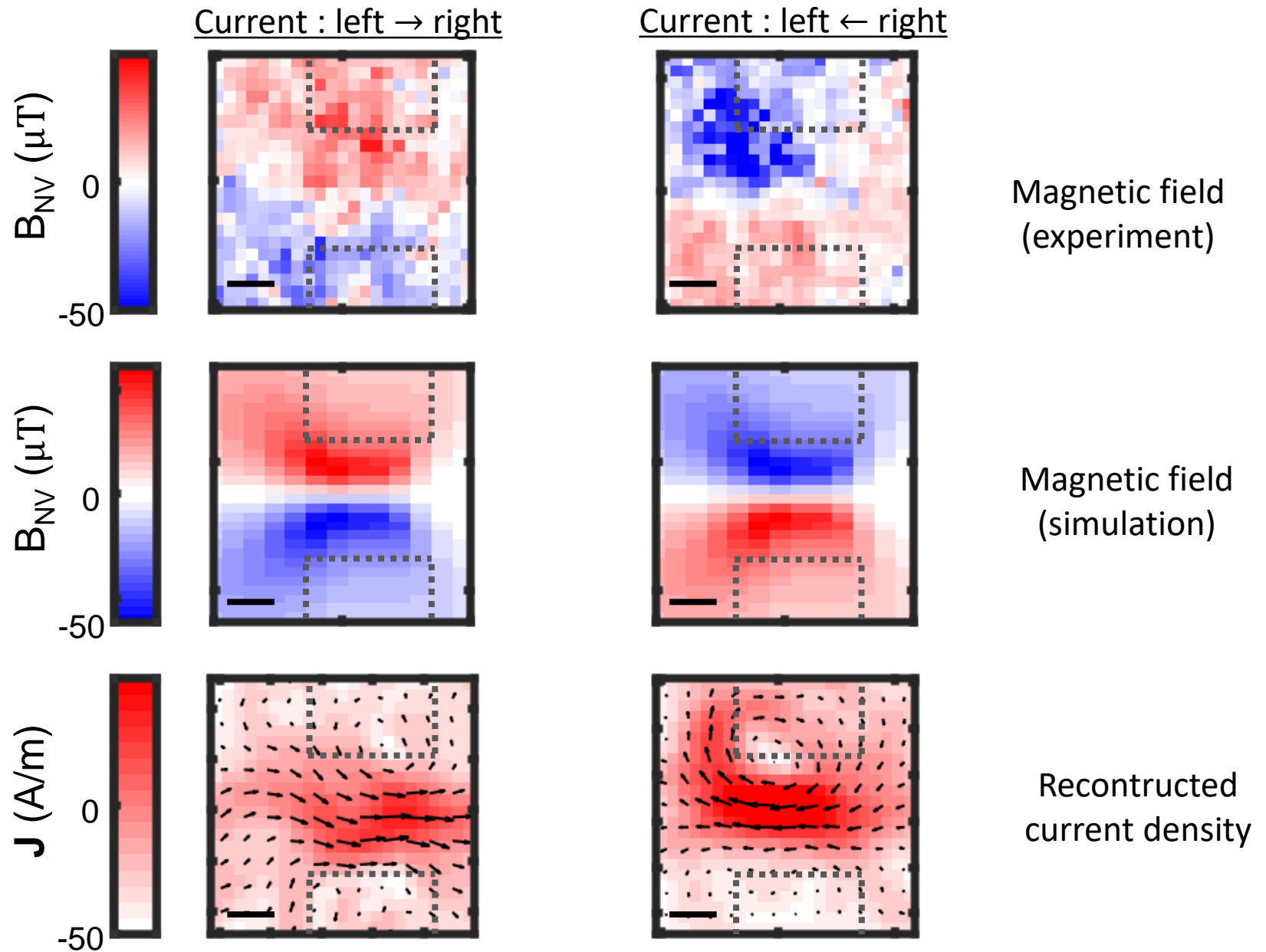
B_{NV} Simulation

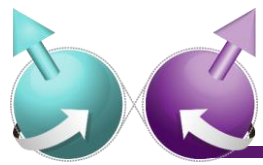


Is a single component of magnetic field enough to reconstruct current profile? Yes!



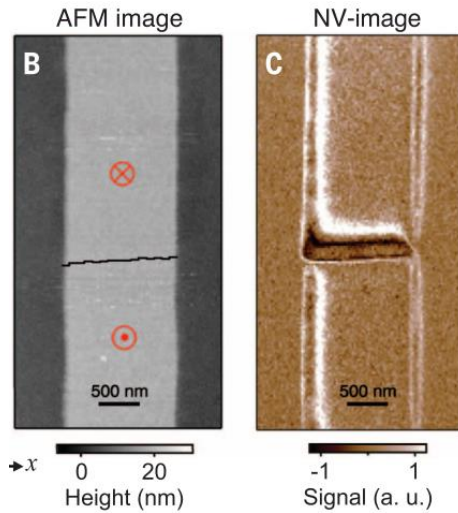
Imaging example with graphene device





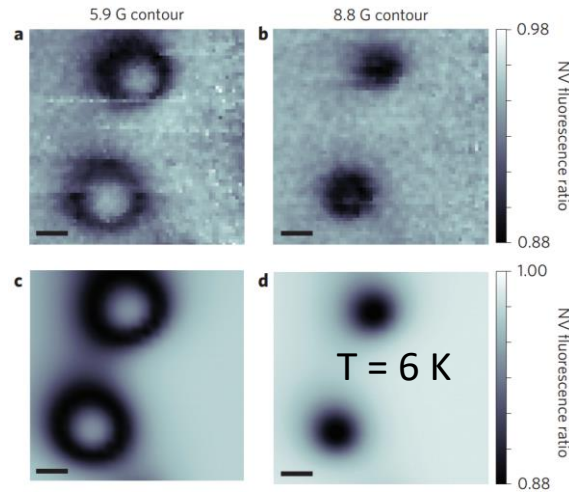
More imaging examples

Domain wall



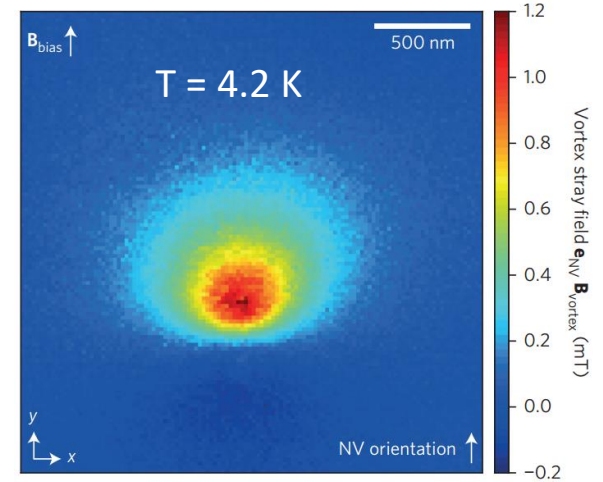
J. P. Tetienne *et al.*, Science (2014)

Superconducting vortices in $\text{BaFe}_2(\text{As}_{0.7}\text{P}_{0.3})_2$



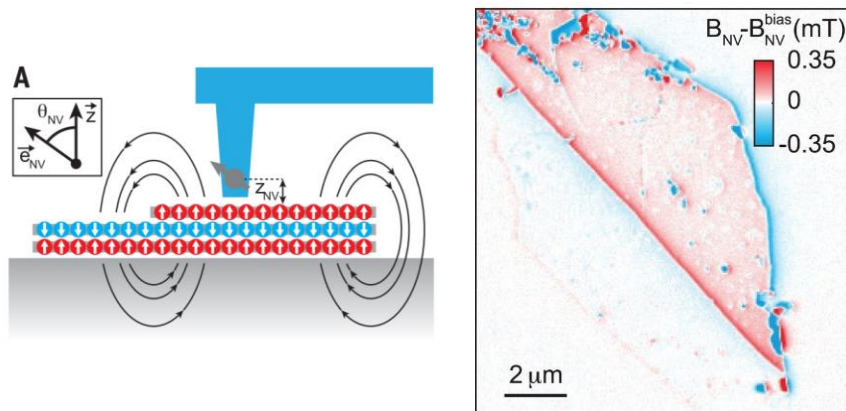
M. Pelliccione *et al.*, Nat. Nano. (2016)

Superconducting vortex in YBCO



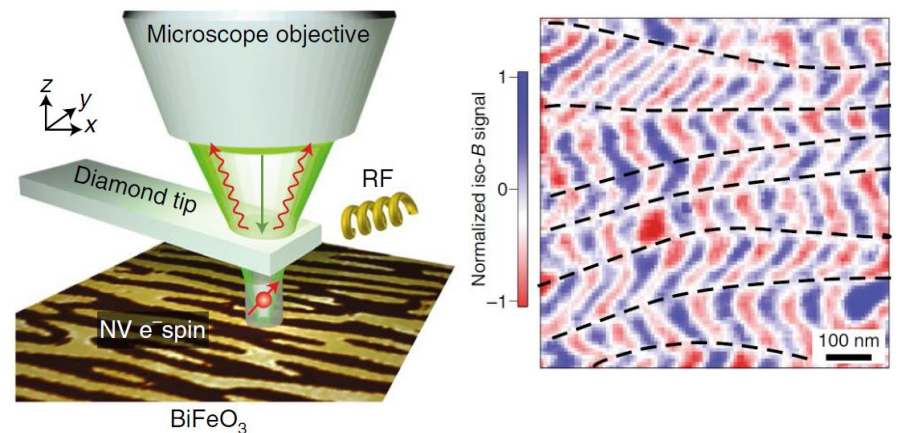
L. Thiel *et al.*, Nat. Nano. (2016)

2D ferromagnetism

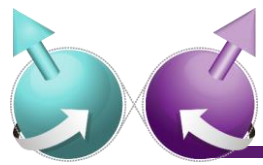


L. Thiel *et al.*, Science (2019)

Anti-ferromagnetic order

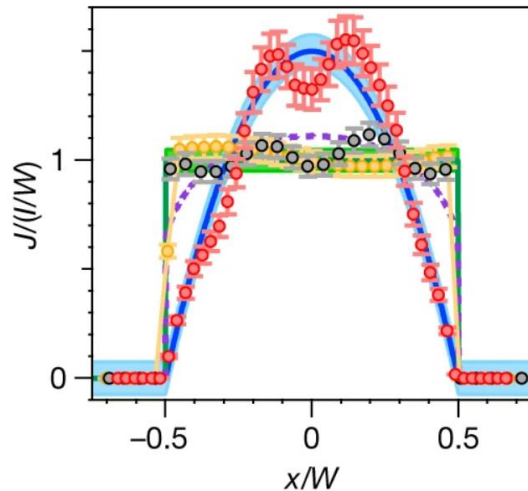
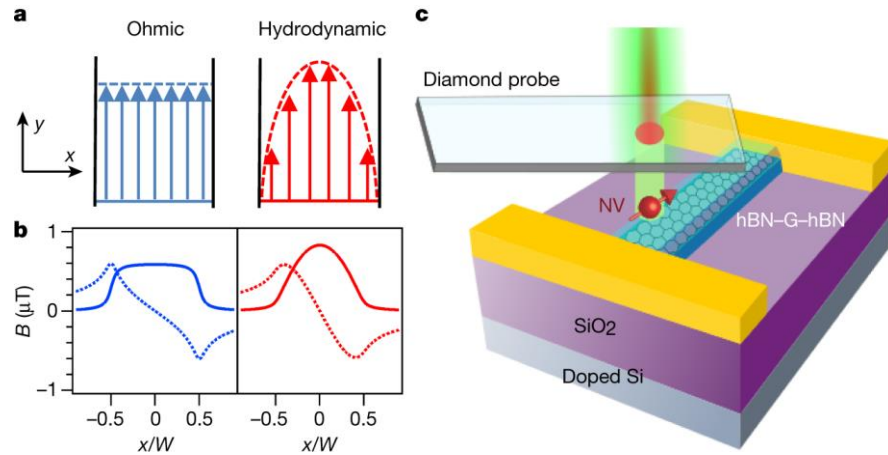


I. Gross *et al.* Nature (2017)



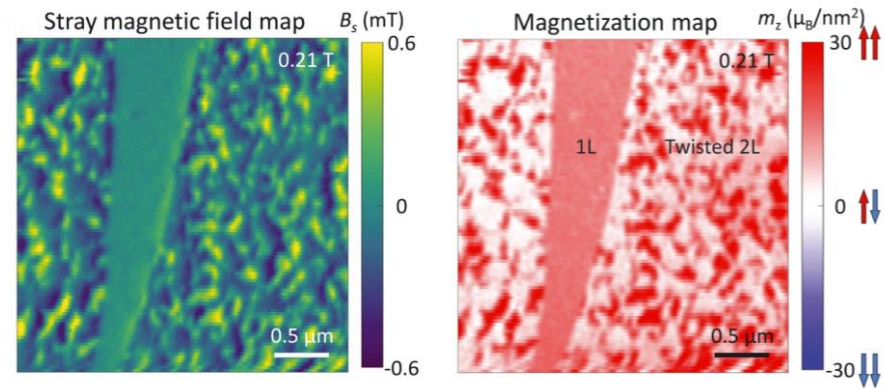
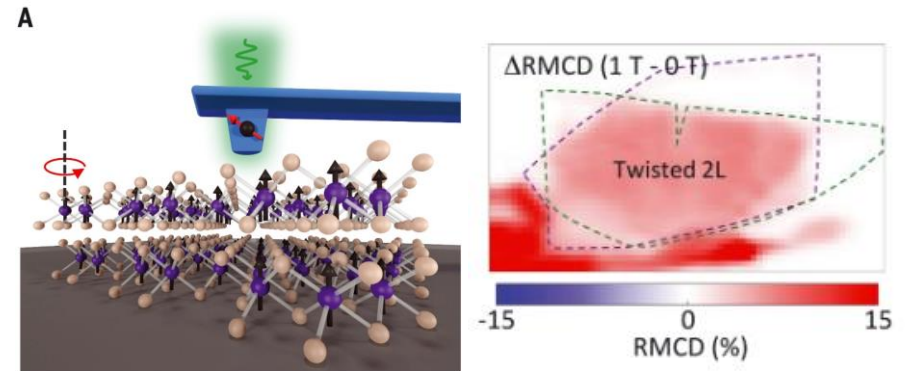
More imaging examples

Imaging viscous flow in graphene

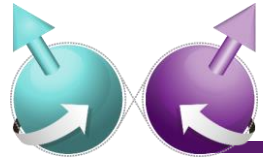


M. J. H. Ku et al. Nature (2020)

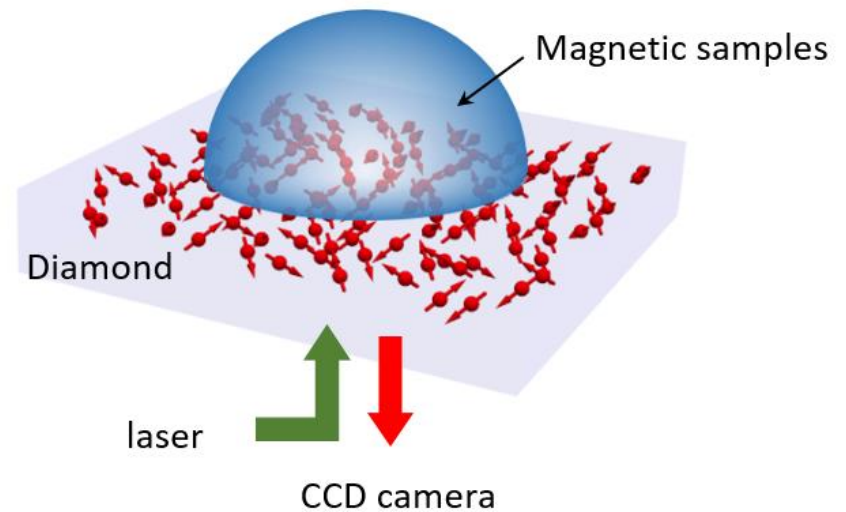
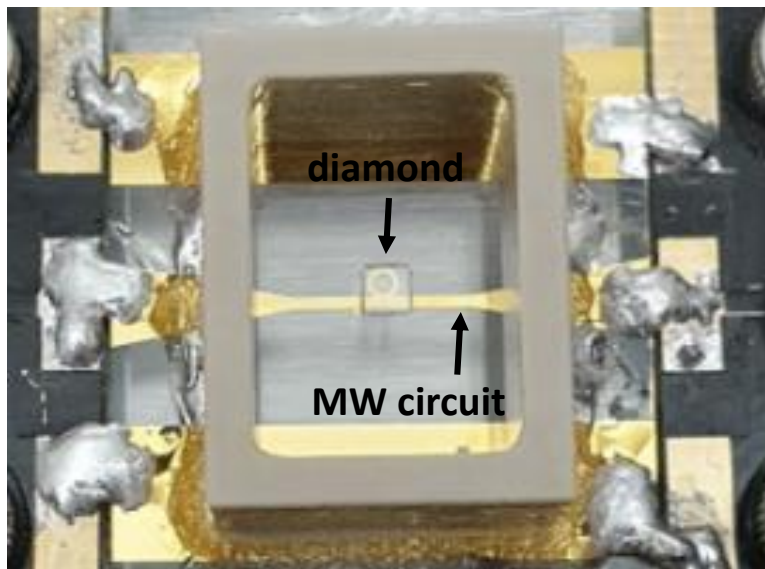
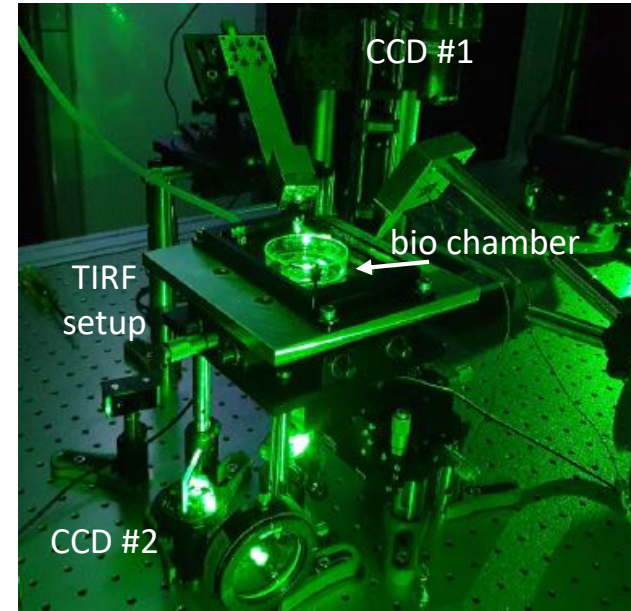
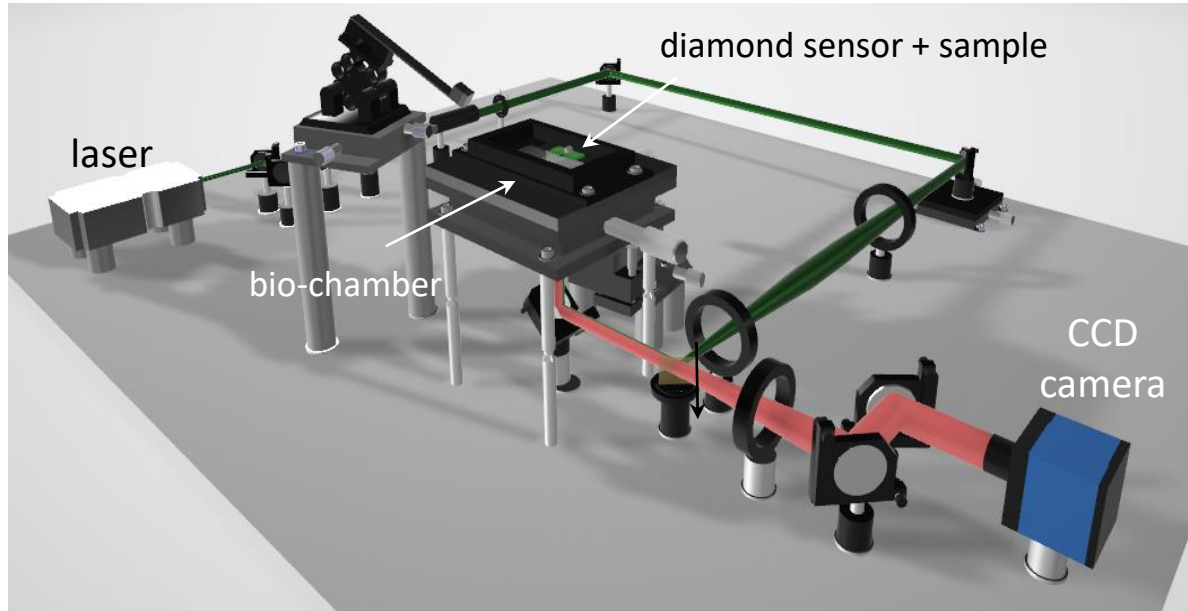
Imaging magnetic domains in twisted CrI₃

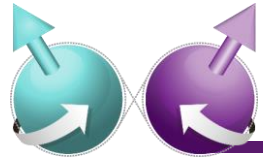


T. Song et al. Science (2021)

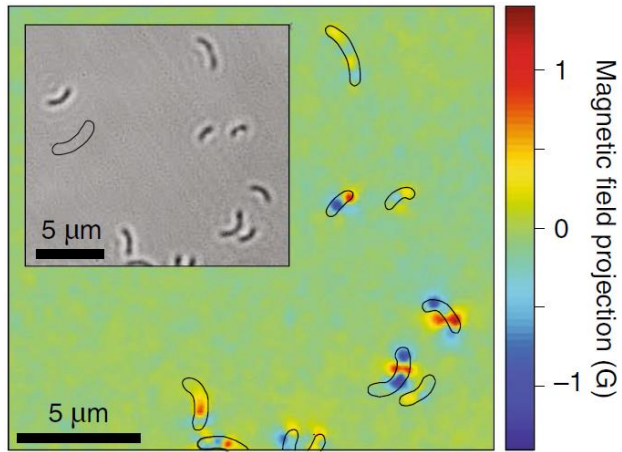


Imaging with wide-field quantum microscope

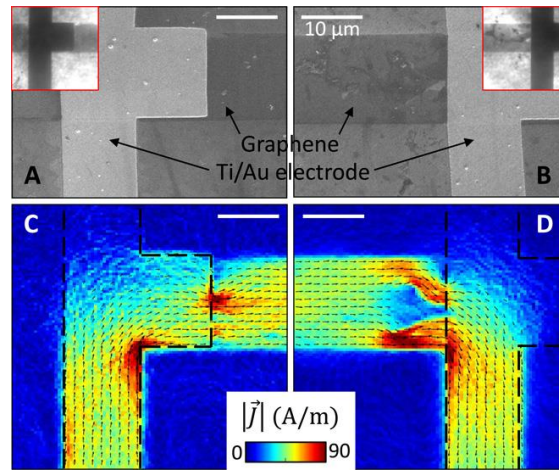




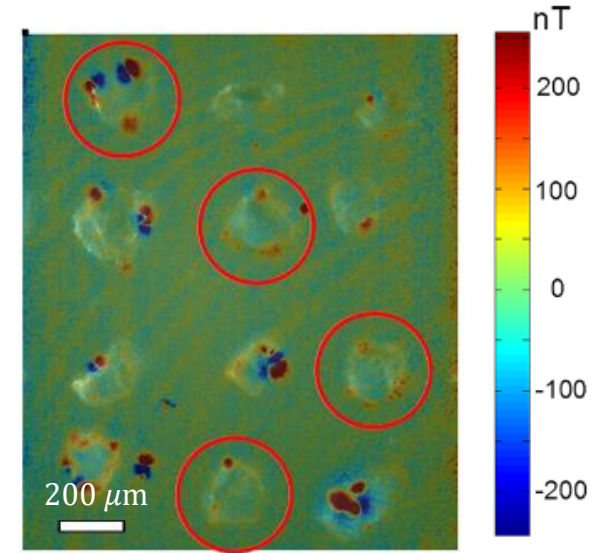
More imaging examples



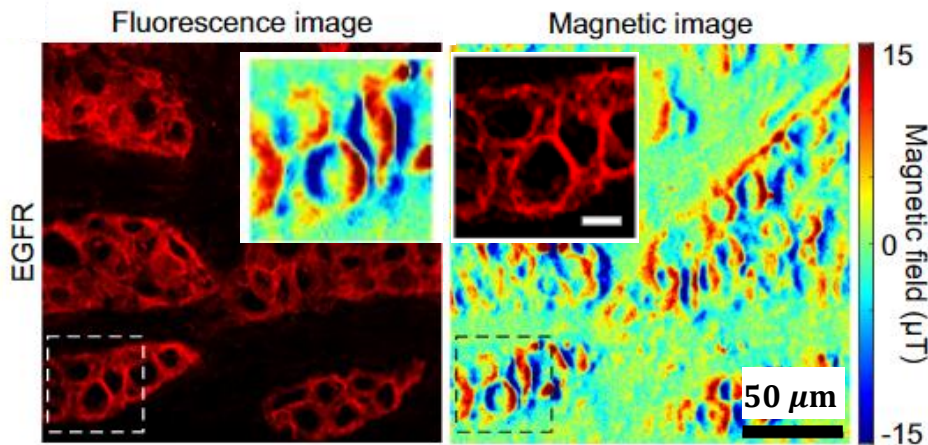
Le Sage et al. Nature (2013)



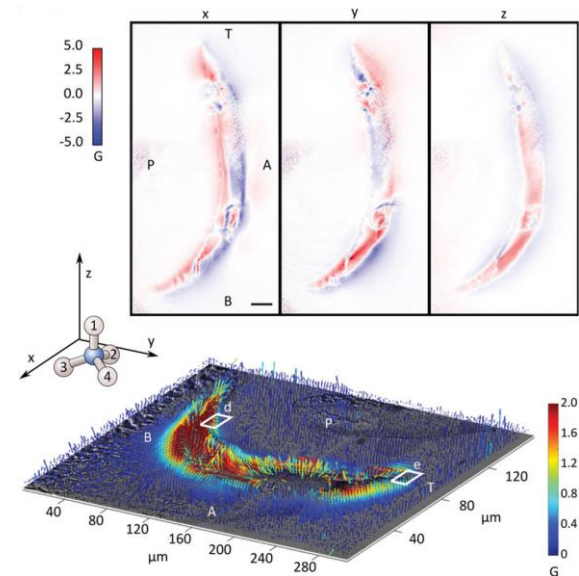
J-T Tetienne et al. Science Advacnes (2017)



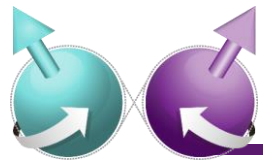
Glenn et. al. Geo. Geophys. Geosys. (2017)



Chen et. al. PNAS (2022)

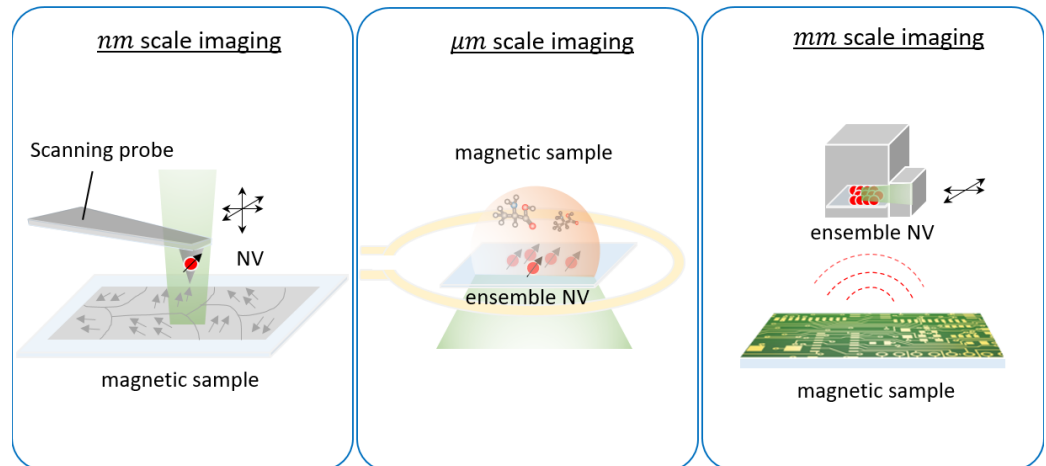
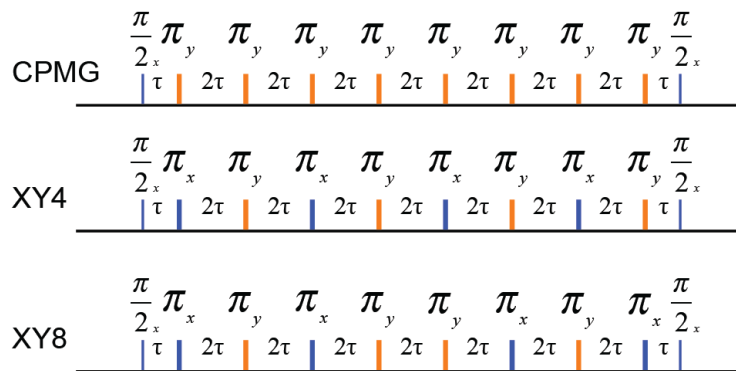


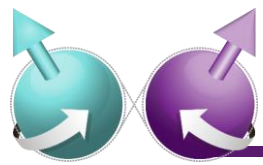
McCoey et. al. Small (2020)



Summary

- 스핀 큐비트 기반 양자센싱 기초 원리 (e.g. Ramsey, echo, dynamical decoupling, etc.)
- 다이아몬드 NV 센터 소개
- NV 센터 기반 양자 센싱 소개
- NV 센터 기반 양자 이미징 소개





Summary

- Quantum sensing, quantum metrology (양자센싱, 양자계측)
- 측정은 모든 물리 실험의 기본
- 양자센싱 및 이미징은 양자현상에 기반한 물리 실험의 새로운 방법론 제공
- 중시계 등 다양한 기초·응용 물리 실험에 활용 가능

